

ABSTRACT

Calibration Methodology for a Microwave Non-Invasive Glucose Sensor

Melanie J. McClung, M.S.B.M.E.

Mentor: B. Randall Jean, Ph.D.

Non-invasive measuring techniques for determining biological parameters are more heavily researched with the growth of the biomedical industry. One of the top areas in non-invasive research deals with diabetes. This disease affects more than 20 million people in the United States, and there is an increasing desire to find a testing process that is non-invasive, easy to use, and safe for users.

Microwave technology has improved greatly during recent years and is now seen more often in conjunction with biomedical research. Microwaves are capable of taking measurements of materials inside of a closed volume without the need to come into contact with the material. This makes them ideal for measuring biological parameters, specifically glucose concentrations in the blood.

This thesis expands on the development of a microwave sensor to non-invasively measure blood glucose levels and will examine the possibility of developing a calibration for a device using the microwave sensor.

Calibration Methodology for a Microwave Non-Invasive Glucose Sensor

by

Melanie J. McClung, B.S.E.C.E.

A Thesis

Approved by the Department of Electrical and Computer Engineering

Kwang Y. Lee, Ph.D., Chairperson

Submitted to the Graduate Faculty of
Baylor University in Partial Fulfillment of the
Requirements for the Degree
of
Master of Science in Biomedical Engineering

Approved by the Thesis Committee

B. Randall Jean, Ph.D., Chairperson

Robert J. Marks II, Ph.D.

Dennis A. Johnston, Ph.D.

Accepted by the Graduate School
May 2008

J. Larry Lyon, Ph.D., Dean

Copyright © 2007 by Melanie J. McClung

All rights reserved

TABLE OF CONTENTS

LIST OF FIGURES	vi
LIST OF TABLES	xi
GLOSSARY	xiv
ACKNOWLEDGMENTS	xix
DEDICATION	xx
CHAPTER ONE	
Introduction	1
CHAPTER TWO	
Diabetes and Glucose	3
CHAPTER THREE	
Glucose Testing	7
CHAPTER FOUR	
Microwaves and Measurement	13
Microwaves	13
Permittivity and S-Parameters	14
Measurement Tools	17
CHAPTER FIVE	
Microwaves and The Body	21
Uses of Microwaves in Biological Applications	21
Permittivity and Biological Modeling	23
Previous Studies	26
CHAPTER SIX	
Design of a Microwave Glucometer	29
Basis for Project	29
Improvements for a New Resonant Sensor	31
Designing and Creating the Device	34
The Enclosure	34
FlexiForce Sensor	35
Force Sensor and LED Circuit	36
Microcontroller Board	39

Spiral Sensor	40
Mounting of the Sensor	44
VNA Program	46
CHAPTER SEVEN	
Studies	47
Study One – “The Soda Test”	47
Study Two – Developing a Calibration Algorithm	55
Experiment One	55
Side Experiment	62
Experiment Two	64
Experiment Three	68
CHAPTER EIGHT	
Conclusions and Final Recommendations	81
APPENDIX A	
Circuit Schematic, Board Layout and Device Bill of Materials	86
Circuit Schematic	86
Circuit Board Layout Views	87
Circuit and Device Bill of Materials	89
APPENDIX B	
Device Instructions, Checklist, and Consent Form	91
Device Instructions	91
Checklist for Information and Instructions Given to Every Participant in the Test	95
Consent Form	96
APPENDIX C	
Excel Data and Regression Results for the “Soda Test”	99
APPENDIX D	
Excel Data and Regression Results for Developing a Calibration Algorithm	106
Regression Data for Participants with the Least Noisy Data Sets	106
Regression Data for All Participants from Twenty-in-a-Row Test	107
Second Regression Results and Charts for all Participants from Second Experiment	109
Group	109
Participant #1	110
Participant #2	112
Participant #3	114
Participant #4	116
Participant #5	118
Participant #4-2	120

PCA Results from the Second Experiment	122
BIBLIOGRAPHY	124

LIST OF FIGURES

Figure 1:	Process of normalizing blood glucose levels in the body	4
Figure 2:	Treatments for diabetes among adults in the United States	6
Figure 3:	Blood glucose meters	8
Figure 4:	The GlucoWatch and Glucoband blood glucose monitoring systems	10
Figure 5:	The electromagnetic spectrum	13
Figure 6:	Vector Network Analyzer	15
Figure 7:	A two-port network	16
Figure 8:	Probes for use with a dielectric probe kit: (a) actual picture of high temperature probe and (b) a schematic of the probe	18
Figure 9:	Rectangular waveguide	18
Figure 10:	Dielectric constant versus frequency for different biological tissues	23
Figure 11:	Dispersion regions for tissue	24
Figure 12:	a.) Time dependence of ϵ' at 10 kHz in a hamster tail b.) Time dependence of blood glucose in a hamster using a glucose meter	27
Figure 13:	Blood glucose response to an increase in blood glucose measured by a resonant sensor	30
Figure 14:	Blood glucose response to an increase in blood glucose measured by a radiometer	31
Figure 15:	The VNA with glucometer program running	33
Figure 16:	The VNA connected to the microwave glucometer device	33
Figure 17:	Front and rear of the device	34

Figure 18:	Inside of the device showing all connections, power supply, microcontroller board, and force sensor circuit board	35
Figure 19:	FlexiForce sensor	35
Figure 20:	Wheatstone bridge circuit	37
Figure 21:	Voltage window schematic	37
Figure 22:	Completed force sensor and LED circuit board	39
Figure 23:	Tern 586-Engine-P microcontroller board	39
Figure 24:	Model of the thumb film, dry skin, wet skin, fat, blood, and muscle	41
Figure 25:	Top and bottom of sensor board	41
Figure 26:	Graph of varying values for epsilon using the thumb configuration, 0-2 GHz	43
Figure 27:	Graph of varying values for epsilon using the thumb configuration, 3-5 GHz	43
Figure 28:	Standard view and exploded view of thumb guide, sensor, SMA connectors, and metal pieces	44
Figure 29:	Spiral resonant sensor mounted between the metal plate and the Ultem finger guide	45
Figure 30:	a.) The silicon thumb mold and b.) The mold placed over a user's thumb while on top of the resonant sensor	45
Figure 31:	"Soda Test" glucose level versus time	48
Figure 32:	Trace data from the low pressure range	49
Figure 33:	Trace data from the high pressure range	49
Figure 34:	Closer view of null '1' from low pressure data traces	50
Figure 35:	Closer view of null '1' from high pressure data traces	50
Figure 36:	Frequency shift in trace data for low pressure traces	51
Figure 37:	Frequency shift in trace data for high pressure traces	52

Figure 38:	Inverted plot of frequency shift plotted along with the actual measured glucose values for the low pressure traces	52
Figure 39:	Inverted plot of frequency shift plotted along with the actual measured glucose values for the high pressure traces	53
Figure 40:	Chart plotting the predicted values of glucose against the actual measured values of glucose. (Second regression - low)	54
Figure 41:	Chart plotting the predicted values of glucose against the actual measured values of glucose. (Second regression - high)	55
Figure 42:	Histogram of the residuals for low and high pressure data sets	58
Figure 43:	Residuals vs. expected values for low and high pressure data sets	59
Figure 44:	Residuals vs. applied pressure for low and high pressure data sets	59
Figure 45:	Chart Frequency shift of the null for one participant for low and high data sets	63
Figure 46:	Frequency areas for least noisy data sets	66
Figure 47:	Histogram of residuals from PCA regression	69
Figure 48:	Residuals versus applied force from PCA regression	70
Figure 49:	Residuals versus expected glucose values from PCA regression	70
Figure 50:	Composite regression results before outliers were removed (predicted versus actual glucose values in mg/dL)	79
Figure 51:	Composite regression results after outliers were removed (predicted versus actual glucose values in mg/dL)	80
Figure A.1:	Circuit schematic	86
Figure A.2:	Silkscreen view of the circuit board showing pads and part labels	87
Figure A.3:	Circuit board layout showing pads and top copper layer	87
Figure A.4:	Circuit board layout showing pads and bottom copper layer	88
Figure A.5:	Circuit board layout showing top copper layer, bottom copper layer, silkscreen, pads, and part labels	88

Figure C.1:	Chart plotting the predicted values of glucose against the actual measured values of glucose. (Low)	100
Figure C.2:	Chart plotting the predicted values of glucose against the actual measured values of glucose. (High)	102
Figure C.3:	Chart plotting the predicted values of glucose against the actual measured values of glucose. (Second regression - low)	104
Figure C.4:	Chart plotting the predicted values of glucose against the actual measured values of glucose. (Second regression - high)	105
Figure D.1:	Predicted values of glucose versus actual values of glucose for least noisy participants at 1.05 GHz	106
Figure D.2:	Predicted values of glucose versus actual values of glucose for least noisy participants at 2.44 GHz	106
Figure D.3:	Predicted values of glucose versus actual values of glucose for least noisy participants at 3.66 GHz	107
Figure D.4:	Predicted values of glucose versus actual values of glucose for all participants at 0.53 GHz	107
Figure D.5:	Predicted values of glucose versus actual values of glucose for all participants at 0.97 GHz	108
Figure D.6:	Predicted values of glucose versus actual values of glucose for all participants at 2.66 GHz	108
Figure D.7:	Group predicted glucose values versus actual glucose values (mg/dL)	109
Figure D.8:	Participant #1 predicted glucose values versus actual glucose values (mg/dL)	110
Figure D.9:	Participant #1 predicted glucose values versus actual glucose values (mg/dL) after the first difference method was applied	111
Figure D.10:	Participant #2 predicted glucose values versus actual glucose values (mg/dL)	112
Figure D.11:	Participant #2 predicted glucose values versus actual glucose values (mg/dL) after the first difference method was applied	113

Figure D.12:	Participant #3 predicted glucose values versus actual glucose values (mg/dL)	114
Figure D.13:	Participant #3 predicted glucose values versus actual glucose values (mg/dL) after the first difference method was applied	115
Figure D.14:	Participant #4 predicted glucose values versus actual glucose values (mg/dL)	116
Figure D.15:	Participant #4 predicted glucose values versus actual glucose values (mg/dL) after the first difference method was applied	117
Figure D.16:	Participant #5 predicted glucose values versus actual glucose values (mg/dL)	118
Figure D.17:	Participant #5 predicted glucose values versus actual glucose values (mg/dL) after the first difference method was applied	119
Figure D.18:	Participant #4-2 predicted glucose values versus actual glucose values (mg/dL)	120
Figure D.19:	Participant #4-2 predicted glucose values versus actual glucose values (mg/dL) after the first difference method was applied	121
Figure D.20:	Predicted glucose values versus actual glucose values (mg/dL) after PCA was applied	122
Figure D.21:	Predicted glucose values versus actual glucose values (mg/dL) after the first difference method and PCA were applied	123

LIST OF TABLES

Table 1:	Various techniques for non-invasive measurement of glucose using optical methods	11
Table 2:	IEEE acceptable SAR levels for human exposure over the frequency range 3MHz - 6GHz	22
Table 3:	Parameters for use in the Debye equation for modeling certain tissues	25
Table 4:	Blood sugar data from “Soda Test”	48
Table 5:	R Square values from principal component analysis	60
Table 6:	R Square values for each individual participant	61
Table 7:	R Square values from regression at new frequencies	64
Table 8:	Results from PCA	71
Table 9:	R Square values from individual data sets for the second Experiment	72
Table 10:	Regression results from PCA after the first difference method was applied	74
Table 11:	R Square values from individual data sets for the second experiment using the first difference method	75
Table 12:	Comparison of R Square values for PCA on the original data and on the first difference data	76
Table 13:	Comparison of R Square values from individual data sets	77
Table 14:	Comparison results for participant #4	78
Table 15:	PCA comparison results for participant #4	79
Table A.1:	Circuit and device bill of materials	90

Table C.1:	Low pressure and high pressure glucose values and frequencies where the minimum value of the null occurs	99
Table C.2:	Regression output for low pressure data	99
Table C.3:	Residual output for low pressure data	100
Table C.4:	Regression output for high pressure data	101
Table C.5:	Residual output for high pressure data	101
Table C.6:	Low pressure and high pressure glucose values and frequencies where the minimum value of the null occurs after four data points were removed	102
Table C.7:	Regression output for modified low pressure data	103
Table C.8:	Residual output for modified low pressure data	103
Table C.9:	Regression output for modified high pressure data	104
Table C.10:	Residual output for modified high pressure data	105
Table D.1:	R Square values and their corresponding frequencies	106
Table D.2:	R Square values and their corresponding frequencies	107
Table D.3:	R Square values and their corresponding frequencies for the whole group	109
Table D.4:	R Square values and their corresponding frequencies for participant #1	110
Table D.5:	R Square values and their corresponding frequencies after the first difference method was applied for participant #1	111
Table D.6:	R Square values and their corresponding frequencies for participant #2	112
Table D.7:	R Square values and their corresponding frequencies after the first difference method was applied for participant #2	113
Table D.8:	R Square values and their corresponding frequencies for participant #3	114

Table D.9:	R Square values and their corresponding frequencies after the first difference method was applied for participant #3	115
Table D.10:	R Square values and their corresponding frequencies for participant #4	116
Table D.11:	R Square values and their corresponding frequencies after the first difference method was applied for participant #4	117
Table D.12:	R Square values and their corresponding frequencies for participant #5	118
Table D.13:	R Square values and their corresponding frequencies after the first difference method was applied for participant #4-2	119
Table D.14:	R Square values and their corresponding frequencies for participant #4-2	120
Table D.15:	R Square values and their corresponding frequencies after the first difference method was applied for participant #5	121
Table D.16:	R Square values for each participant after PCA was applied	122
Table D.17:	R Square values for each participant after the first difference method and PCA were applied	123

GLOSSARY

2-hour postprandial blood sugar test (2-hour PC) - a test that measures blood glucose exactly 2 hours after an individual eats a meal to determine how food affects the blood glucose level in the body.

active sensor - microwave sensor that provides its own source of microwave radiation to illuminate its target.

ADC - Analog to digital converter

Advanced Glycation Endproducts (AGEs) - result of a chain of chemical reactions after an initial glycation reaction.

attenuation - a decrease in a property per unit area of a wave or a beam of particles, occurring as the distance from the source increases.

bio-electromagnetic resonance - (BEMR) is a technology based on the detection of a change of electrical impedance in the human body caused by an externally applied glucose-specific electromagnetic wave.

c – the speed of light (3×10^8 m/s)

CST Microwave Studio - a microwave modeling software created and distributed by CST (Computer Simulation Technology) abbreviated in this paper as CST.

diabetes mellitus - a disorder of carbohydrate metabolism characterized by inadequate production or utilization of insulin.

dielectric constant - the real part of permittivity, ϵ' .

dispersion region - region of decreasing dielectric constant.

electrochemistry - the branch of chemistry that deals with the chemical changes produced by electricity and the production of electricity by chemical changes.

f - frequency

Fasting Blood Sugar test (FBS) - a test that measures blood glucose after fasting for at least 8 hours. It often is the first test done to check for diabetes.

FDA - United States Food and Drug Administration

ferrocyanide - a salt of ferrocyanic acid usually obtained by a reaction of cyanide with Iron sulphate.

fluorophores - component of a molecule which causes a molecule to be fluorescent.

FR4 - Flame Resistant 4, material typically used for making printed circuit boards with a dielectric constant of 4.

glucagon - a hormone secreted by the pancreas that acts in opposition to insulin in the regulation of blood glucose levels.

glucometer - a medical device for determining the approximate concentration of glucose in the blood.

gluconic acid - a colorless, water-soluble acid obtained by the oxidation of glucose.

glucose - a monosaccharide sugar, $C_6H_{12}O_6$, occurring widely in most plant and animal tissue. It is the principal circulating sugar in the blood and the major energy source of the body.

glucose oxidase - obtained from the fungus, *Aspergillus niger*, it is a dimeric protein with a molecular weight of about 160 kD and is strongly specific for beta-D-glucose (the type of glucose in blood).

hyperglycemia - an abnormally high level of glucose in the blood.

hypoglycemia - an abnormally low level of glucose in the blood.

hysteresis - the lagging of an effect behind its cause.

IEEE - Institute of Electrical and Electronics Engineers

insulin - a polypeptide hormone, produced by the beta cells of the islets of Langerhans of the pancreas, that regulates the metabolism of glucose and other nutrients.

interstitial fluid - liquid found between the cells of the body that provides much of the liquid environment of the body.

iontophoresis - a painless alternative to drug injection in which a weak electrical current is used to stimulate drug-carrying ions to pass through intact skin

IR - infrared, the part of the invisible spectrum that is contiguous to the red end of the visible spectrum and that comprises electromagnetic radiation of wavelengths from 800 nm to 1 mm.

islets of langerhans - irregular clusters of endocrine cells scattered throughout the tissue of the pancreas that secrete insulin and glucagon.

ketoacidosis - acidosis with an accumulation of ketone bodies; occurs primarily in diabetes mellitus.

lancet - a sharp-pointed and commonly two-edged surgical instrument used to make small incisions.

LED - Light Emitting Diode

loss factor - the imaginary part of permittivity, ϵ'' .

microwave - An electromagnetic wave with a wavelength between that of infrared and short waves (1cm to 1m).

minimally invasive method - a method that does not use subcutaneous sampling or sensors in fatty tissue to collect blood but instead uses percutaneous needles or sensors in the dermal layer.

non-invasive method - a method that requires no puncturing of the skin for testing purposes.

open-ended coaxial probe - a contact sensor used to measure the permittivity of a material as a function of a signal reflected by the material.

passive sensor - detects the naturally emitted microwave energy within its field of view.

PC - personal computer

PCA - Principal Component Analysis

percutaneous - pertains to any medical procedure where access to inner organs or other tissue is done via needle-puncture of the skin.

permeability - a measure of the change in magnetic induction produced when a magnetic material replaces air, expressed as a coefficient or a set of coefficients that multiply the components of magnetic intensity to give the components of magnetic induction.

permittivity - a measure of the ability of a material to resist the formation of an electric field within it, equal to the ratio between the electric flux density and the electric field strength generated by an electric charge in the material.

PTFE - polytetrafluoroethylene, a synthetic fluoropolymer with an extremely low coefficient of friction.

Raman spectroscopy - a spectroscopic technique that relies on inelastic scattering, or Raman scattering of monochromatic light, usually from a laser in the visible, near infrared, or near ultraviolet range.

rectangular waveguide - a metal box, open at either one or both ends, that restricts the three dimensional "free space" propagation of an electromagnetic wave to a single dimension in order to measure the permittivity of a material.

reflection - the return of a wave after striking a surface.

relative permittivity - ϵ_r , a unitless ratio of the permittivity of an object to the permittivity of free space.

relaxation - momentary delay in the dielectric constant of a material caused by the delay in molecular polarization with respect to a changing electric field in a dielectric medium.

resonant sensor - a sensor that senses shifts in S-parameters of a material in order to determine the material's permittivity.

Random Blood Sugar test (RBS) - also known as the casual blood glucose test, it measures blood glucose regardless of when an individual last ate.

RS232 - (Recommended Standard 232) is a standard for serial binary data signals connecting between a *DTE* (Data terminal equipment) and a *DCE* (Data Circuit-terminating Equipment).

S-Parameters - scatter parameters, describe the performance of a two-port Network.

$|S_{11}|$ - The response of a sensor at port 1 as a result of a signal input at that port, reflection.

$|S_{21}|$ - The response of a sensor at port 2 as a result of a signal input at port 1, transmission.

SAR – specific absorption rate, is the time rate at which radio-frequency electromagnetic energy is imparted to an element of mass of a biological tissue.

SMA connector - a type of coaxial radio-frequency connector.

stripline - a microwave transmission structure that consists of a trace between two ground planes separated by a substrate.

subcutaneous - situated or lying under the skin, as tissue.

transmission - the broadcasting of electromagnetic waves from one location to another, as from a transmitter to a receiver.

transverse electric waves (TE) - (Transverse Electric) waves that have no electric field in the direction of propagation.

transverse magnetic waves (TM) - (Transverse Magnetic) waves that have no magnetic field in the direction of propagation.

UART - universal asynchronous receiver/transmitter, a piece of computer hardware that translates data between parallel and serial interfaces.

Ultem - a dielectric material with a dielectric constant of 6 at microwave frequencies.

VNA - Vector Network Analyzer, a device used to measure the S-parameters of a microwave circuit over a specified frequency range.

volar - located on the same side of the body as the palm of the hand.

Wheatstone bridge - a measuring instrument used to measure an unknown electrical resistance by balancing two legs of a bridge circuit.

ϵ_0 - the permittivity of free space (8.85×10^{-12} F/m)

ϵ_∞ - the electrical permittivity of a material at very high frequencies

λ - wavelength

τ_n - the time constant for a material used in the Debye equation

ω - angular frequency ($2\pi f$)

ACKNOWLEDGMENTS

Thanks to Dr. Jean for keeping me motivated and always volunteering to contribute a lot of data. Thanks to Dr. Marks for looking at everything from a different perspective and keeping the project interesting. Also, thanks to Brandon for lending me your programming expertise.

DEDICATION

To my parents who, although they didn't understand any if this,
still seemed interested the whole time

CHAPTER ONE

Introduction

Diabetes is a disease that affects 20.8 million people in the United States, with an estimated 6.2 million people remaining undiagnosed. [1] The invasiveness of the testing procedure for diabetes plays a contributing role to the fact that nearly one-third of the population with diabetes goes undiagnosed. It is for this reason that a method for non-invasively monitoring glucose levels is highly desirable for patients with diabetes which would allow for more frequent and possibly continuous monitoring without the pain that is associated with current commercial glucose monitors.

Over the course of the last fifty to sixty years the increase in the uses of microwaves for everyday applications has grown exponentially. Microwaves are used in many applications today, ranging from ground mapping to cell phones, to every type of radar in use. Because microwaves are capable of measuring various parameters inside of a closed volume, through harmless penetration, they have become ideal for advancements in biological measurement applications. Applications of microwaves in the medical field include, and are not limited to, microwave tomography scanning systems, breast tumor detection, RF/Microwave ablation for treatment of cardiac arrhythmias, obstructive sleep apnea and benign prostatic hypertrophy, microwave balloon angioplasty, microwave assisted lipoplasty, and electrothermal arthroscopic surgery. [2]

This research presents a microwave resonant sensor for use in non-invasively measuring the glucose concentrations in a patient through the thumb. The microwave sensor

presented functions as a receiver gathering information from the material with which it is in contact. This ensures that there is no possibility of electromagnetic radiation effects on the body. The aims of this research are to improve on previous designs of a microwave resonant sensor, create a device, for use with a vector network analyzer, to take data from the resonant sensor, implement the use of a pressure sensor, confirm previous results using the ‘Soda Test’, and develop a methodology for creating a calibration algorithm for the microwave non-invasive glucose sensor to help pave the way for future advancements in non-invasive glucose monitoring..

CHAPTER TWO

Diabetes and Glucose

In 2002 the United States spent \$132 billion dollars on diabetes, with \$92 billion stemming from direct medical expenditures and \$40 billion from lost work time, disability, and premature mortality [3]. Because of the seriousness and variability of the disease, regular testing for diabetics is required where number of tests per person vary from one to four times each day. Test strips used in daily testing are relatively expensive, costing around \$1.00 per strip [4]. Over a year of testing at least twice per day, the average patient will spend \$730 on test strips alone. By 2010 an estimated 14.5 million people will be diagnosed with costs near \$156 billion, and in 2020 an estimated 17.4 million people will be diagnosed with costs near \$192 billion [3]. Due to the increase in the population with diabetes and the increase in the costs of diabetes it is fast becoming necessary to develop new ways to test diabetes that are non-invasive, less expensive, and easy to use at home.

Diabetes Mellitus, more commonly known only as diabetes, is “a disease in which the body does not produce or properly use insulin” [5]. There are many types of diabetes that affect different kinds of individuals and are treated in slightly different ways. Type 1 diabetes is the most serious type and affects 5-10% of the diabetic population. It is a disease that “usually develops during childhood or adolescence and is characterized by a severe deficiency of insulin secretion, resulting from atrophy of the islets of Langerhans, and causes hyperglycemia and a marked tendency toward ketoacidosis” [5, 6]. The most common form of diabetes is Type 2 diabetes which affects 90-95% of the diabetes population. This is a

common form that “develops especially in adults and most often in obese individuals and that is characterized from hyperglycemia resulting from impaired insulin utilization coupled with the body’s inability to compensate with increased insulin production” [5, 6]. Type 2 diabetes can be prevented in individuals with pre-diabetes by closely monitoring diet and exercise.

Insulin and glucagon are hormones found in the body that maintain an exceptionally tight range of blood sugar levels in the body. The production of glucagon and insulin by the pancreas is the determining factor in whether or not an individual has diabetes, hypoglycemia, or another blood sugar problem. As shown in figure 1, the level of blood glucose in the body determines whether the pancreas secrete glucagon or insulin. As the blood glucose level in the body rises, the amount of insulin secreted by the pancreas increases, and as the blood glucose level decreases the insulin secretion also decreases.

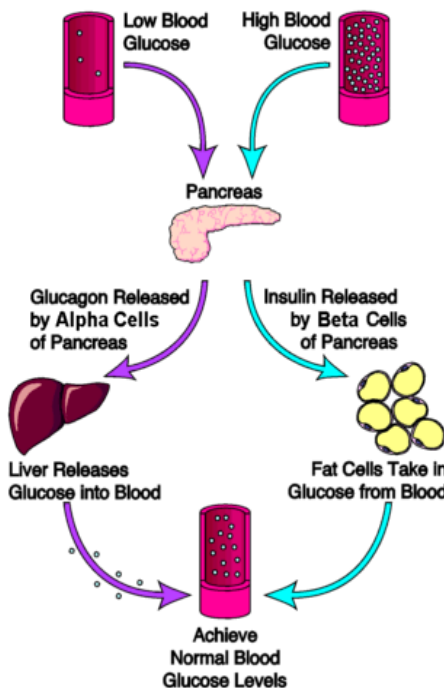


Figure 1: Process of normalizing blood glucose levels in the body [7]

Some cells in the body such as muscle cells, red blood cells, and fat cells absorb glucose out of the blood to lower high blood glucose levels to a more normal range. During periods when blood glucose is low, such as during exercise or between meals, the pancreas secretes glucagon into the body. This secretion affects the liver and causes it to release stored glucose to raise the blood glucose level in the body to a normal range. A normal blood glucose range is from 70 - 110 milligrams per deciliter (mg/dL). Hypoglycemia occurs when the blood glucose level falls below 70 mg/dL, hyperglycemia occurs when the level exceeds 180 mg/dL, and an individual is diagnosed with diabetes when the level exceeds 200 mg/dL after drinking a glucose enriched drink. [7]

Based on death certificate data, 224,092 deaths were attributed to diabetes in 2002. This makes diabetes the fourth leading cause of death by disease in the United States [1]. Many of these deaths result from the complications of diabetes, which include heart disease and stroke, high blood pressure, blindness, kidney disease, nervous system disease, amputations, dental disease, and pregnancy complications.

One factor that increases the mortality rate from diabetes is the lack of treatment. Type 1 diabetics must have insulin delivered by injection or a pump, while most Type 2 diabetics can control their blood glucose through healthy eating, exercise, losing excess weight, and taking oral medication. In statistics for adults with diagnosed diabetes, 57% take oral medication only, 16% take insulin only, 12% take both insulin and oral medication, and 15% do not take either insulin or oral medications. This is shown in the pie chart in figure 2 [1]. Type 1 diabetics typically only test themselves one to two times daily, when somewhere around four to six times is required for proper monitoring. This can result in life-threatening

results due to uneven insulin usage. It is this lack of treatment that is the primary reason for new ideas and developments for non-invasive ways to measure blood glucose levels

Treatment with insulin or oral medications
among adults with diagnosed diabetes—
United States, 2001–2003

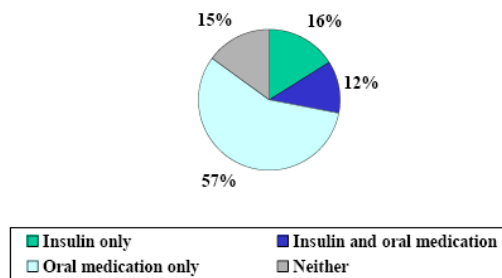


Figure 2: Treatments for diabetes among adults in the United States [1]

CHAPTER THREE

Glucose Testing

Blood sugar tests are used to evaluate blood glucose levels, diagnose or screen for diabetes, and monitor patients who have diabetes. Dietary carbohydrates taken in by the body during eating are converted to glucose in the blood and excess glucose is converted for energy storage. Some cells such as red blood cells and cells in the brain are almost entirely dependent on blood glucose as a source of energy. The brain, in fact, requires that glucose concentrations in the blood remain within a certain range in order to function normally. Concentrations of less than about 30 mg/dL or greater than about 300 mg/dL can produce confusion or unconsciousness [8]. There are three tests used to test for the disease at medical institutions: the fasting blood sugar test (FBS), the 2-hour postprandial blood sugar test (2-hour PC), and the random blood sugar test (RBS). The FBS test is the most commonly used test which measures how the patient's body responds, after fasting for at least 8 hours, to a large amount of sugar into their system. A reading above 139 mg/dL is normal, while a reading above 200 mg/dL is diagnosed as diabetes. Readings in the middle show a potential for pre-diabetes. The 2-hour PC test is done 2 hours after a patient eats to determine how food affects the body's glucose levels. The RBS test is done at random at any point in the day and a reading of 200 mg/dL or more along with other symptoms, such as increased thirst or unexpected weight loss, indicate that the individual has diabetes.

Home glucose tests are used by diabetics, when away from a doctor's office or hospital, to measure the amount of glucose in their blood in order to monitor and regulate

their blood glucose levels. Typically, testing has to be done at least once a day, but may have to be done several times a day for patients that require insulin to maintain their blood glucose level. Testing is done with a special device, often times called a glucose monitor, but other names are glucose meter or glucometer. Various types of glucometers are pictured in figure 3.



Figure 3: This figure shows four different blood glucose meters from 1993 to 2005. Sample sizes taken by the meters vary from 30 to 0.3 μ L and test times vary from 2 minutes to 5 seconds. [9]

Along with home glucose tests is another test done at a medical institution that gives the patient an overview of their average blood glucose levels from the past 2 to 3 months. This test is called an A1C test, but is also known as a glycated hemoglobin test or a HbA1c test. Hemoglobin in the red blood cells links up with sugars, such as glucose. For individuals with diabetes there is more sugar in the blood so more red blood cells glycate with the glucose molecules. The percent of A1C in the blood is an overview of average blood glucose control over the life of the red blood cell, or approximately 120 days. This test should be conducted at least twice a year as a way of determining if a treatment plan is working, a way to show how healthy choices affect diabetes control, and a way to confirm

self-testing results. This test does not replace daily testing using a commercial glucose meter because it does not measure day-to-day control.

All invasive blood glucose monitors require the user to prick a finger, palm, or forearm with a lancet so that a small droplet of blood can be collected. These devices use electrochemistry of the testing strip to determine glucose levels. Each strip contains ten layers of spacers and chemicals, including glucose oxidase and microcrystalline potassium ferricyanide. The blood flows into the strip by capillary action and the glucose in the blood reacts with the glucose oxidase to form gluconic acid. This then reacts with the layer of ferricyanide to form ferrocyanide. The electrode inside of the device oxidizes the ferrocyanide, which generates a current directly proportional to the glucose concentration [10].

Most glucose meters, available for purchase at local drug stores, are capable of reading glucose levels between 0 mg/dL and 600 mg/dL. The ranges vary between meters and the readings are not linear over the entire range, therefore readings that are either very high or very low are open for interpretation and need to be confirmed by repeated measurements or measurements taken by a different meter. [11]

There are several factors, however, that will have an effect on the results of a test with a traditional glucometer: rubbing alcohol, water, or soap from cleaning the testing area intermixing with the drop of blood, the drop of blood being either too small or too large, the blood level being exceptionally high or low, or a wet test strip which is usually caused by humidity [12]. According to the FDA, the goal of all future Self Monitoring Blood Glucose systems should be able to achieve a variability of 10% at glucose concentrations of 30-400mg/dL 100% of the time. With current systems, measurements should be within 15% of

the results of the reference measurements and approximately 50-70% of individuals, who receive some sort of formal training, are capable of obtaining a result within 20% of the reference method [13]. However, the accuracy is greatly decreased when the results are affected by the factors listed previously, thus contributing to the inventions of non-invasive blood glucose monitors that eliminate these factors.

A minimally invasive method is one that does not use subcutaneous sampling or sensors in fatty tissue to collect blood. Instead it uses percutaneous needles or sensors in the dermal layer where there are less nerve endings at sites other than the fingers to collect or react with interstitial fluid or blood. However, there are no FDA approved minimally invasive devices with sensors or sampling probes for continuous monitoring [14]. Non-invasive methods require no puncturing of the skin for testing purposes. Most methods use infrared light sensors which shine light on the skin and measure IR absorption or transmission wavelengths which are specific to glucose. Another sampling technique draws interstitial fluid through virtually intact skin. This method uses reverse iontophoresis to pull out the fluid or lasers to create micropores in the dead layer of skin from which to collect the fluid. Glucose in the interstitial fluid can be correlated with blood glucose, therefore, requiring that calibration be done with a blood sample obtained from finger-stick methods. [14]

There are several types of non-invasive blood glucose monitors for home use that have been proposed, some of which have been approved by the FDA. The Glucoband is a non-invasive glucose monitor that uses bio-electromagnetic resonance to measure the blood glucose levels of the human body. This device is worn like a wrist watch and displays results of the test on an LCD screen within a few minutes. The GlucoWatch system is a device that

is portable and can be worn on the wrist to take glucose measurements throughout the day similar to the Glucoband. This device uses a low electric current that pulls fluid from the skin. This fluid is collected on gel disks and analyzed for blood glucose concentration and then displayed on the screen. Pictures of the GlucoWatch and Glucoband are pictured below in figure 4.



Figure 4: The GlucoWatch and Glucoband blood glucose monitoring systems [15, 16]

Besides the FDA approved blood glucose monitors, several other methods have been addressed and considered. LighTouch, a device patented by Professor Joseph Chaiken, a professor in the Department of Chemistry at Syracuse University, uses Raman spectroscopy to measure the glucose levels in blood. A laser is focused onto the fingertip and the colored light exiting the other side of the finger is analyzed where the different colors exiting the finger represent different quantities and chemicals in the tissue [17].

A prototype device, labeled "Scout", is a non-invasive device that is designed to replace initial diabetes diagnosing methods by making use of "advanced glycation endproducts," or AGEs [18]. The device uses various wavelengths of light on an individual's forearm which causes the AGEs to emit a fluorescent light signature, indicating diabetes risk.

Another technique being researched are optical methods. In optical glucose monitoring a beam of light is focused onto the body, which is then modified by the tissue after transmission through the target area. The absorbed light is due to the chemicals in the skin and the diffuse light escaping the tissue produces a “fingerprint” or an optical signature. Changes in the optical signature such as wavelength, polarization, or intensity of light are used to determine the concentration of glucose in the test area [4]. Table 1 lists various optical techniques and a brief description of each.

Table 1: Various techniques for non-invasive measurement of glucose using optical methods [19]

Near Infrared Spectroscopy (NIR)	Raman Spectroscopy	Photoacoustic Spectroscopy	Scatter Changes	Polarization changes	Mid-Infrared Spectroscopy
Absorption or emission data in the 0.7 to 0.5 μm region of the spectrum are compared to known data for glucose	Laser light is used to induce emission from transitions near the level excited	Laser excitation of fluids is used to generate an acoustic response and a spectrum as the laser is tuned	The scattering of light can be used to indicate a change in the material being examined.	The presence of glucose in a fluid is known to cause a polarization preference in the light transmitted	Absorption or emission data in the 2.5 to 25 μm region are examined and used to quantitate glucose in a fluid

These methods for non-invasive monitoring all remain in the process of study, but there are limitations that exist for each of these methods, as found in Tura *et al.* [20]. Because of the limitations that exist for various methods of non-invasive monitoring, a non-invasive monitoring method that would be available for everyday use by the public is far from realization. Everyday numerous institutions and research organizations use new and different technology in hopes of creating a device that can be used by diabetics everywhere as a daily non-invasive way for measuring their blood glucose levels.

CHAPTER FOUR

Microwaves and Measurement

Microwaves

The electromagnetic spectrum covers a range of frequencies from 0 to 10^{24} Hz, which represent different types of waves and is pictured in figure 5.

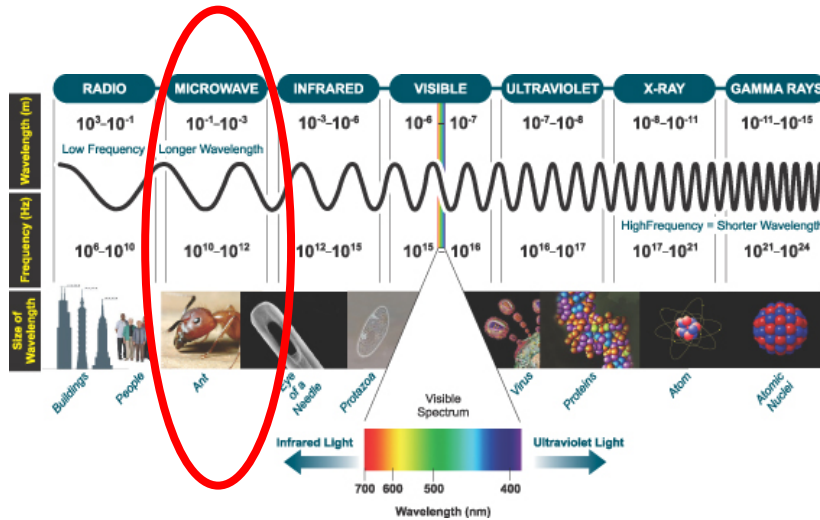


Figure 5: The electromagnetic spectrum

Some of the most common types of waves encountered are radio waves, UHF waves, microwaves, infrared rays, visible light, and x-rays. Each type of wave has a different wavelength and corresponds to a different frequency range in the electromagnetic spectrum. Microwaves occupy the frequencies in the electromagnetic spectrum ranging from 300 MHz to 300 GHz, which is a subset of the radio portion of the spectrum [21].

The wavelengths of microwaves can be determined by the equation

$$\lambda = \frac{c}{f} \quad (1)$$

and are found to be between 1cm and 1m. Because of these longer wavelengths, microwaves are more capable of penetrating through various materials. Most measurement tools used today tend to only be able to measure wavelengths up to 50GHz.

Permittivity and S-Parameters

All materials contain charged particles that, when in contact with electric or magnetic fields, produce secondary fields. The electric and magnetic fields across a material result in conduction, polarization, or magnetization of the particles in that material. Polarization of the particles results in the material acting as a dielectric [22].

When the electric field passes through the dielectric medium, the medium has an effect on the electric field called permittivity (ϵ). Permittivity is essentially the ability of the material to transmit (or “permit”) an electric field and is determined by the material’s ability to polarize its particles under the influence of an electric field [23]. The relative permittivity (ϵ_r) of a material is also called the dielectric constant and is “an experimentally measurable parameter” [22]. The relative permittivity is a ratio of the permittivity of a material to the permittivity of free space.

$$\epsilon_r = \frac{\epsilon}{\epsilon_0} \quad (2)$$

When an electric field is applied across a conducting medium an equation for complex permittivity has to be used.

$$\epsilon = \epsilon' - j\epsilon'' \quad (3)$$

The real part of the complex permittivity is the dielectric constant (relative permittivity) of a material, or the energy storage of that material. The imaginary part is the loss factor, or the amount electric field energy lost when passing through a material [24]. Most biological materials have a permeability close to that of free space, so permeability is not a concern during tests involving blood glucose levels, allowing the tests to focus on the frequency variations of the relative permittivity [25]. Because the dielectric properties of a material are dependent upon its molecular structure, a change in the molecular structure will cause the dielectric properties of the material to change. Measuring the dielectric properties of a material can indirectly measure other properties that have a correlation to the molecular structure of the material. This can be important when the property of interest is difficult to measure directly.

Most measurements involving microwaves and permittivity are taken using a vector network analyzer, or VNA. A VNA is a device that is used to measure the S-parameters of a microwave circuit over a specified frequency range and is pictured in figure 6.

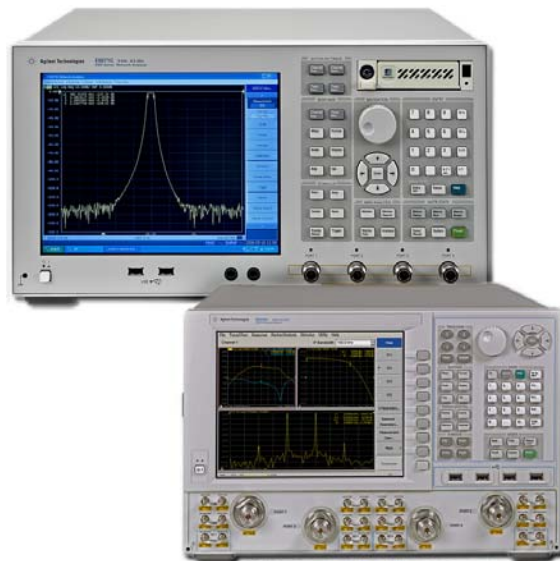


Figure 6: Vector Network Analyzer

S-Parameters, also known as scatter parameters, describe the performance of a two-port network completely. They relate to the traveling waves that are scattered or reflected when a network is inserted into a transmission line with a certain characteristic impedance, and they also represent the linear behavior of a two-port network. $|S_{11}|$ and $|S_{21}|$ are the two parameters of interest in this study and are determined by measuring the magnitude and phase of the incident, reflected, and transmitted signals when the output is terminated in a perfect load. The $|S_{11}|$ parameter represents reflection, which is a response at the port from which the signal was sent out and the $|S_{21}|$ parameter represents transmission, which is a response at the opposite port from which the signal was sent [26]. Figure 7 below represents a two port network.

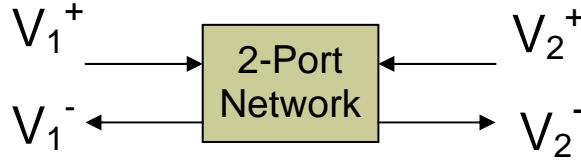


Figure 7: A two-port network

Equations for the S-parameters of a two-port network can then be derived. First is a matrix equation that relates the incoming and outgoing voltage waves:

$$\begin{bmatrix} V_1^- \\ V_2^- \end{bmatrix} = \begin{bmatrix} S_{11} & S_{12} \\ S_{21} & S_{22} \end{bmatrix} \begin{bmatrix} V_1^+ \\ V_2^+ \end{bmatrix} \quad (4)$$

The $|S_{11}|$ parameter represents the input port voltage reflection coefficient,

$$S_{11} = \left. \frac{V_1^-}{V_1^+} \right|_{V_2^+=0} \quad (5)$$

the $|S_{12}|$ parameter is the reverse voltage gain,

$$S_{12} = \left. \frac{V_1^-}{V_2^+} \right|_{V_1^+ = 0} \quad (6)$$

the $|S_{21}|$ parameter is the forward voltage gain,

$$S_{21} = \left. \frac{V_2^-}{V_1^+} \right|_{V_2^+ = 0} \quad (7)$$

and the $|S_{22}|$ parameter is the output port voltage reflection coefficient.

$$S_{22} = \left. \frac{V_2^-}{V_2^+} \right|_{V_1^+ = 0} \quad (8)$$

Measurement Tools

Dielectric probe kits, radiometers, wave guides, and sensors are all types of devices that can be connected to a VNA and used to measure a material's response to microwave energy using S-parameters. Dielectric probe kits are used to measure the complex permittivity of a material. The open-ended coaxial probes, shown in figure 8, feature hermetic glass-to-metal seals, which make them resistant to corrosive or abrasive chemicals and they can also withstand a wide temperature range, allowing for measurements using frequency and temperature [27]. Measurements are typically made by attaching the probe to a probe stand and immersing the probe into liquids or semi-solids. However, it is required that the solid material and the probe maintain a smooth, gap-free contact [27]. This makes it very difficult to measure the permittivity of blood in a non-invasive manner since the human body is not a material that would allow a gap-free contact with the probe. In this case, dielectric probe kits are typically used when a sample of blood outside of the body is available.

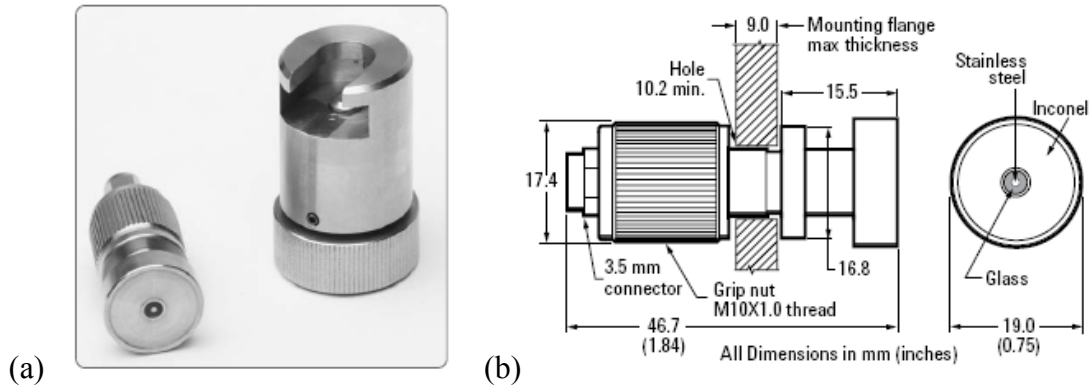


Figure 8: Probes for use with a dielectric probe kit: (a) actual picture of high temperature probe and (b) a schematic of the probe [27]

Another method used to measure the permittivity of materials is the waveguide. A waveguide restricts the three dimensional "free space" propagation of an electromagnetic wave to a single dimension. Waveguides are low loss, which means that the wave can travel along the guide without large attenuation [28]. A rectangular waveguide supports transverse electric (TE) and transverse magnetic (TM) modes which mean that there is no electric (for TE) or magnetic (for TM) fields in the same direction as the propagating electromagnetic wave. The most commonly used type of waveguide is the rectangular waveguide, shown in figure 9.

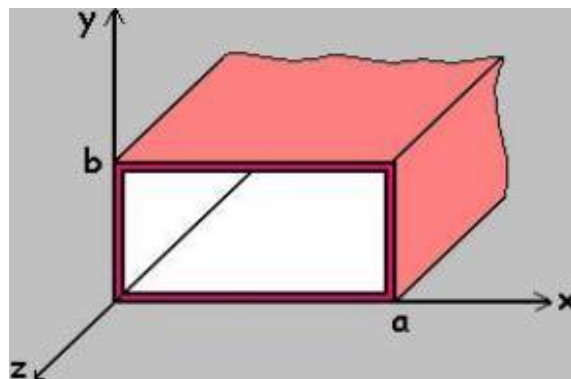


Figure 9: Rectangular waveguide [29]

A rectangular waveguide is essentially a box built of metal that can be either open-ended or closed on one end. The guiding of waves through the waveguide is accomplished by the bouncing of the waves obliquely between the walls of the guide [22]. A waveguide filled with a dielectric material will have different cutoff frequencies, where no propagation occurs for a certain range of frequencies, for each mode available to the waveguide. These cutoff frequencies will be dependent on the material in the waveguide and the permittivity of the material will be dependent on the cutoff frequency [21]. A VNA can pass a swept frequency signal into a waveguide where it is converted to an electromagnetic wave. When the swept frequencies reach the cutoff frequency of the waveguide, the wave propagates through the guide where it is detected and sent back to the VNA. It is difficult to measure permittivity of a material that is not a liquid or a semi-solid in a waveguide since the object under test would not fill the entire waveguide. This makes a waveguide a poor choice for non-invasively measuring the permittivity of a part of the human body. Also, more simple methods for calculating permittivity from the swept frequencies can only be done at the cutoff frequencies, which would severely limit the results for permittivity since it can depend on many different frequencies. There are complex mathematical models that can calculate permittivity for swept frequencies, but these are very complex and require advanced analysis programs and computers.

Sensors are devices that are ideal to measure blood since they are able to make use of lower frequencies and, therefore, longer wavelengths, in order to better penetrate through the skin and fat layers of the human body. Resonant techniques are capable of accurate measurements at a discrete set of frequencies and have been used for numerous applications in the past, including moisture measurements and sensing solutions. Microstrip patch

antennas and ring resonators have been the most widely used types of resonant sensors in the past, but for this type of application a planar resonant sensor is examined. The planar resonant sensor requires no contact with the material under test and can be placed directly on the body. A resonant sensor works when fringing fields interact with the dielectric that the sensor is constructed from and energy is coupled into it. This coupled energy causes a shift in the resonant frequency of the sensor where the shift is dependent on the relative permittivity of the material under test [30]. As the permittivity of the material changes a change can be seen in its S-parameters, which is either a peak or valley in the frequency response, corresponding to the sensor's resonant frequency. Because of the multi-frequency response characteristic of a microwave resonant sensor it is capable of isolating a response from one specific parameter in an environment where many parameters can change [31]. A resonant sensor is also able to obtain useful information from both the reflection and transmission of the signal. There are two parameters that contain useful information when using a resonant sensor: $|S_{11}|$ and $|S_{21}|$. Sensor configuration is based on the shift in the $|S_{11}|$ and $|S_{21}|$ parameters from a known change in the load permittivity [26].

CHAPTER FIVE

Microwaves and the Body

Uses of Microwaves in Biological Applications

Microwaves are present in society today more than ever before. They can be found daily in use with cell phones, radars, wireless internet connections, and satellite communications. Also, many new medical procedures are making use of microwave technology. Because of the increased use of microwaves in daily life the issue of human exposure to this radiation has been a concern for a number of years. Most recently, the main concern has been with the amount of exposure from constant use of cell phones. This radiation is measured in SAR, which is the specific absorption rate or the time rate at which radio-frequency electromagnetic energy is imparted to an element of mass, of a biological tissue. All devices that are designed and approved for use have to meet stringent standards concerning SAR levels that make the devices harmless to human tissues. According to the Institute of Electrical and Electronics Engineers standards there are different acceptable SAR levels for whole body or partial body radiation, which are dependent on the environment in which the radiation is taking place. These standards for exposure between 3MHz and 6GHz can be found in Table2 [32].

Microwaves are becoming more commonly used in medical technology today. There are many different uses for microwaves, including the areas of tomography, therapeutic medicine, and thermography.

Table 2: IEEE acceptable SAR levels for human exposure over the frequency range 3MHz - 6GHz [32]

Type of Environment	Whole Body Exposure	Partial Body Exposure	Wrists, Ankles, Hands, and Feet Exposure
Controlled Environment	0.4 W/kg	8 W/kg	20 W/kg
Uncontrolled Environment	0.08 W/kg	1.6 W/kg	4 W/kg

Tomography is a way of using microwaves for two-dimensional or three-dimensional imaging. For three-dimensional imaging it uses numerous transmitters arranged along a vertical line with a receiver rotating around the object being imaged. Some applications of tomography also have the object rotating on its own axis. Waves are transmitted through the object and received by the antennas, which are then used to reconstruct the object formation using spatial distributions of the dielectric constant. Two-dimensional imaging techniques are used in breast cancer detection where multiple transmit/receive antennas are used with multiple channels. Correlations are observed between the dielectric constant and radiographic density [2].

In therapeutic medicine microwaves have been used in thermal procedures for patients suffering from loose shoulder joints, back pain, and liver cancer. Microwaves are also being used as ablation for treatment of cardiac arrhythmias and benign prostatic hypertrophy since microwaves have better penetration depth and can better target and heat the tissue that needs treatment [2]. Diathermy is a technique used for muscle relaxation and is a method for heating deep tissue electromagnetically through induction.

Thermography is a type of imaging that detects radiation in the infrared range of the electromagnetic spectrum. Infrared radiation is emitted by all objects based on their temperature. The amount of radiation increases with temperature so therefore, thermography

allows one to see variations in temperature. Thermography has been most commonly used by the military and secret services, but has found a new use as a method for medical imaging [33].

Microwaves in medical applications have been making large steps in recent years since microwave technology, like ultrasounds, allow doctors to see inside of the body without the ionizing radiation found in x-rays. To better understand how microwaves can be used in medical applications it is important to understand how microwaves affect and interact with the body.

Permittivity and Biological Modeling

The effects of microwaves on biological tissue are dependant on the field in the tissue, or rather the power deposited in a unit mass of tissue. Permittivity of human tissues shows noticeable changes with the change in applied microwave frequency as seen in figure 10 [2].

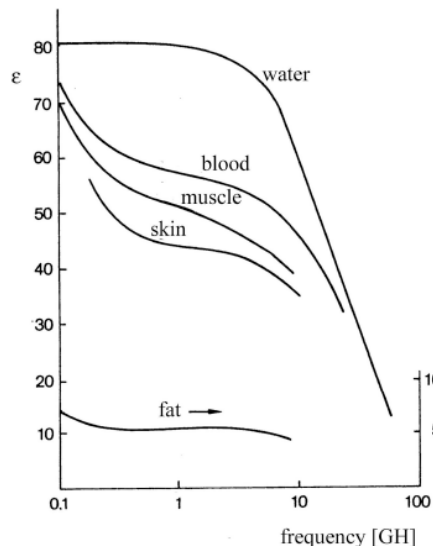


Figure 10: Dielectric constant versus frequency for different biological tissues [2]

Water is the most abundant molecule in the human body and has different content percentages in varying tissues in the body. Permittivity is a property dependant on water content due to the polarization of the water molecules in the presence of an applied electromagnetic field. An increase in the frequency of the applied field causes the molecules to line up slower than is required and some of the energy is stored in the tissues. Thus the tissues do not ‘permit’ all of the energy to pass though and the permittivity decreases with increasing frequencies [21].

The real part of relative permittivity drops off in distinct steps as the frequency increases; therefore, it experiences something called dispersion, which is reflected in figure 11 [25]. Each dispersion region occurs at different frequencies and represents different effects of electromagnetic waves on the body.

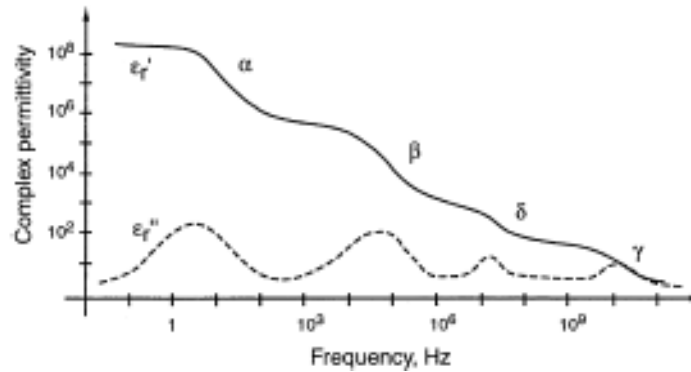


Figure 11: Dispersion regions for tissue [34]

The α dispersion region is associated with interfacial polarizations as a result of Maxwell-Wagner relaxation caused by cell membranes building up charge. As the charge builds up the cell membrane acts like a short circuit and β dispersion occurs. δ dispersion is a weak relaxation that occurs as bound water forms around cells. At the end of δ dispersion the dielectric constant begins to appear like that of water since water is the most abundant

dielectric material in tissues. The next dispersion region, γ dispersion, occurs at the relaxation frequency of bulk water in the tissues. [2, 34]

Each dispersion region is the manifestation of a polarization mechanism characterized by a constant τ which gives the Debye equation relating complex relative permittivity as a function of angular frequency.

$$\hat{\epsilon}(\omega) = \epsilon_{\infty} + \frac{\Delta\epsilon}{1 + j\omega\tau} \quad (9)$$

Since biological tissues are complex in both structure and composition, distribution parameters have to be taken into account. As a result the second order Debye equation is formed,

$$\hat{\epsilon}(\omega) = \epsilon_{\infty} + \sum_n \frac{\Delta\epsilon}{1 + j\omega\tau} \quad (10)$$

which can be used, along with the parameters given in table 3, to predict the dielectric behavior of a tissue. Models for biological tissues were created for simulation in CST, where the parameters in table 3 were used to determine the permittivity of the models [35]. Data found from simulations involving this model are presented in Chapter 5.

Table 3: Parameters for use in the Debye equation for modeling certain tissues [35]

Type of Tissue	ϵ_{∞}	$\Delta\epsilon_1$	τ_1 (ps)	$\Delta\epsilon_2$	τ_2 (ns)	$\Delta\epsilon_3$	τ_3 (μ s)
Blood	4.0	56	8.38	5200	132.63	0.0	0.00
Fat	2.5	9	7.96	35	15.92	3.3×10^4	159.15
Muscle	4.0	50	7.23	7000	353.68	1.2×10^6	318.31
Skin (Wet)	4.0	32	7.23	1100	32.48	0.0	0.00
Skin (Dry)	4.0	39	7.96	280	79.58	3.0×10^4	1.59

Previous Studies

There has been little work done in the area of blood glucose and permittivity correlations. Because of this there is minimal research, but the research that has been done suggests that a correlation exists between blood glucose and permittivity. The following studies used microwave measurement techniques other than a resonant sensor to measure the permittivity and relate it to blood glucose concentration.

Ismail *et al.* [36] conducted a study in which they used a wave guide to measure the permittivity of blood samples in Plexiglas vials. The authors measured the $|S_{11}|$ and $|S_{21}|$ parameters of the vials containing blood and used one of their previous methods for determining the permittivity. They concluded that the measured and calculated values for the human blood were in agreement.

In Nikawa *et al.* [37] the authors conducted a study in which they placed glucose solutions of varying concentration into a thin acrylic resin container where an open-ended coaxial probe (dielectric probe kit) in conjunction with a VNA was implemented to measure the permittivity of the solutions. Here the authors obtain results of permittivity for given glucose concentrations and conclude that there is a possibility for non-invasive measurement of blood sugar.

Park *et al.* [38] measured the correlation between blood glucose and permittivity using an impedance analyzer. A new needle-type sample cell was pinned on the tail of a hamster and the permittivity was measured. Comparisons were done using a commercial glucose meter typically used by diabetes patients. The authors provide graphs, shown in Figure 12, that show a non-linear relationship between glucose and permittivity. In conclusion, the authors state that the “blood glucose of a hamster and the dielectric constant

values of a hamster's tail were the same as time goes on. Indirectly this indicates that the value of the relative permittivity is correlated with the value of blood glucose.” [38]

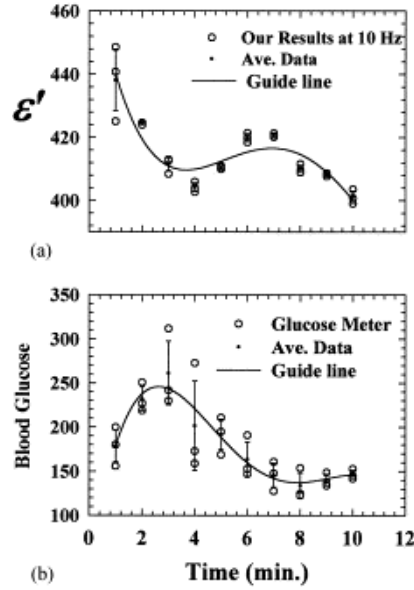


Figure 12: a.) Time dependence of ϵ' at 10 kHz in a hamster tail
b.) Time dependence of blood glucose in a hamster using a glucose meter [38]

A study conducted by Borges *et al.* [39] used a polymetric waveguide as an optical bio-sensor. In this study, a structure called an Anti Resonant Reflecting Optical Waveguide (ARROW) was used for measurement. The change in glucose concentration of a blood sample was represented as a change in the index of refraction of the same blood sample. Through this change the optical field in the first guide is perturbed and, as a result, energy is coupled to the second guide where the glucose concentration is proportional to the power output of the second guide. The simulation results of this study showed a percentage of optical power variations relative to input power that are indicative of this device being nearly twice as sensitive as conventional device architectures. The authors also state that redesigning the structure for a longer wavelength could further enhance the device sensitivity.

Caduff *et al.* [40] presents a non-invasive continuous glucose monitoring system using dielectric spectroscopy for use in a frequency range from 1 to 200 MHz. Dielectric spectroscopy is a way of measuring the impedance pattern of the material under test. The device in this study is roughly the size of a wristwatch, which holds an open ended resonant sensor circuit to the skin for measurement. The authors select the range of 1 to 200 MHz because it stays inside of the β -dispersion region allowing for a better retention of sensitivity without encountering problems with electrode polarization from the α -dispersion region. Results are based on the shift of the resonant frequency (a null at a specified frequency) of the sensor which they conclude changes with glucose concentrations. In the end, it is determined that it is potentially viable to create a non-invasive sensor using this method, but the experiments conducted were met with limited success.

CHAPTER SIX

Design of a Microwave Glucometer

Basis for Project

This project stems from the work done previously by Eric Green [41], concerning the design and implementation of a microwave resonant sensor for non-invasive blood glucose monitoring. The conclusions, concerning the correlation to blood glucose concentrations in Mr. Green's study, stemmed from one test, the soda test. This is a test in which sugar was added to the body by ingestion of a high sugar drink, after fasting, to see if the microwave sensor could detect a change in the frequency maximums over a given time period. The experiment used pulsed frequencies sent through a sensor on the arm to take measurements of the $|S_{21}|$ parameter. As can be seen in figure 13, the frequency maximums over time of the $|S_{21}|$ parameter change with the addition of glucose into the body.

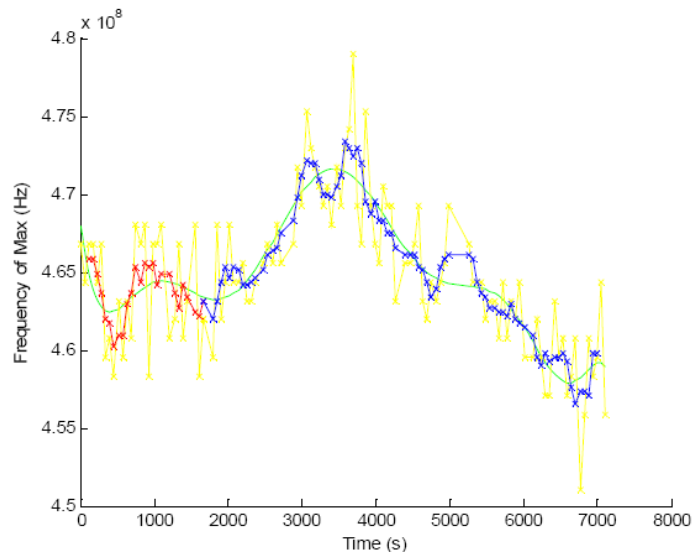


Figure 13: Blood glucose response to an increase in blood glucose measured by a resonant sensor [41]

This showed that the permittivity of the body changes with the addition of glucose into the body, which most likely means that there was a change in the blood permittivity. In other words, there is a possibility that a microwave sensor can be designed and calibrated to use as an instrument for non-invasively determining blood glucose concentrations in the body. One main concern with this test, though, is that there are no actual glucose values to correlate with the frequency shifts.

As an experiment in another thesis, written by Laura Ballew [42], another soda test was conducted, except that it was done using a radiometer instead of a resonant sensor. Radiometers are devices that use passive sensing, whereas other devices, such as radar in aircraft or spaceships, use active sensing.

A radiometer can measure the power in electromagnetic radiation and can be applied to detectors operating any wavelength in the electromagnetic spectrum. Radiometers detect noise-like radiation which can then be used to determine a material or an object's microwave properties. These devices are very sensitive and useful since they can detect many of the frequencies and intensities that a material or object emits. In the soda test the user drank a high sugared soda a few minutes into the test and obtained readings from the radiometer over a period of an hour and a half. As can be seen from the results in figure 14 there is an increase in the radiation emitted from the body shown by an increase in the voltage output. This is indicative of the body's radiation changing as the permittivity in the body changes. Therefore it is also concluded from this experiment that the changes of permittivity in the body are coordinated with changes in the body's blood glucose level. However, there are still no actual values of glucose to correlate with the voltage output of the radiometer.

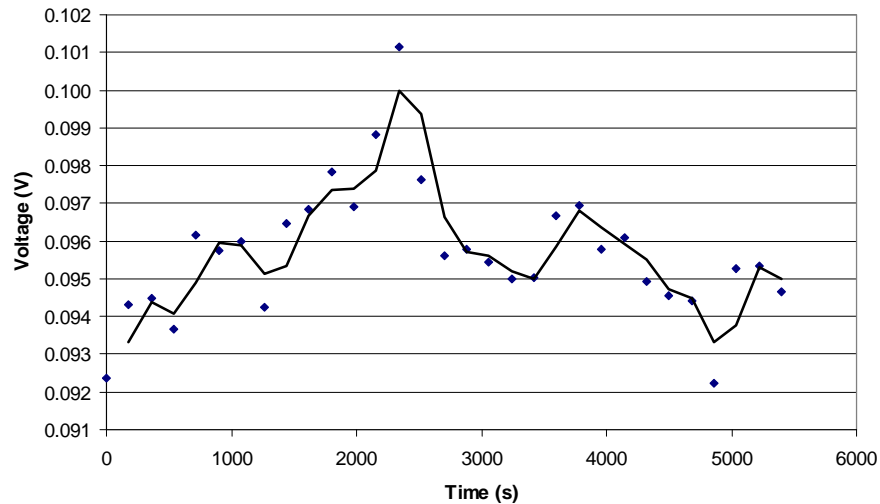


Figure 14: Blood glucose response to an increase in blood glucose measured by a radiometer [42]

Improvements for a New Resonant Sensor

Results of the test conducted by Mr. Green provide data that point to the capability of creating a device to non-invasively measure blood glucose concentrations. The first goal of this thesis was to improve upon the previous microwave sensor design and build a device that is simple for the user. The device designed here captures and saves data from the microwave sensor using an Agilent E5071B VNA which then can be taken and analyzed in order to determine if a calibration algorithm for the sensor is possible.

Before starting this study, however, more tests were run using the existing microwave sensor. During many tests and after much data processing, it was found that the original sensor design and its method of use faced many possible errors during a test. The first concern was of the area of the body used in testing. Although the volar side of the wrist does allow for less fat and increased blood flow, it is difficult to position the sensor in the same place for each test, therefore, creating a situation where the results of the tests are affected by the position of the sensor on the body. Therefore, it was decided to create a sensor that can be used with the thumb.

Another error, which was of greater concern, was the amount of pressure applied to the sensor. As an individual applies more pressure to the sensor, the area contact between the thumb and the sensor increases and the amount of blood in the thumb over the sensing area spreads out. As a result, the trace data from the VNA had a possibility of varying when the applied pressure varied. However, with the original resonant sensor design this theory of varying applied pressures could not be tested. Also, movement of the thumb from side to side had a noticeable effect on the frequency shift as well as amplitude changes in the trace data. Therefore, an Ultem thumb guide is created and attached to the sensor, thereby limiting thumb placement and movement on the sensor. Also, a mold is created for each user that virtually eliminates any thumb movement on the sensor.

The last main error concerned the cables connecting the sensor to the VNA. On the original resonant sensor the cables were physically soldered to the sensor board and the opposite end was connected directly to the VNA. The solder connection between the cable and the board proved to be crude and unstable after many uses and the cable wire started to fray, becoming separated from the sensor. Therefore, several connectors need to be used and bolted to the device in order to eliminate movement of the cables during use.

All of these factors were taken into consideration in the final design of the device. It is designed to be concealed inside of a metal enclosure with the microwave sensor protruding from the front. LED lights on the front of the enclosure and a user program from the VNA provide the user with feedback from the device. Ports on the rear of the enclosure are used for secure connections to outlet power, the VNA, and a computer. To use the device one merely has to open a program on the VNA, start the program, and press their thumb to the microwave sensor at two different pressures, following the directions and feedback provided

by the program. The device makes taking data fast and simple, and it removes much of the error that was encountered when using the original standalone resonant sensor. The pictures in figures 15 and 16 show the VNA with the glucometer program running and the glucometer device connected to the VNA.

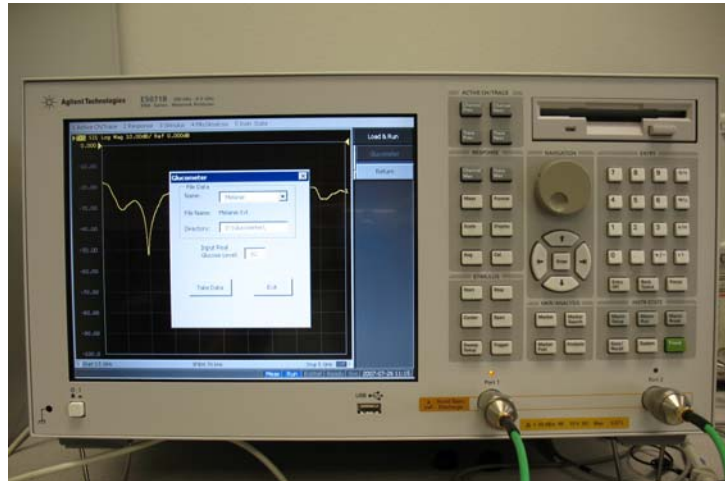


Figure 15: The VNA with glucometer program running

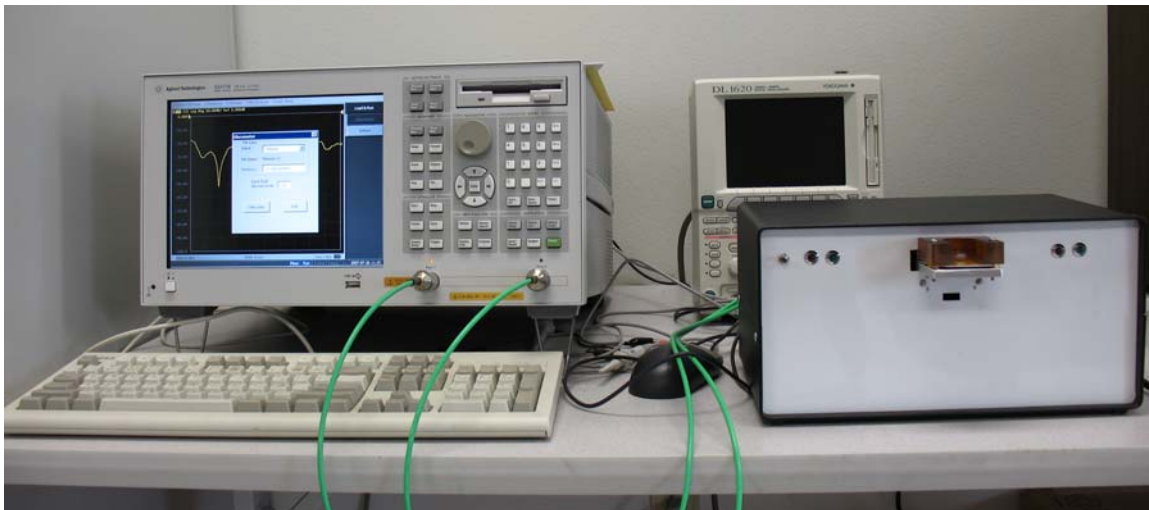


Figure 16: The VNA (left) connected to the microwave glucometer device (right)

Designing and Creating the Device

The Enclosure

The enclosure selected to house the power supply, microcontroller board, force sensor and LED board, the resonant sensor hardware, and all interconnecting wires is an aluminum rack enclosure that consists of a front, back and two side panels for easy assembly and access. There are ventilation holes in the rear panel for air flow to the power supply, which is mounted inside to the bottom of the enclosure using aluminum standoffs. The power supply is a Condor HAD12-0.4-A+ with both positive and negative 12 volt outputs at 0.4 amps, which is required for operation of the LM324 amplifier found in the circuit. At a size of 4.80 x 4.00 x 2.25 inches and a weight of 2 pounds, the power supply is small enough to be mounted inside of the enclosure. Along with the power supply, the microcontroller board, the force sensor, and the LED circuit board are also mounted in the same fashion. Four LEDs, a power on/off switch, and the resonant sensor are all mounted on the front of the enclosure with two SMA connectors, a power cord socket, and two RS232 serial ports mounted in the rear. Figures 17 and 18 show the front and rear of the device, as well as a view of all internal parts and connections.



Figure 17: Front (left) and rear (right) of the device

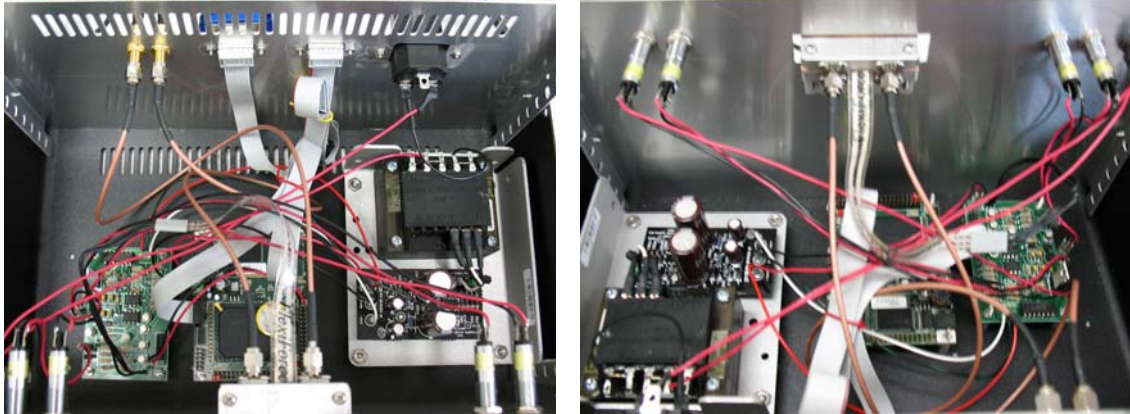


Figure 18: Inside of the device showing all connections, power supply, microcontroller board, and force sensor circuit board

FlexiForce Sensor

The force sensor from Tekscan, Inc. is a lightweight, thin, flexible printed circuit that can measure forces up to 1000 lbs. A FlexiForce sensor with a force range of 0-25 lbs. was sufficient for this application. The active sensing area consists of a 0.375 inch diameter circle on the end of the sensor. Each sensor consists of two layers of a polyester film substrate. On top of one of the substrate layers is a layer of thin conductive silver material and a layer of pressure sensitive ink. The two layers of substrate are glued together with an adhesive with the silver material extending from the sensing area to the connectors at the opposite end of the sensor. (See figure 19).



Figure 19: FlexiForce sensor

The sensors are capable of being trimmed for different lengths, ranging from 2 inches to 8 inches. Inside of a circuit the sensor acts like a variable resistor ranging from 200k Ω to 5M Ω with the latter representing the value for unloaded resistance. As larger pressures are applied to the sensor the resistance decreases. For the sensor to give proper outputs a “puck” must be used so that all of the applied pressure falls inside of and is distributed evenly across the sensing area. A puck is essentially a piece of rigid material that evenly distributes the load over the sensing area. The sensor provides voltage feedback proportional to applied pressure through the microcontroller board. This voltage feedback is used to determine if the glucose readings change with different applied pressures on the resonant sensor. Therefore, this force sensor is mounted directly underneath the resonant sensor so that a force is only applied to the force sensor when a force is applied to the resonant sensor.

Force Sensor and LED Circuit

This circuit was designed to provide feedback of applied pressure to the microcontroller and also to the user with LEDs. A full schematic of the circuit can be found in Appendix A. The first stage of the schematic makes use of a 5V voltage regulator to lower the voltage from the power supply to a range that is acceptable for the Tern microcontroller board. A Wheatstone bridge is used in conjunction with two voltage followers to decrease hysteresis in the signal. The force sensor is used as a variable resistor in the Wheatstone bridge, represented by R_2 in figure 20. When a pressure is applied to the sensor the resistance in that leg of the Wheatstone bridge changes and, as a result, the voltage at the two output points of the bridge, *out1* and *out2*, also changes.

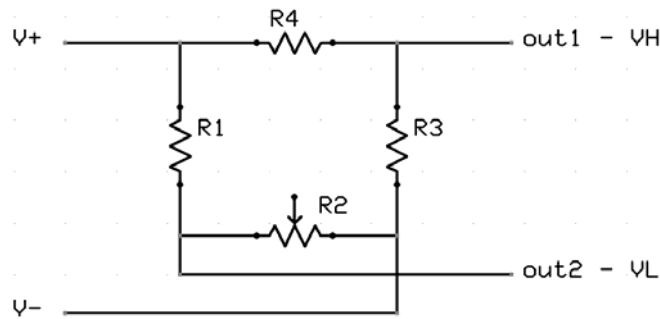


Figure 20: Wheatstone bridge circuit

These two voltages are then sent through voltage followers so that the noise in the signal is drastically decreased. A Wheatstone bridge was chosen instead of a voltage divider on the basis that it is more stable and provides a less noisy output. Next, in this stage of the circuit, is a differential amplifier, which takes the two outputs from the Wheatstone bridge, takes the difference, and amplifies it up. This is done so that the maximum voltage rests at and does not exceed 5V. 5V is the maximum voltage that will be measured because as a pressure is applied to the force sensor, the voltage will decrease as a result of a decrease in the resistance of the force sensor.

The next stage in the circuit uses a voltage window configuration designed with comparators to set a range of voltages that are considered acceptable. (See figure 21)

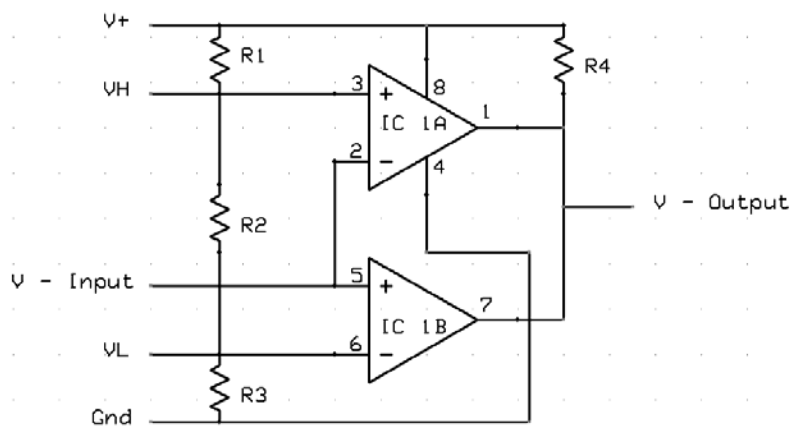


Figure 21: Voltage window schematic

For this application it is desired to have a low pressure range and a high pressure range. Therefore, two voltage windows are needed, one for the low range and one for the high range. The input voltages from the force sensor will be higher for low applied pressures and lower for high applied pressures. The three resistors providing inputs to the comparator are chosen, based on what the desired voltage ranges should be. The following equations are used to determine this range:

$$V_L = I_L(R_3) \quad (11)$$

$$V_H = I_L(R_2 + R_3) \quad (12)$$

$$V_+ = I_L(R_1 + R_2 + R_3) \quad (13)$$

Where V_L is the lower limit on the voltage range, V_H is the upper limit on the voltage range,

V_+ is the voltage from the power supply, I_L is the current through the resistors, and

R_1 , R_2 , and R_3 are the three resistors. When the input voltage is below V_L the output of IC

1A is low and when the input voltage is above V_H the output of IC 1A will also be low.

Therefore, the voltage window exists when both outputs are high. This signal from the voltage window then gets sent through a transistor configuration so that when both outputs are low the red LED is turned on and when both outputs are high the green LED is turned on.

The transistor and LED configuration is identical for the second voltage window stage which is designed for lower voltages representing a higher applied pressure. The completed circuit board can be seen in figure 22. Through use of the Tern microcontroller board the LEDs on the circuit board become obsolete and feedback about the pressure ranges can be sent from the Tern board directly into the VNA program for feedback to the users.



Figure 22: Completed force sensor and LED circuit board

Microcontroller Board

The microcontroller board from Tern, Inc., shown in figure 23, is a complete C/C++ programmable independent controller based on a 32-bit 133 MHz AMD Elan SC520 which supports 32 programmable I/O lines that can be used as general discrete I/O. It also includes two industrial standard 16550-compatible UARTs with RS232 drivers that support baud rates up to 1.152 M baud. A synchronous serial interface on the board is used for bi-directional communication. The 16-bit parallel ADC supports analog signal acquisition from 0-5V at a conversion rate of 1MHz.

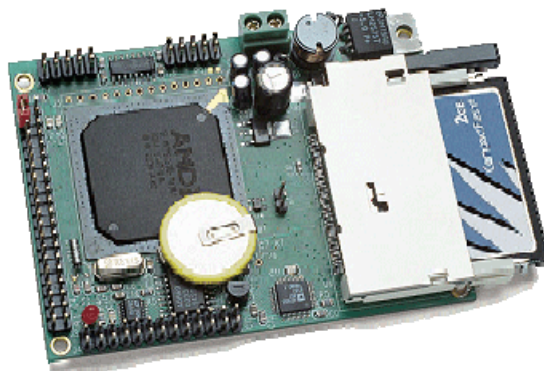


Figure 23: Tern 586-Engine-P microcontroller board

The 586-Engine-P is first programmed through a PC using RS232. After initial programming of the 586, it is capable of interfacing between the force sensor and LED board and the VNA. With the use of the 586 the LEDs, intended for user feedback, are not necessary. This is because the 586 is programmed to acknowledge the voltage ranges from the force sensor circuit and send the information to the VNA which then provides user feedback using words through the glucometer program on the VNA.

Spiral Sensor

The design for a new single spiral resonant sensor is based off of the sensor design by Mr. Green [41]. The previous design was a result of various attempts to design a planar resonant sensor that provided the best frequency shift when materials of varying permittivity were under test. In the end, a sensor was designed with a single circular spiral centered at one end of a stripline board made from FR4 substrate with the transmission lines for connection to the VNA at the opposite end. The details of the sensor construction can be found in Green *et al.* For the new design it was desired that the spiral be redesigned to enable use of the sensor in conjunction with the thumb instead of the wrist. Therefore, it was necessary to create an ovular spiral instead of a circular spiral to ensure that the entire sensing area can be entirely covered by the thumb of a smaller than average person. Using CST and the second order Debye equation, a model of the layers of the body was created so that the simulation of the sensor would provide results consistent with those that would be found when used in conjunction with real human tissue. The model, shown in figure 24, consists of a layer of cover film, a 0.015mm layer of dry skin, a 0.3mm layer of wet skin, a 0.2mm layer of fat, a 0.5mm layer of blood, and a 2mm layer of muscle.

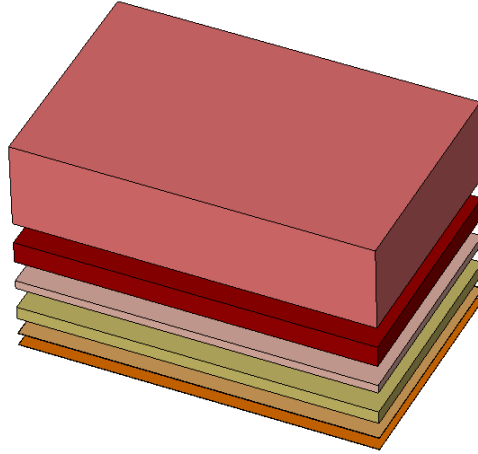


Figure 24: Model of the thumb film, dry skin, wet skin, fat, blood, and muscle

To create the resonant sensor, two separate boards had to be designed. Both boards are made from Rogers RO3000 Series high frequency circuit materials. This material is a ceramic-filled PTFE composite with consistent mechanical properties, regardless of the selected dielectric constant, making them ideal for stripline and multilayer board designs. In this application 0.025 inch RO3006 was selected with a dielectric constant of 6.15 and copper cladding of 2 oz/ft². For the first board, the spiral and half ground plane were etched onto one side with transmission lines on the opposite side. Both sides of the board are shown in figure 25. Holes were drilled through the board so that the spiral on the top side could be electrically connected with the transmission lines on the bottom side.

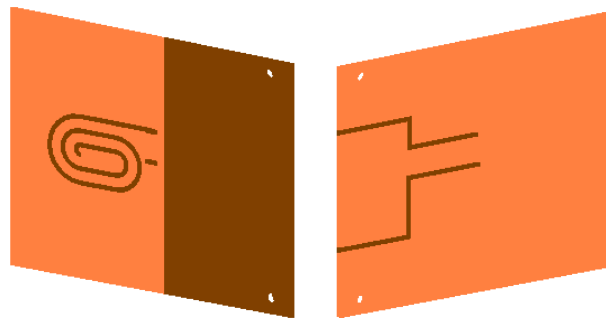


Figure 25: Top of the sensor on the left and the bottom of the top board (the inside) on the right

For the second board, one side was stripped of all copper and the other side retained all of the copper to act as a ground plane. Using Rogers R/flex 2001 bonding film, the two boards were adhered together with the transmission line side of the first board and the non-copper side of the second board in contact with each other. Two SMA tab connectors were soldered to the lines on the first board to ensure a secure mounting to the board before bonding the two boards together. The bonding of the boards with the transmission lines in the middle created a stripline structure. This was ideal to ensure that the waves traveling down the lines into the VNA remain contained before entering the cable attached to the VNA. R/flex 2100 coverfilm was attached to the top of the sensor to add physical protection, which has no effect on the performance of the sensor.

A simulation in CST of this board design in contact with the model designed for the human thumb was implemented using varying values for the dielectric constant of blood over a frequency range of 0 to 2 GHz. As shown in figure 26 the dielectric constant of blood changes causing a shift of the trace in frequency. Noticeably, the shift in frequency is greater as the frequency range increases showing a larger gap between each trace. A different frequency range of 3 to 5 GHz was used in figure 27, which shows an even larger increase in the frequency shift. This could prove to be a useful range because with a larger frequency shift it could, potentially, be easier to determine if the frequency shifts are consistent with changes in glucose as long as there is not an increase in noise in the signal. In the actual implementation of the sensor as glucose levels in the blood change the change in the dielectric constant of the blood will produce a frequency shift in the trace data. Therefore, obtaining trace data in a range of 3 to 5 GHz, where the frequency shifts are larger could prove to enhance the accuracy of the sensor.

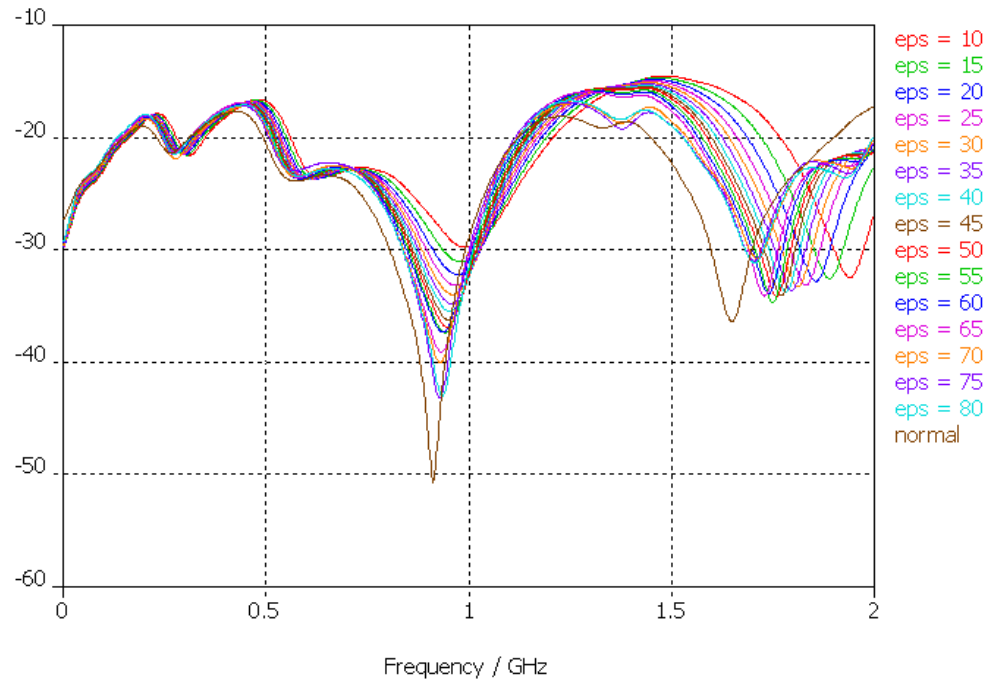


Figure 26: Graph of varying values for epsilon using the thumb configuration. 0-2 GHz

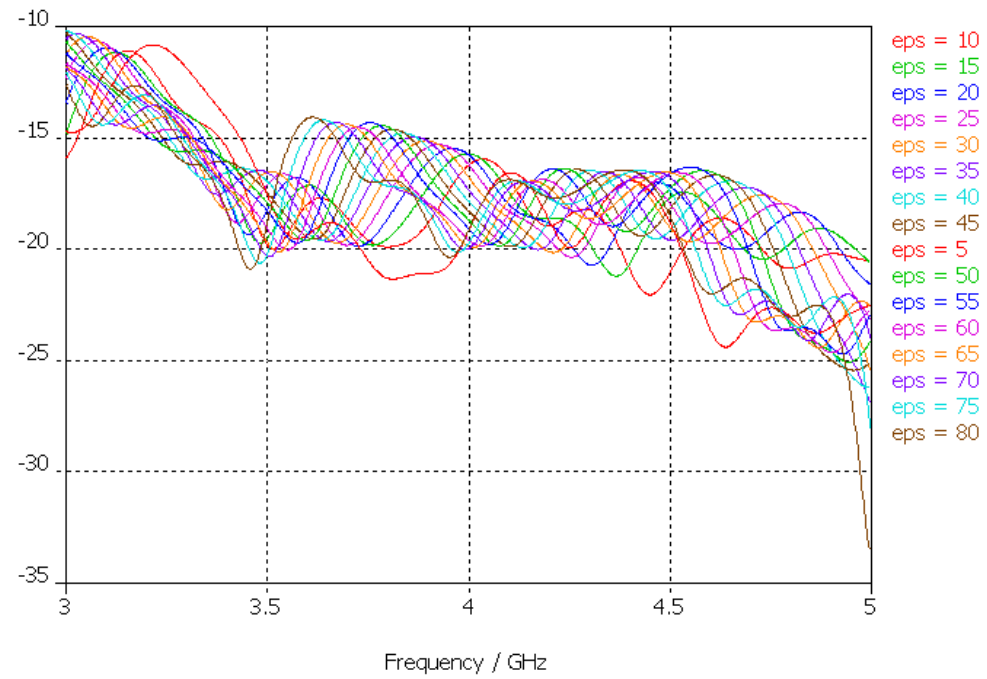


Figure 27: Graph of varying values for epsilon using the thumb configuration. 3-5 GHz

Mounting of the Sensor

In order to ensure that the resonant sensor would not be able to move around during and in between tests and cause adverse effects during the testing process, it had to be mounted onto the enclosure. For mounting the resonant sensor in the enclosure properly, special metal pieces were designed that hold the sensor in place and also connect the ground side of the SMA connector to the ground of the sensor. Two metal pieces were created so that the resonant sensor and the FlexiForce sensor are placed between the pieces. The force sensor was mounted on the bottom side of the resonant sensor, under the center of the spiral, in order for the pressure applied by the thumb to be concentrated directly on the force sensor. Another piece, crafted out of Ultem, was designed as a guide for the thumb and is located on top of the resonant sensor with a cutout for access to the spiral strip. This thumb guide serves to decrease the amount of error due to movement when a user places their thumb onto the spiral area of the sensor. A SolidWorks drawing of these pieces, with the sensor, is shown in figure 28 with an actual picture of the mounted sensor found in figure 29.

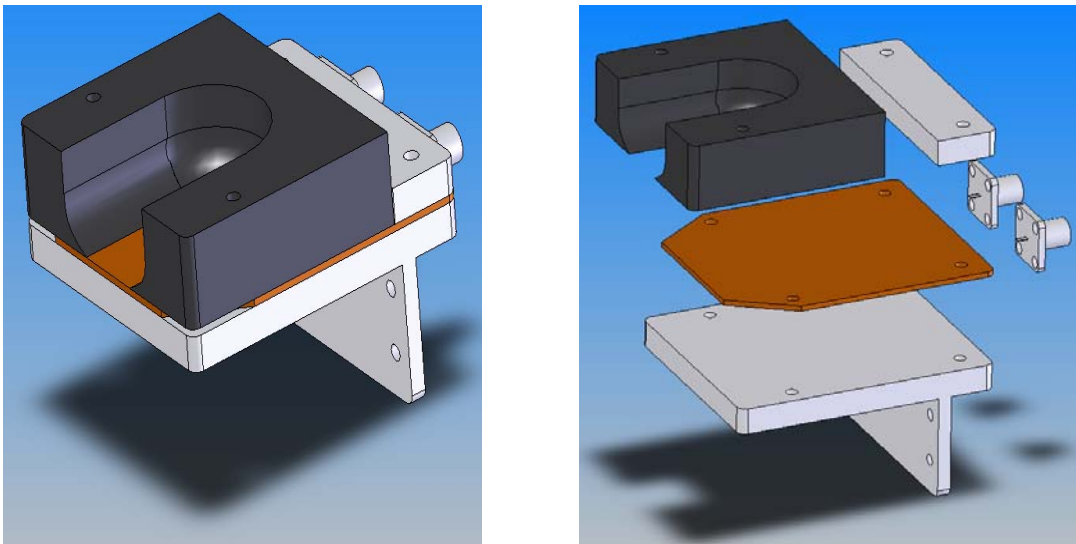


Figure 28: Standard view and exploded view of thumb guide, sensor, SMA connectors, and metal pieces

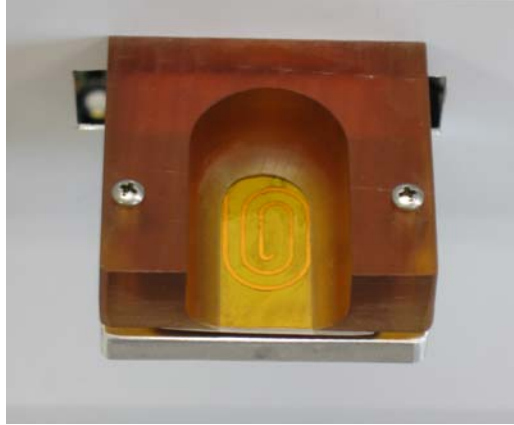


Figure 29: Spiral resonant sensor mounted between the metal plate and the Ulem finger guide

As an additional measure to prevent movement of the thumb on the sensor, a silicon mold was made for each user. The mold was made of equal parts, by weight, of Smooth-On Equinox 35 Fast Set Silicone Putty 1A and 1B kneaded together. This compound was placed over the user's thumb while it is in the guide and pressed down until it filled in all of the empty space on top of the user's thumb. After the putty cured, it was placed over the user's thumb each time a reading is taken by the VNA program. The thumb mold can be seen below in figure 30. This additional molded guide greatly reduces the amount of movement from the thumb and ensures that the user places their thumb in the same place on the sensor in every test.

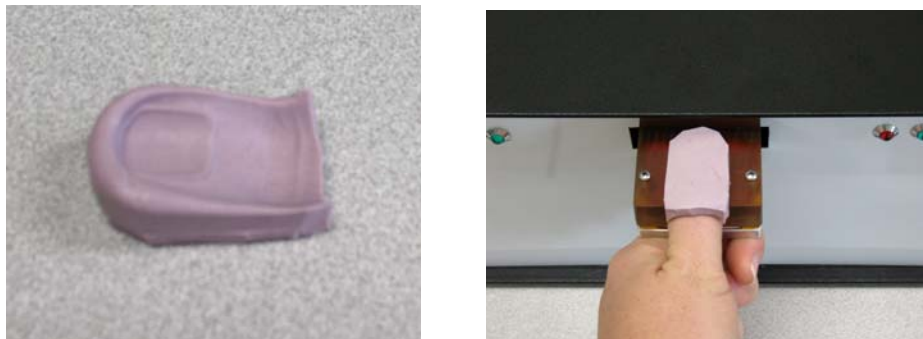


Figure 30: a.)The silicon thumb mold and
b.) the mold placed over a user's thumb while on top of the resonant sensor

VNA Program

The user program, for taking and storing trace data on the VNA, is a Microsoft Visual Basic program and was written directly into the programming interface in the VNA. To use the program, the user loads the program from the Macro Setup menu on the VNA and enters their name and actual glucose level into the provided boxes. The actual glucose level is found using a commercial One Touch Ultra Smart glucose meter which is provided to the users during the test. After this is done the button to start capturing the data is clicked and the user follows the instructions on the screen. It first asks for a low pressure reading. There is a status bar at the bottom of the screen with a smaller box representing the desired pressure range. The user presses their thumb down on the sensor and keeps the status bar inside of the range markings until the VNA captures the data, which takes about 2 seconds. After this data is captured and stored, the program asks for a high pressure reading and the user follows the same steps, except pressing harder until the status bar is kept in between the new range markers and the VNA can capture the data. Each user's name with their entered glucose level, voltage output from their applied pressure, and the date and time is recorded in a text file labeled with the user's name. Each set of trace data is saved to the hard drive on the VNA and is saved with the user's name, the date, and the time that the data was captured. A text document is also saved that contains the date of the test, time of the test, actual glucose level, and a voltage reading representing the pressure applied to the force sensor. The document outlining the steps for using the program and the device can be found in Appendix B.

CHAPTER SEVEN

Studies

Study One – The “Soda Test”

This is an experiment conducted with the sole purpose of determining if the frequency shift in the response of the resonant sensor closely matches the response of the body when a high amount of sugar is introduced. The test makes use of a commercial One Touch Ultra Smart glucose meter, the microwave glucometer designed for this study, and a 20 oz. bottle of soda with a sugar content near 65g. In this experiment the participant drinks the high sugared soda, after fasting for at least 8 hours. In this particular experiment a 20 oz. bottle of Dr. Pepper with 67.5g of sugar was used and the individual conducting the test was also the participant. This test closely resembles the fasting blood sugar test done at a physician’s office where the patient drinks a glucose rich drink, typically 50g of sugar, after fasting, in order to determine how the patient’s glucose levels rise and fall.

To start the experiment the participant tested their blood sugar level twice in 6 minute intervals with the commercial glucose meter. Immediately after taking each sample the participant then took a reading with the non-invasive microwave device. The soda was then introduced to the participant’s system immediately after the first two tests and was ingested as quickly as they could drink it. Following the drinking of the soda, the participant continued to take readings with the commercial glucose meter and the non-invasive microwave device in 6 minute intervals for a period of an hour and a half from the start of the experiment. After an hour and a half had passed the test was concluded and the data was

collected. The times and blood sugar data from the commercial glucose meter are shown in Table 4.

Table 4: Blood sugar data from “Soda Test”

Low Pressure Time (h:mm:ss)	High Pressure Time (h:mm:ss)	Glucose Level (mg/dL)
8:11:27	8:11:36	85
8:17:18	8:17:25	85
8:22:52	8:22:59	87
8:28:22	8:28:34	83
8:34:56	8:35:05	102
8:40:22	8:40:29	113
8:46:54	8:47:02	148
8:52:13	8:52:18	151
8:58:53	8:59:02	129
9:04:25	9:04:33	128
9:10:47	9:10:57	131
9:16:18	9:16:24	127
9:22:28	9:22:36	113
9:28:20	9:28:27	113
9:34:36	9:34:45	109
9:40:27	9:40:33	103
9:46:43	9:46:53	97

Data of the participant’s glucose level versus time from table 4 was plotted in figure 31.

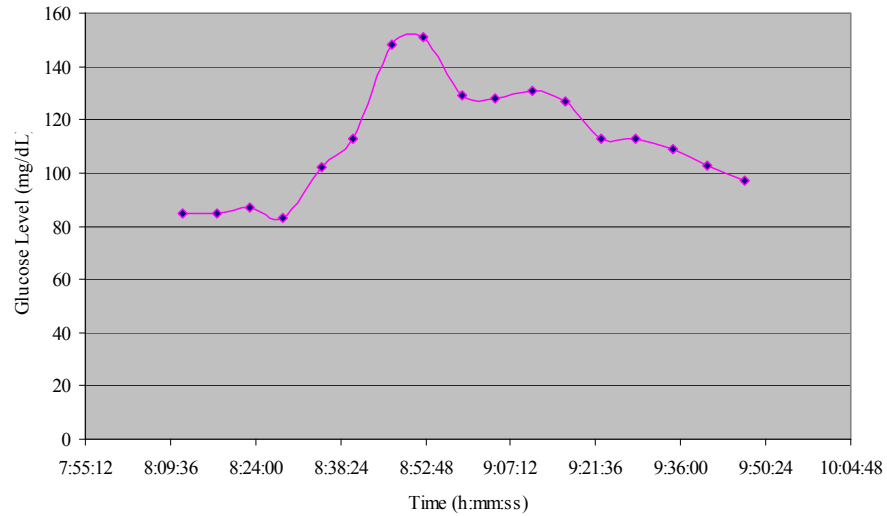


Figure 31: “Soda Test” glucose level versus time

Trace data was collected in two different pressure ranges where the y-axis represents frequency over a range from 3.5GHz to 5 GHz and the x-axis represents the amplitude in dB. (See figures 32 and 33).

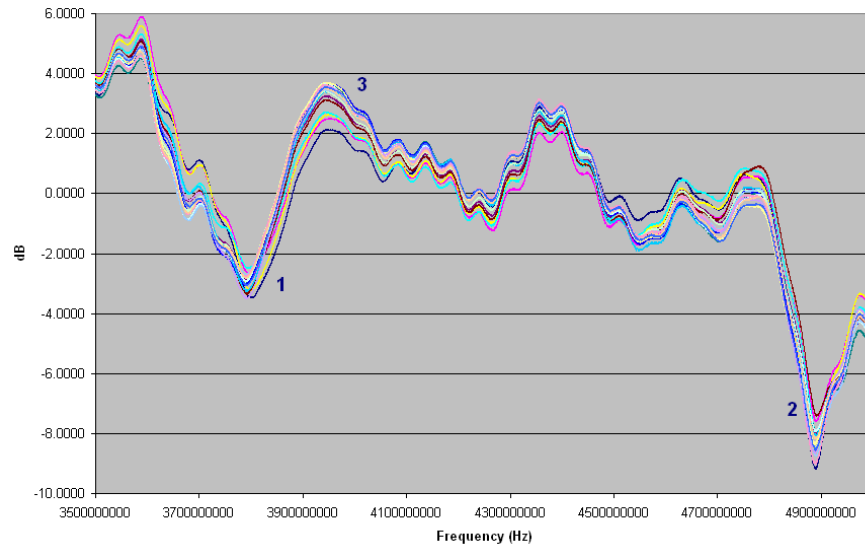


Figure 32: Trace data from the low pressure range

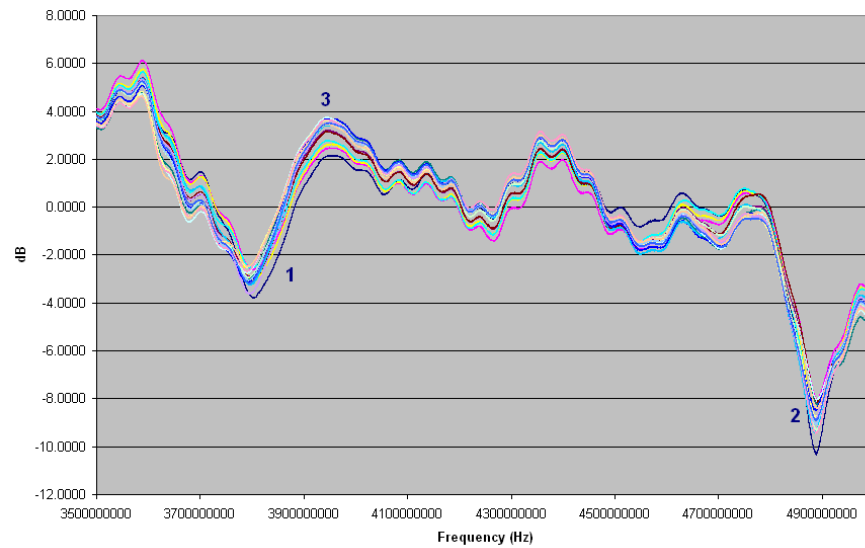


Figure 33: Trace data from the high pressure range

A program was written in Matlab which would find the frequency in each trace where the minimum values at the null labeled with a '1' in figures 32 and 33 occurred. A closer view of the data at this null for each plot is shown in figures 34 and 35.

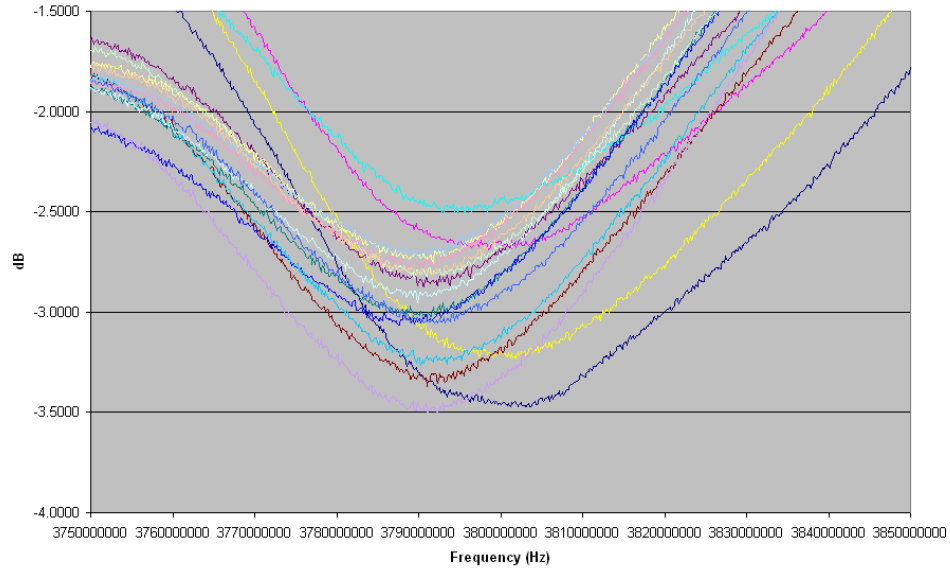


Figure 34: Closer view of null '1' from low pressure data traces

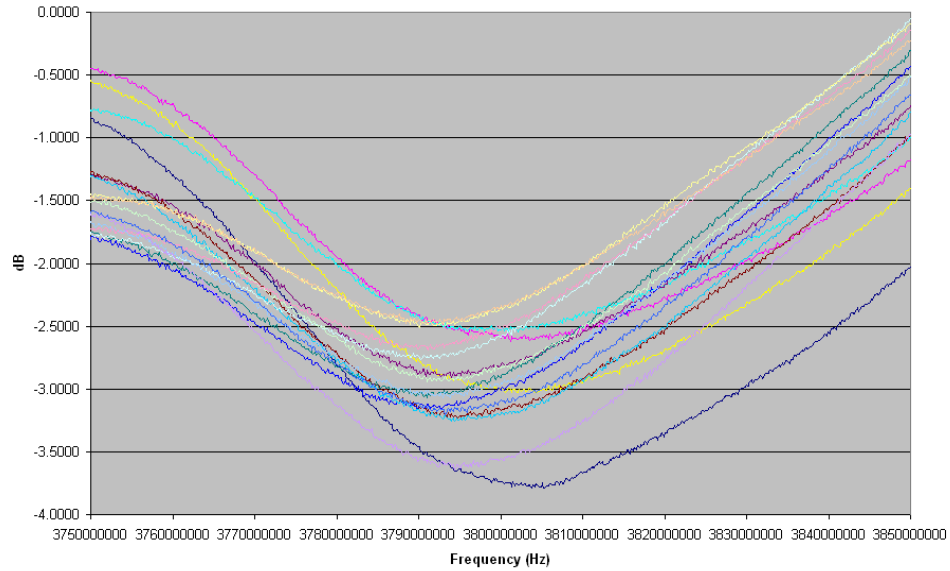


Figure 35: Closer view of null '1' from high pressure data traces

The frequency at which the minimum occurred for each trace was found and is plotted versus time in figures 36 and 37. According to the table of glucose values, the frequency shift in the trace data should show an increase followed by a slow decrease, but instead it shows a decrease followed by a slight increase. It can be noted here that as the glucose values increase, the frequency does not increase, but rather decreases, which is indicative of an inversely proportional relationship between the frequency shift and actual glucose values. This is due to the fact that a null was used instead of a peak. In the first ‘soda test’, conducted by Mr. Green, it was found that the frequency shifted up as the glucose levels increased when the maximum was tracked at a peak. This is expected because the wavelength of the signal changes as a result of a change in the dielectric constant of the material. The dielectric constant changes with respect to the glucose levels in the blood, causing the wavelength of the signal to change, which in turn causes a frequency shift to the left in a minimum and a frequency shift to the right in a maximum.

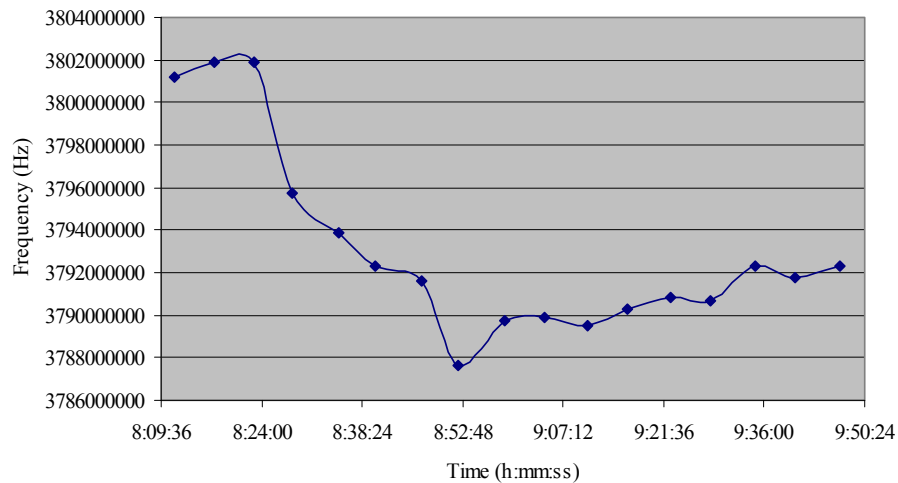


Figure 36: Frequency shift in trace data for low pressure traces

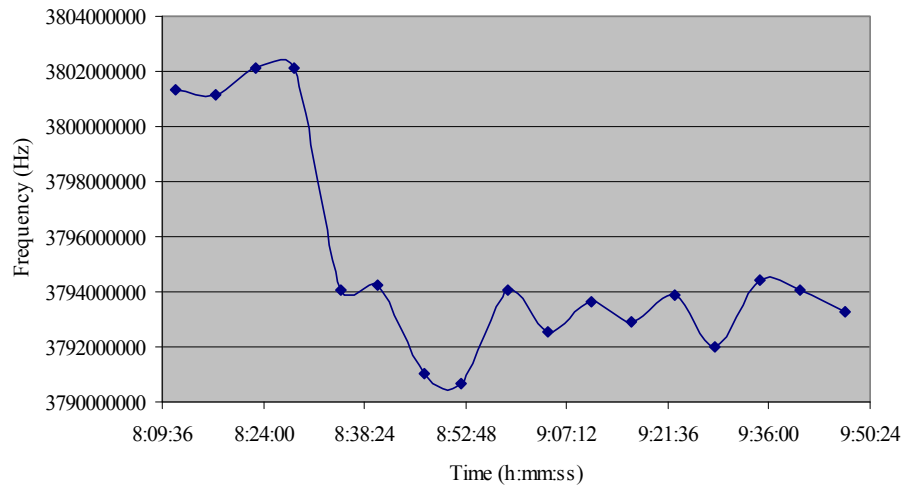


Figure 37: Frequency shift in trace data for high pressure traces

After the data was inverted, it was plotted with the actual glucose values on a secondary axis and plots like those shown in figures 38 and 39 were created. From these plots it is visually obvious that there is a correlation between the shift in frequency of the data and the actual glucose level.

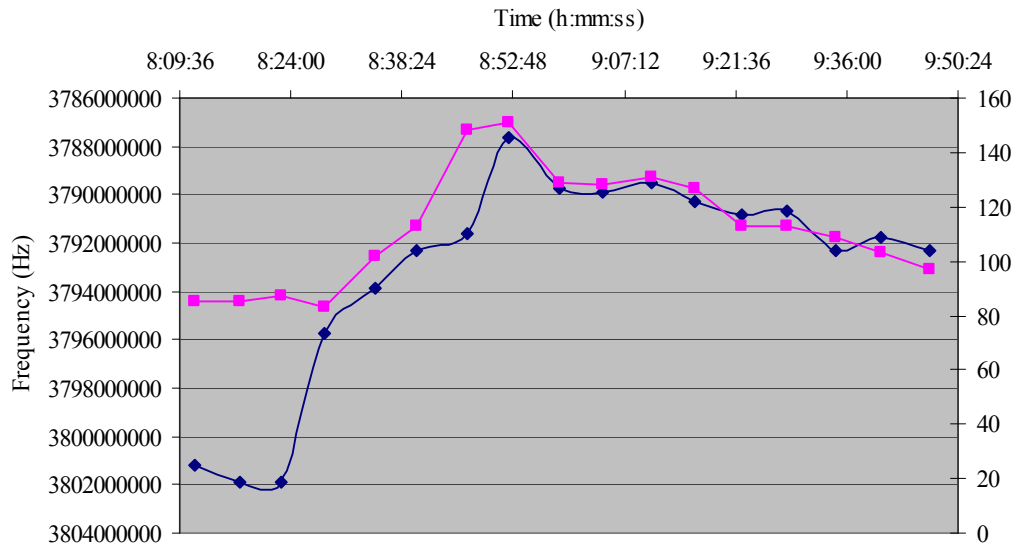


Figure 38: Inverted plot of frequency shift plotted along with the actual measured glucose values for the low pressure traces

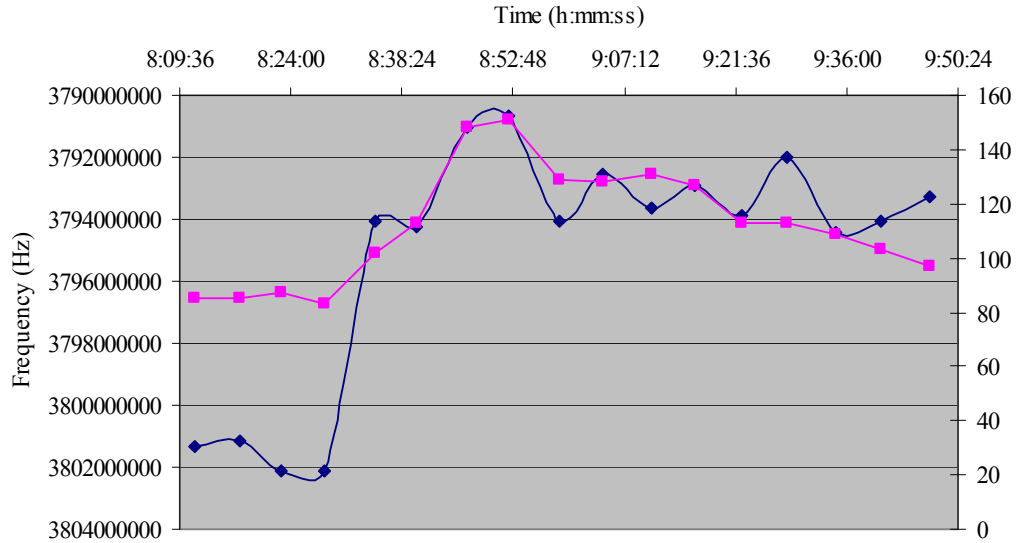


Figure 39: Inverted plot of frequency shift plotted along with the actual measured glucose values for the high pressure traces

Further analysis on the data was done to show that what is seen visually in the plots is backed up by statistical proof. Linear regressions are done on the data throughout this entire study as a way of analyzing the data. In a regression the observed data is modeled by a linear combination that is dependent on one or more independent variables and represents a straight line. The dependent variables are subject to error, while the independent variables, called regressors, are error free. Each residual in a regression analysis is the difference between the observed value and the predicted value calculated by the model. In linear regression, R square represents the square of a correlation coefficient between the original and the modeled data. The R square value is a measure of how well a regression line approximates real data points. An R square value of 1.0, means that the model explains all variability in the predicted values, while an R square value of 0 indicated no relationship between the observed values and the values predicted by the model. R square values from 0 to 1.0 can be represented as percent correlations from 0-100%

A linear regression was performed on both the low pressure data and the high pressure data. The R square value for the low pressure data is 0.68998 and 0.65012 for the high pressure data. Four data points were removed from each set of data because their standard residual values were beyond ± 15 . A second linear regression was done on the data with the three points removed and the R square values for low pressure and high pressure data were found to be 0.79933 and 0.84517 respectively. After the second linear regression was done it can be seen that the R square values improved by 0.109348 and 19505 respectively. The R square values show that the correlation between glucose values and frequency shift is 79.9% for the low pressure data and 84.5% for the high pressure data and provides a firm foundation for continuing research for a calibration algorithm for the non-invasive microwave device. A full set of regression data can be found in Appendix C with the final correlation plots after the second regression pictured in figure 40 and 41.

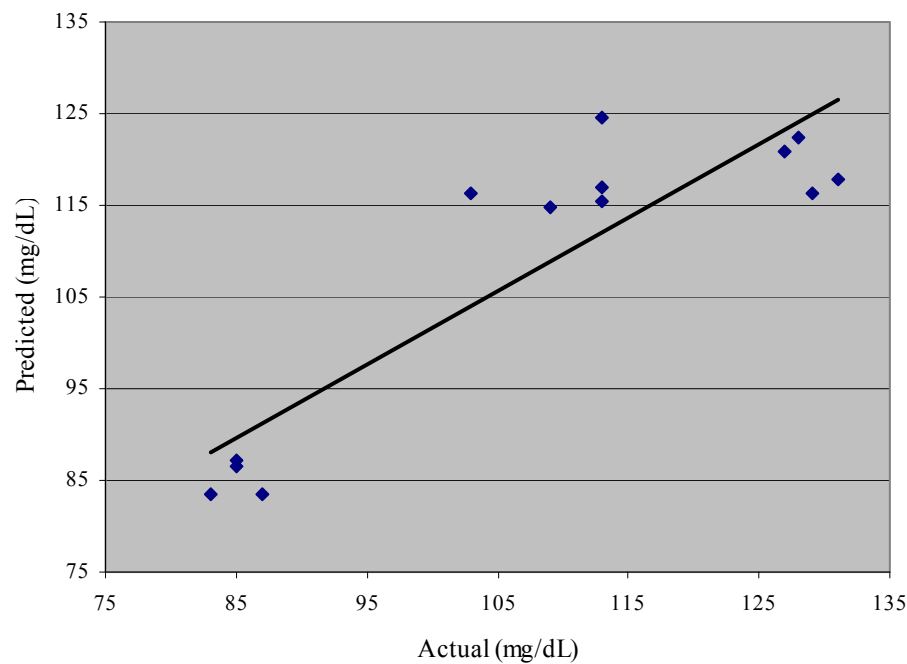


Figure 40: Chart plotting the predicted values of glucose against the actual measured values of glucose. (Second regression - low)

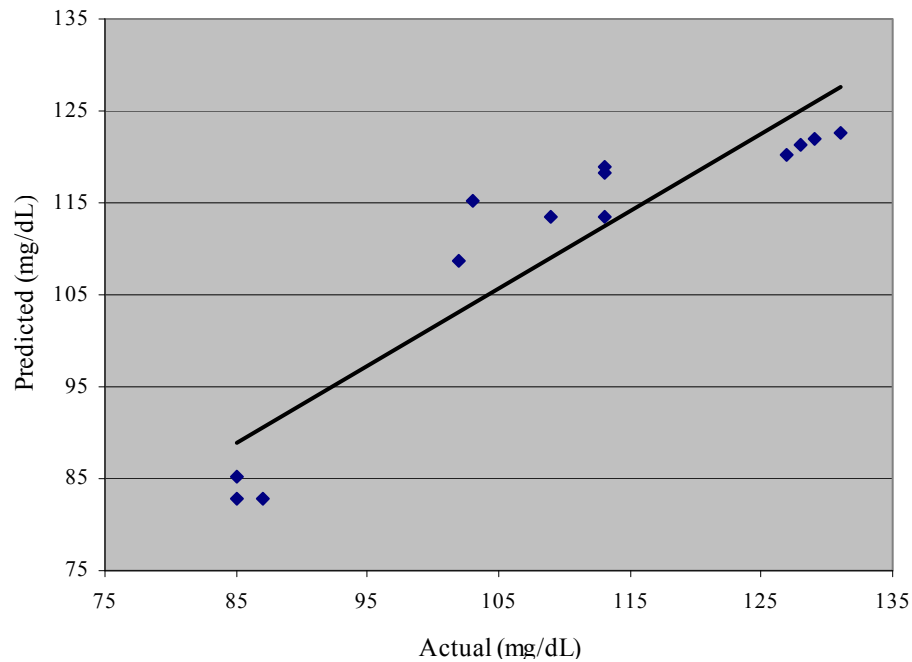


Figure 41: Chart plotting the predicted values of glucose against the actual measured values of glucose. (Second regression - high)

The data appears somewhat non-linear in these two final plots. This is due to the small range of data and the low number of data points available in the analysis. If other data also showed non-linear tendencies, then this would be considered, but data from later experiments, which have more data points, shows that the relationship is linear.

Study Two – Developing a Calibration Algorithm

Experiment One

The second study conducted for this device is lengthy and involved multiple participants. The data obtained from this experiment will be used to determine if it is possible to formulate a calibration algorithm for the resonant sensor for each individual user and for the entire group of participants as a whole. Permission to conduct an experiment involving voluntary human participants was obtained from the Baylor University Institutional Review Board. Each participant was given a consent form that outlined the test and what

was involved in the test. They were required to read the document, sign it, and obtain a signature from the person obtaining consent. A copy of this consent form can be found in Appendix B. Upon giving their consent each participant was shown how to use the device for the experiment. The person obtaining consent and giving instructions to the participants followed a checklist while giving the instructions which can be found in Appendix B.

The first step in the experiment was creating a silicon thumb mold for each participant which ensured consistent placement and decreased movement of the thumb. These molds were stored in a plastic segmented container with name labels for each user on top of the container. The second step was to begin collecting data. The user was asked to administer a traditional glucose test on him/herself with a One Touch Ultra Smart glucose meter. This glucose meter was used by each participant every time the test was done. The user pricked him/herself with a small lancet and applied a drop of blood to a test strip which was inserted into the glucose meter. The glucose meter then provided a reading of the user's glucose level in mg/dL. The participant then entered their name and glucose level into the program on the VNA and clicked the "Take Data" button. Immediately, after clicking the button, the participant placed their thumb on the microwave sensing device along with their thumb mold and followed the directions on the VNA. The VNA captured and stored the trace data and glucose level data in a folder for each participant. A minimum of 10 trials was required for each participant, but the participants were allowed to take more than 10 trials, if they wished. The data collected from the experiment aided in determining if a calibration algorithm could be produced for this device, and in determining if changes needed to be made to the device or any of the testing procedures.

The first step in analyzing the data was to take all of the data traces from every participant and combine them into one large data set in an Excel file. This data set, comprised of 8000 frequency points and their corresponding amplitude values, was then subjected to principal component analysis (PCA) where the first half of the data, representing the 4000 lower frequencies, were examined. This was because the last half of the data contained more noise which masked slight shifts in the data caused by the changing levels of glucose. Principal component analysis is a technique that reduces the number of dimensions of a data set while retaining most of the information in the set. The information that is retained after PCA is the most important information in the data set, while the reduced data in the data set is the redundant data. The amount of information that is retained in the signal can be specified in the PCA algorithm. For all PCA done in this study the energy was set to 90%, meaning that 90% of the data is retained after PCA is preformed. For both the low pressure and high pressure data in this data set the dimensions were reduced from 4000 to 9. The matrix containing the nine dimensions of data was then regressed against the actual glucose levels.

The residuals obtained from a regression can contain unexplained systematic tendencies. In order to determine that the means of collecting the data did not introduce any systematic tendencies into the data, the table of the residuals from the regression was taken and studied. Histograms, shown in figure 42, were created for the low and high pressure data sets to determine if the residuals closely resembled a sample of a normal distribution centered at zero.

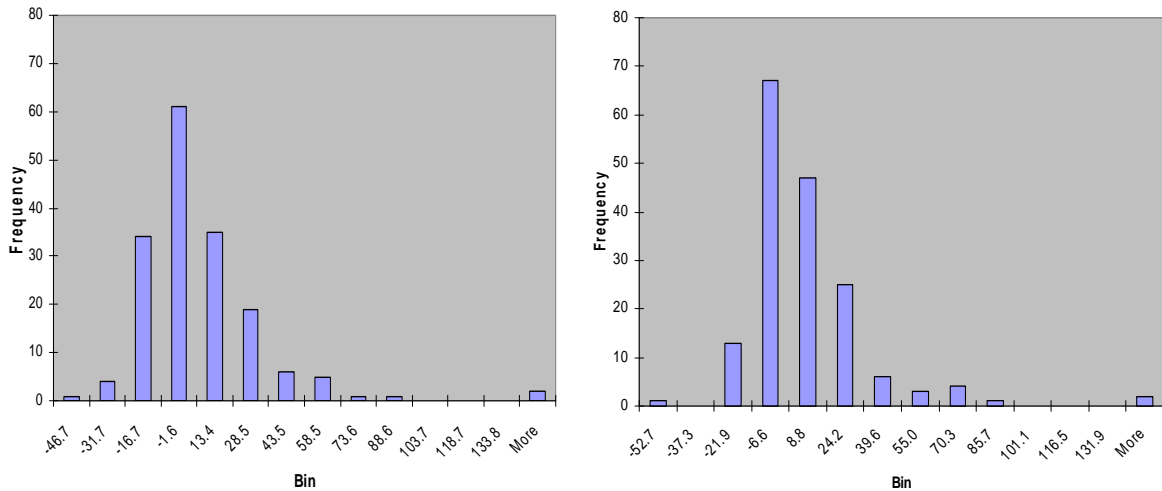


Figure 42: Histogram of the residuals for low and high pressure

For each set of data a normal distribution was seen with a few extreme outliers. These outliers were examined and found that the data points that cause the outliers are extremely high values of glucose, which are rare in the data. When a regression is run on the data, it treats these high reported values as outside of normal even though the values are reported correctly. In order for the regression to treat this data as normal there would have to be more high values in the data set.

Another examination of the data was done on the relation between the size of the residuals and the expected values. For the mathematical model to be represented correctly these two variables should have no relation to each other. If there was a constant percentage error in the glucose values then the resulting plot would have a funnel-like appearance caused by the absolute value of the residuals increasing with the size of the observations, but as can be seen in figure 43 there is no such tendency. This confirms that there is no relation between the residuals and the expected values.

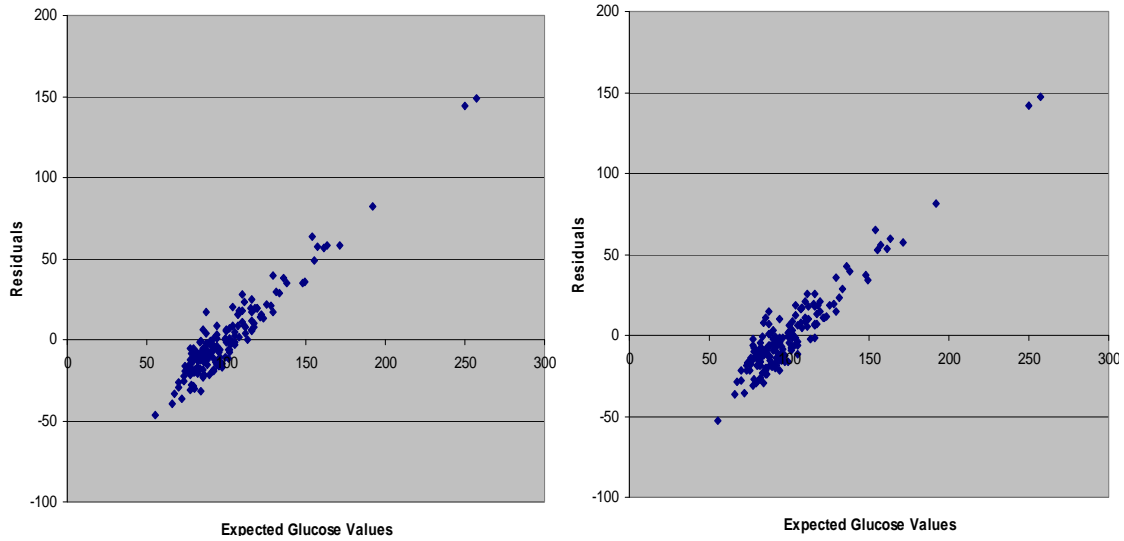


Figure 43: Residuals vs. expected values for low and high pressure data sets

The last examination of the residual data is done to ensure that there is no relation between the residuals and the applied pressures on the sensor. As can be seen from figure 44, there are no tendencies in the data which corresponds to there being no relationship between the data and the applied pressures. These different examinations show that the model does not contain obvious inadequacies and further analysis on the data can proceed with more assurance.

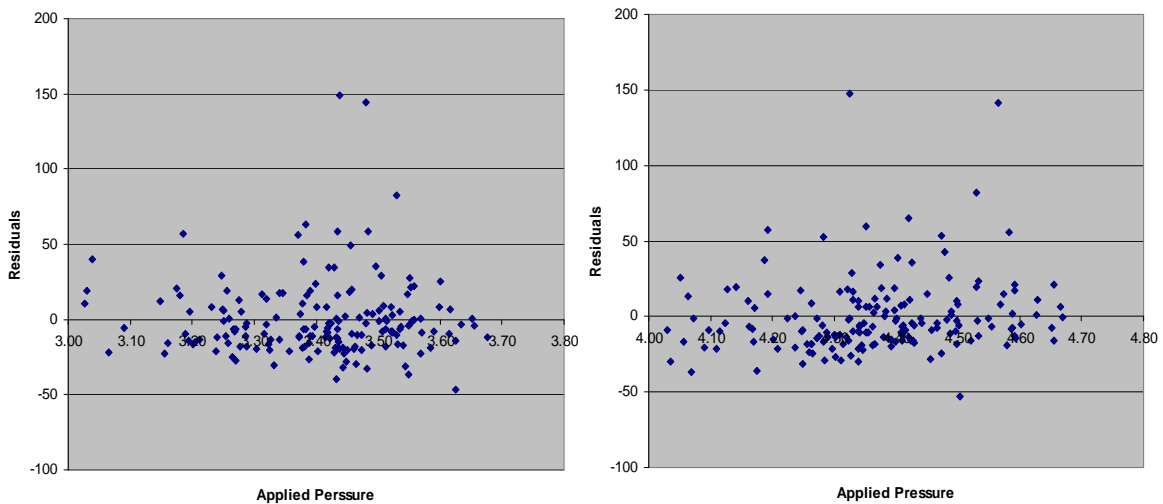


Figure 44: Residuals vs. applied pressure for low and high pressure data sets

After the analysis on the residuals was done and the results showed that the data had no systematic tendencies, outliers were removed from the data based upon their standard residuals. The data was then regressed again against the actual glucose values. This process provided low R square values, shown in table 5, which leads to a conclusion that there is virtually no correlation to glucose in either the low pressure or high pressure data.

Table 5: R Square values from principal component analysis

First Regression	<i>R Square</i>	Second Regression	<i>R Square</i>
Low Pressure Data	0.0943573	Low Pressure Data	0.1368321
High Pressure Data	0.115037	High Pressure Data	0.16974632

This provides confirmation that when data from different individuals is combined there is no correlation to glucose in the data. This revelation was somewhat expected because the biological and physiological makeup of each participant's thumb is different. As a result, the data was re-analyzed to find if a correlation could be found for each individual participant's data.

The second step in analyzing the data was to examine each participant's data individually. The data for each participant, that finished the minimum of ten trials, was collected and compiled into an Excel file for each participant. There is a null that occurs around 3.78 GHz in each set of data, which was examined for the analysis. The following procedure was applied to each participant's data set. All data was collected and plots were made of all traces to confirm the frequency range of the null. For each trace the frequency at which the null occurred was recorded along with the participant's actual glucose value, which was measured previously during the testing process. The frequencies were plotted versus the trial number and the glucose values were also plotted on the same graph versus the trial number. These plots were only created to provide a visual relation between the

frequency shift and the glucose values. To further analyze this data a linear regression was performed on the frequency values at the null and the actual glucose levels. Outliers were selected from the data set due to their high standard residual values and were then removed. Another regression was done on the remaining data. From this second regression the R square values are noted and can be found in table 6.

Table 6: R Square values for each individual participant

First Regression	<i>R Square</i>	Second Regression	<i>R Square</i>
Participant #1		Participant #1	
Low Pressure Data	0.110125	Low Pressure Data	0.102672
High Pressure Data	0.142939	High Pressure Data	0.13863
Participant #2		Participant #2	
Low Pressure Data	0.270872	Low Pressure Data	0.414559
High Pressure Data	0.232609	High Pressure Data	0.700991
Participant #3		Participant #3	
Low Pressure Data	0.431784	Low Pressure Data	0.897485
High Pressure Data	0.366018	High Pressure Data	0.865714
Participant #4		Participant #4	
Low Pressure Data	0.000703	Low Pressure Data	0.11354
High Pressure Data	0.006656	High Pressure Data	0.661892
Participant #5		Participant #5	
Low Pressure Data	0.076658	Low Pressure Data	0.064015
High Pressure Data	0.020784	High Pressure Data	0.379629
Participant #6		Participant #6	
Low Pressure Data	0.030652	Low Pressure Data	0.484136
High Pressure Data	0.430648	High Pressure Data	0.818831
Participant #7		Participant #7	
Low Pressure Data	0.007053	Low Pressure Data	0.081839
High Pressure Data	0.00082	High Pressure Data	0.058109
Participant #8		Participant #8	
Low Pressure Data	0.05519	Low Pressure Data	0.091297
High Pressure Data	0.08555	High Pressure Data	0.191902

From the R square values it can be seen that there is virtually no correlation in the data for each participant. The data sets that show a possible correlation is most likely coincidental and there is actually no correlation between the frequency shift and the glucose

values found by only looking at the frequency shift of a null. As a result of this information a new method was adopted for examining the data.

Side Experiment

In response to the results from the manner in which the data was previously collected and analyzed, a new method was tested to determine if a new method for collecting data would be beneficial in determining if a calibration algorithm is possible. Two participants, with at least 10 trials worth of data each, were selected for this side analysis method. First, the two participants were asked to take twenty readings in a row with the microwave device while their glucose level was constant, which was over a period of approximately two minutes. This new data was plotted as amplitude against frequency. Upon analyzing the plots, it was seen that there was a noticeable frequency shift in the null examined previously in each of the individual data sets. Since the data was taken quickly, while the glucose level remained constant, there should not have been any noticeable shifts in the data. The frequency shift of this null was tracked and was found to shift more than it should at constant levels of glucose for both high and low pressure readings. (See figure 45) In addition, it was noted that the shifts in the low and high pressure plots closely resemble each other showing that, in this pressure range, the amount of pressure applied does not largely affect the frequency shifts.

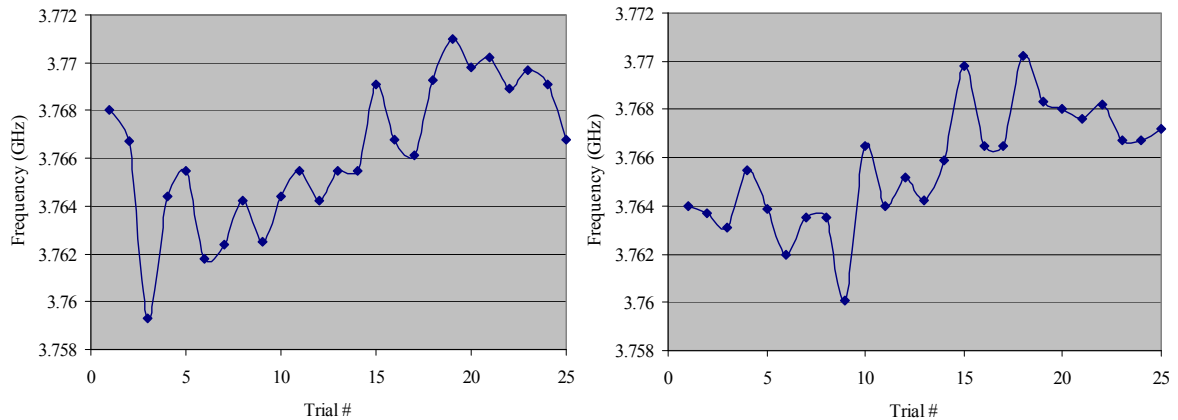


Figure 45: Frequency shift of the null for one participant for low and high pressure data sets

The large shift in the frequency for a constant glucose level shows that there is noise in the null that interfered with the results of the regressions done on each individual data set from the previous analysis. Therefore, the null is not a good place in the data to find a correlation with the glucose level.

Both low pressure and high pressure charts of amplitude versus frequency, in the new sets of data for the two participants, were visually examined to determine where the traces were the most consistent with each other and therefore mostly unaffected by noise. Two areas were chosen from each data set for low and high pressure for both participants. Within each area all trace values for five frequencies were taken out of the data set. These five frequencies were regressed against the glucose values. Outliers were removed based on high standard residuals, and the data was regressed again. The R square values from the regression are found in table 7 and show that there is a good possibility of correlation between frequency shifts and changes in blood glucose levels when areas, with little noise, are found and examined.

Table 7: R Square values from regression at new frequencies

First Regression	<i>R Square</i>	Second Regression	<i>R Square</i>
<i>First Frequency</i>			
Participant #1 (3.725 GHz)		Participant #1	
Low Pressure Data	0.343875	Low Pressure Data	0.667672
High Pressure Data	0.394227	High Pressure Data	0.748498
Participant #2 (3.72 GHz)		Participant #2	
Low Pressure Data	0.286560	Low Pressure Data	0.669854
High Pressure Data	0.334514	High Pressure Data	0.741531
<i>Second Frequency</i>			
Participant #1 (3.83 GHz)	<i>R Square</i>	Participant #1 (3.83 GHz)	<i>R Square</i>
Low Pressure Data	0.237663	Low Pressure Data	0.529567
High Pressure Data	0.367836	High Pressure Data	0.717439
Participant #2 (3.82 GHz)		Participant #2	
Low Pressure Data	0.047930	Low Pressure Data	0.497519
High Pressure Data	0.166638	High Pressure Data	0.599531

Experiment Two

Since it was found that there is a good possibility for a correlation between glucose levels and frequency shifts, another experiment was conducted to collect new data. The resonant sensor was constructed out of a flexible material, so it tended to physically bend with more applied pressure. This slight physical change in the sensor during tests was a cause of some of the noise in the data. Therefore, the resonant sensor mounting was changed so that the force sensor is located under the bottom metal plate and not directly underneath the sensor. By remounting the force sensor under the metal plate the resonant sensor is now mounted flush against the metal plate thereby decreasing the noise in the signal. The pressure applied to the force sensor is now applied by the forefinger when the forefinger and thumb squeeze together around the sensor and metal plate.

With the remounting of the sensor, more of the ground plane of the sensor is in contact with the metal plate and it is physically more flat without the force sensor underneath

it. This caused the trace data to change. Because of this change the trace was re-examined with differing thumb placements and movements. A frequency range from 100 MHz to 5 GHz was selected for this new sensor configuration because there are fewer variations with slight thumb movements, less noise in the data for the lower frequencies, and larger frequency shifts in the higher frequencies. This larger frequency range allows more of the signal to be examined during analysis. Since it was also determined that the applied pressure on the force sensor does not greatly affect the frequency shift, only one pressure range was used for this experiment in order to ensure more consistency throughout the test and aid in decreasing thumb movement.

Again, participants were asked to volunteer for this experiment and all had been previous participants. To begin the experiment the participants were asked to prick themselves once and take twenty readings in a row, over a period of a couple of minutes, while their glucose level was constant. This data was used to determine areas in the data where the frequency remains constant and was least affected by noise. After all participants completed the test, where they took twenty readings in a row, the data was collected and analyzed. Charts were created of all data traces for each participant. Each chart was visually examined to determine areas where their data was very consistent and contained little noise.

After examining each of the charts, it was noted that the data for some participants was noticeably less noisy than others. This is mainly due to the quality of the thumb mold that was created and how consistent the user was at consciously trying to place their thumb in the same position each time. Although the thumb molds are designed to drastically decrease thumb movement there is still some movement that occurs, if the thumb mold does not

encompass a large area of the thumb. This is an area that has a large effect on the test results and will have to be greatly improved for the accuracy of the sensor to improve.

The data sets of the individuals that had the least amount of noise, were combined to see if, in the absence of noise, there could be a correlation between frequency shifts and glucose values for multiple users. In the previous study it was concluded that a correlation could not be found, but this conclusion was reached when using all participants' data regardless of whether it was noisy or not. With the addition of the twenty-in-a-row data collection it was possible to see if data sets were inherently noisy. These least noisy data sets were combined and three frequency areas were found where the traces exhibited less frequency shift due to noise. (See figure 46)

Five consecutive frequencies were selected from each of these areas, along with the amplitude data from each frequency. This data was then regressed against the actual glucose values. Because this is the data from the twenty-in-a-row test, all traces from one participant have the same glucose value. The data from three participants was used so there were only three different glucose values present.

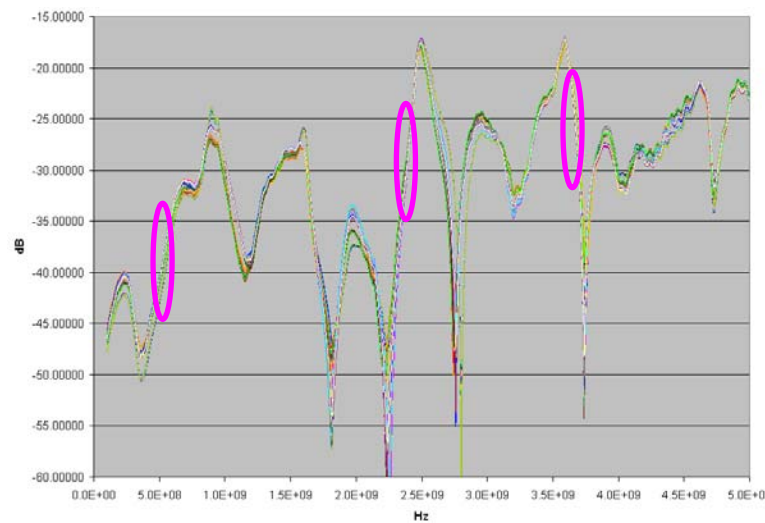


Figure 46: Frequency areas for least noisy data sets

Regression results for each frequency area, 1.05, 2.44, and 3.66 GHz, gave R square values of 0.89235, 0.79288, and 0.85210 respectively. Charts, representing the predicted glucose values versus the actual glucose values, can be found in Appendix D. A 26 mg/dL glucose value spread in the data is not a large spread since glucose values can have a range of 60mg/dL to over 200 mg/dL, depending on the persons involved. This could possibly be a reason that a better correlation was found. However, this analysis shows that consistency in the data can lead to a possible correlation between multiple participants, but, in order for this analysis to be applied in further tests, an improvement will have to be made to the thumb mold so that the data from all participants in the experiment will be consistent. This does show great promise for further experiments.

After thoroughly studying all of the charts and data from every participant, it was decided to take each set of individual data and average all twenty readings together. This was done to essentially average out the noise present in the readings caused by thumb movement, inconsistent thumb placement, and the high sensitivity of the sensor. After the data sets were averaged they were combined to give a new data set of six readings, one for each participant. This new data set was then subjected to regression analysis. Again, three frequency areas were selected which occurred at 0.57, 0.97, and 2.60 GHz. Three frequencies were selected from each area and regressed against the actual values of glucose. The R Square values from the regression were 0.82687, 0.97264, and 0.96846 respectively. Charts, representing the predicted values of glucose versus the actual values of glucose, can be found in Appendix D. These frequency areas were different from the ones selected before and were solely selected from visual analysis of the chart. It can be noted that there are many different frequency areas that contain useful information so it is beneficial to examine many

different areas. The R Square values, found from this regression, show that the implementation of averaging into the analysis process eliminates noise from the data and allows a correlation to be found between glucose values and frequency for multiple participants. However, since there were only six samples for the regression, more data is required to determine, more concretely, if a correlation can actually be found for multiple participants. More data was then collected and the averaging strategy was implemented.

Experiment Three

All of the participants were given instructions for a new test that will allow implementation of the averaging strategy into the analysis. Five out of the six previous participants volunteered for the new test. In addition to implementing the averaging strategy a new, wider, thumb guide was used. The wider thumb guide required that new thumb molds be made. With the wider thumb guide there was more room between the user's thumb and the side of the guide for more silicon molding material to fit. This allowed for more of the thumb to be encompassed by the molding material, further decreasing thumb movement and, therefore, decreasing the noise in the data. Just as before, the participants were asked to prick themselves and enter in their glucose value into the program. However, instead of taking one reading with the commercial glucose meter the participants were asked to take two readings and enter an average of the two values. This was done to recognize and decrease the error in the commercial meter. The VNA was reprogrammed to loop and capture ten readings for each entered value of blood glucose each time the microwave device was used. These ten readings were required in order for the averaging strategy to be implemented. For each of the ten readings taken by the VNA the participants were asked to

remove and replace their thumb just as they would as if it was the first reading. After all of the participants finished the test the data was collected and analyzed.

The newly collected data was analyzed in the same manner as in the twenty-in-a-row test, and, in addition, PCA was also conducted. For each participant's data set the group of ten readings from each entered glucose value were averaged together giving a set of 15 data traces for each participant instead of 150 traces. All of the data sets were subjected individually to PCA as well as a group set of all combined participant's data sets. The results of each analysis were then regressed against the actual values of glucose. As before, the residuals from the group set of data were analyzed to determine if there were any systematic tendencies in the data. From the histogram and plots of the residuals versus the applied force and the residuals versus the expected values, it was determined that there were no systematic tendencies in the data. Figures 47, 48, and 49 show the plots from the analysis.

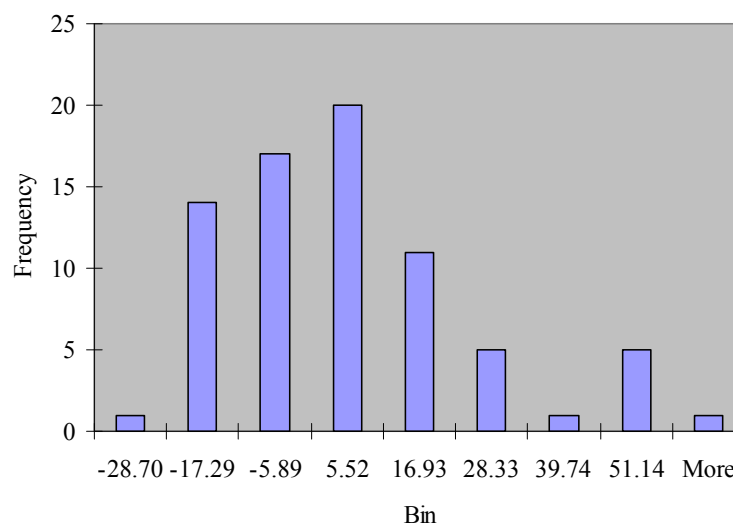


Figure 47: Histogram of residuals from PCA regression

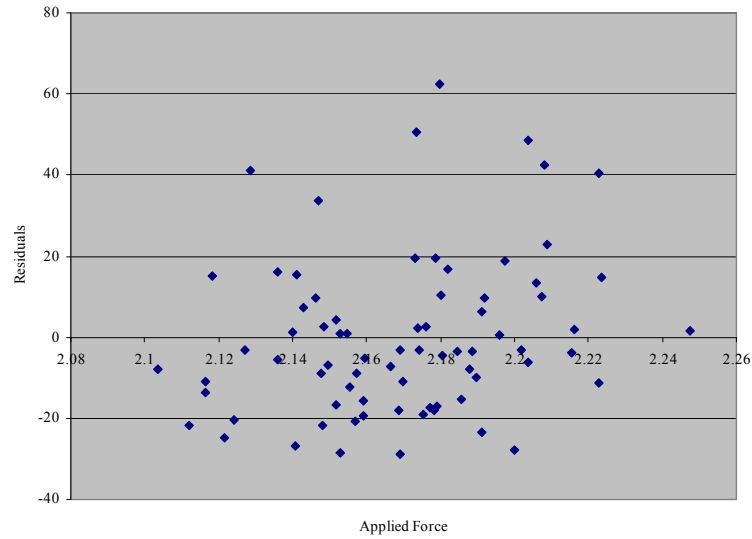


Figure 48: Residuals versus the applied force from PCA regression

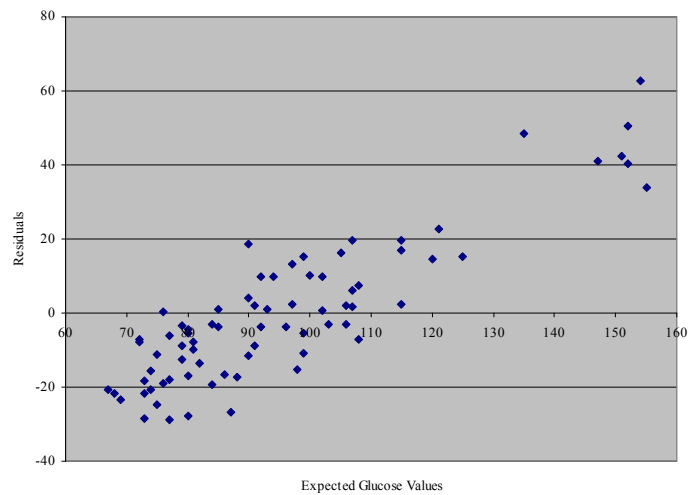


Figure 49: Residuals versus expected glucose values from PCA regression

R Square results from the PCA on the entire set of data and all of the individual sets of data are shown in table 8. The percent of error is based off of the average value of the glucose values for the group or individual. Performing a regression after only doing PCA is not the best way to analyze this data. Although the R Square values from the regression are not very good, the standard error values are acceptable. A standard commercial glucometer requires that it be accurate to within 20% of a person's actual glucose level.

Table 8: Results from PCA

First Regression	<i>R Square</i>	<i>Std. Error</i>	<i>% Error</i>	Second Regression	<i>R Square</i>	<i>Std. Error</i>	<i>% Error</i>
Group Data	0.21648	20.4485	21.4%	Group Data	0.32232	12.6096	14.0%
Individual Data				Individual Data			
Participant #1	0.24880	24.4499	21.4%	Participant #1	0.42888	19.2320	17.6%
Participant #2	0.09245	10.4116	12.2%	Participant #2	0.31813	4.6549	5.70%
Participant #3	0.44155	6.88812	8.80%	Participant #3	0.80301	3.60573	5.90%
Participant #4	0.212042	20.9845	18.6%	Participant #4	0.33575	9.78285	9.10%
Participant #5	0.15018	18.9053	21.5%	Participant #5	0.35029	12.0311	14.3%

As seen from the chart, only three standard error values from the regression fell outside of this range with all of them falling within 1.5% of the range. This error in the data is primarily caused by noise in the sensor and in the device, but it is also caused by the error that is built into the commercial glucometer used to obtain the actual glucose readings for each participant. Charts, showing the predicted glucose values versus the actual glucose values from the regressions, can be found in Appendix D.

An analysis, like that done in the twenty-in-a-row test, was performed on the whole group set of data and for each individual set of data. Several frequency areas were selected from a chart of frequency versus amplitude for the whole set of data for analysis purposes. As was done before, the trace data from five consecutive frequency values in each area were selected from each data set. The data in each area was then regressed against the actual values of blood glucose. Table 9 shows the frequency areas and R square values, for the first regression and the second regression after some data points were removed due to their outlying standard residual values. Charts, of the predicted glucose values versus the actual glucose values after the second regression, can be found in Appendix D.

Table 9: R Square values from individual data sets for the second experiment

First Regression	<i>R Square</i>	Second Regression	<i>R Square</i>
<i>Frequency (GHz)</i>		<i>Frequency (GHz)</i>	
Participant #1		Participant #1	
0.58	0.30998	0.58	0.61039
1.05	0.60188	1.05	0.90840
1.60	0.37475	1.60	0.59002
1.75	0.74685	1.75	0.89527
2.43	0.29193	2.43	0.57555
2.50	0.08821	2.50	0.25776
3.63	0.42272	3.63	0.73125
Participant #2		Participant #2	
0.14	0.53302	0.14	0.58761
0.51	0.35600	0.51	0.28169
0.94	0.22947	0.94	0.61869
2.43	0.21255	2.43	0.15362
2.55	0.35689	2.55	0.32964
3.00	0.39816	3.00	0.69224
3.65	0.33379	3.65	0.67200
Participant #3		Participant #3	
0.16	0.32997	0.16	0.69352
0.55	0.06433	0.55	0.24865
0.99	0.26695	0.99	0.68509
1.74	0.34482	1.74	0.78069
2.45	0.01540	2.45	0.51082
2.54	0.33445	2.54	0.47968
3.63	0.31225	3.63	0.71609
Participant #4		Participant #4	
0.14	0.31246	0.14	0.64868
0.47	0.28114	0.47	0.35283
1.72	0.50579	1.72	0.91247
2.00	0.25353	2.00	0.29950
2.50	0.34390	2.50	0.71261
3.05	0.25887	3.05	0.35149
3.63	0.25487	3.63	0.64073
Participant #5		Participant #5	
0.50	0.25311	0.50	0.84169
1.05	0.17807	1.05	0.60105
1.71	0.46704	1.71	0.82231
2.43	0.12459	2.43	0.66176
2.55	0.24082	2.55	0.65247
3.07	0.41024	3.07	0.64104
3.64	0.33113	3.64	0.66619

The results from the set of group data were not very good, but were somewhat expected. Since there are many different factors that affect the sensor response and each person is different, the results were not expected to correlate well. This was seen in earlier experiments where the group data did not correlate. However, the results from this experiment are better than the results obtained previously which leads to a conclusion that this method of gathering and analyzing data was better than the previous methods. It is still possible that a correlation for a group set of data could be found, but this would require a larger test population, with a larger number of trials and a more controlled test environment to decrease the effects of user actions/errors on the results. Also, a different test setup would be required that would virtually eliminate noise from the sensor response. This would also include obtaining an instrument that would measure actual glucose levels more accurately than a commercial glucose meter.

Although the results of this new test method were much better than the previous results, they are not good enough for a proper correlation and creation of a calibration algorithm. In response to the results of this data and the data from the PCA, a new method was applied to magnify the slight shifts in frequency in the data, which is where all of the information in the data is found. In order to do this the first difference method was applied, which is similar to taking the first derivative of a set of data. When the first difference method is applied the second data point in one trace is subtracted from the first data point in the same trace, the third from the second, the fourth from the third, and so on until the end of the data trace is reached. This is then done for all traces in the data set. The first difference method was applied to all of the individual data sets which were then subjected to individual PCA. This analysis was done on the set of group data, despite the poor results from the

previous analysis, in order to determine if a correlation is at all possible for a set of group data. The results of the PCA were regressed against the actual values of glucose and can be found in table 10.

Table 10: Regression results from PCA after the first difference method was applied.

First Regression	<i>R Square</i>	<i>Std. Error</i>	<i>% Error</i>	Second Regression	<i>R Square</i>	<i>Std. Error</i>	<i>% Error</i>
Group Data	0.51122	19.5066	20.0%	Group Data	0.75959	9.3000	10.2%
Individual Data				Individual Data			
Participant #1	0.38784	27.66813	24.17%	Participant #1	0.97359	6.33365	5.60%
Participant #2	0.19124	11.34915	13.25%	Participant #2	0.91465	2.75469	3.29%
Participant #3	0.26470	10.20383	12.98%	Participant #3	0.74147	6.98679	8.94%
Participant #4	0.37076	19.84379	17.59%	Participant #4	0.401566	17.71493	15.81%
Participant #5	0.51375	16.82213	19.03%	Participant #5	0.91084	6.79759	8.23%

The results from PCA in table 10 show much improvement over the results from PCA in table 8. In table 10 there is only one value outside of the 20% tolerance that is acceptable for a commercial glucose meter which occurred in the first regression before outliers were removed. Also, the R Square values are extremely improved, with three out of the five above 90%, when the first difference method was applied.

The same method for analyzing the individual data was again implemented after the first difference method was applied to the data. The regression results from this analysis are found in table 11. Charts, showing the predicted glucose values versus the actual glucose values from the regression on the PCA data and the second regression on the following data, can be found in Appendix D.

From visually comparing the results from table 8 to those in table 10 and the results from table 9 to those in table 11, it can be seen that the first difference method made an immense improvement in the results of both analyses. To see how great the improvement

was table 12 contains a comparison analysis of the PCA between the original data and the original data after it was subjected to the first difference method.

Table 11: R Square values from individual data sets for the second experiment using the first difference method

First Regression	<i>R Square</i>	Second Regression	<i>R Square</i>
<i>Frequency (GHz)</i>		<i>Frequency (GHz)</i>	
Participant #1		Participant #1	
0.58	0.39828	0.58	0.67228
1.05	0.52786	1.05	0.90875
1.60	0.09711	1.60	0.67411
1.75	0.87959	1.75	0.96362
2.43	0.29542	2.43	0.74118
2.50	0.16811	2.50	0.52326
3.63	0.25724	3.63	0.59381
Participant #2		Participant #2	
0.14	0.52304	0.14	0.80384
0.51	0.33398	0.51	0.84369
0.94	0.13858	0.94	0.77567
1.75	0.09326	1.75	0.68465
2.55	0.24125	2.55	0.69328
3.00	0.73263	3.00	0.69461
3.65	0.36797	3.65	0.68769
Participant #3		Participant #3	
0.16	0.33856	0.16	0.80663
0.55	0.09656	0.55	0.76823
0.99	0.29225	0.99	0.90365
1.74	0.33374	1.74	0.88084
2.45	0.22022	2.45	0.85329
2.54	0.41529	2.54	0.93808
3.63	0.31578	3.63	0.75672
Participant #4		Participant #4	
0.14	0.33344	0.14	0.83795
0.47	0.34587	0.47	0.17869
1.72	0.47303	1.72	0.89776
2.00	0.21569	2.00	0.47220
2.50	0.39512	2.50	0.79519
3.05	0.28797	3.05	0.30987
3.63	0.27942	3.63	0.86979
Participant #5		Participant #5	
0.50	0.27994	0.50	0.89253
1.05	0.38111	1.05	0.89155
1.71	0.65343	1.71	0.97659
2.43	0.28008	2.43	0.70702
2.55	0.73092	2.55	0.90437
3.07	0.22308	3.07	0.54319
3.64	0.32709	3.64	0.89781

Table 12: Comparison of R Square values for PCA on the original data and on the first difference data

Participant	Original PCA	First Difference PCA	Difference	% Difference
	<i>R Square</i>	<i>R Square</i>		
Group	0.322	0.759	0.437	135.71%
Participant #1	0.429	0.974	0.545	127.03%
Participant #2	0.318	0.915	0.597	187.52%
Participant #3	0.803	0.741	-0.062	-7.67%
Participant #4	0.336	0.402	0.066	19.60%
Participant #5	0.350	0.911	0.561	160.08%

There was a large improvement in R Square values when the first difference method was applied. This can be seen in the percent difference in the R Square values between the original data and first difference data. Only one participant's R Square value decreased, but it was very minimal compared to increases of more than 100% in other participant's data. Also, there was an immense improvement in the group R Square values, which gives more hope that a calibration can be found for a set of group data. Table 13 shows the same type of comparison, but with the data from the frequency area analysis instead of PCA.

This comparison gives a nice representation of how much improvement there was when the first difference method was applied before regressions on the data were conducted. There are very few places where the data, using the first difference method, had lower R Square values than the original data. It is possible that this is partly due to the areas that were selected for the analysis. With each frequency area being only visually selected it is very possible that a frequency area slightly above or below the selected one would have provided a better result. Also, there could be numerous other frequency areas in the data, which contain less noise, which would provide equally good or better results.

Table 13: Comparison of R Square values from individual data sets

Frequency (GHz)	Regular Regression	First Difference Regression	Difference	% Difference
	R Square	R Square		
Participant #1				
0.58	0.61039	0.67228	0.06189	10.14%
1.05	0.90840	0.90875	0.00035	0.04%
1.60	0.59002	0.67411	0.08409	14.25%
1.75	0.89527	0.96362	0.06835	7.63%
2.43	0.57555	0.74118	0.16563	28.78%
2.50	0.23767	0.52326	0.28559	120.16%
3.63	0.73125	0.59381	-0.13744	-18.80%
Participant #2				
0.14	0.58761	0.80384	0.21623	36.80%
0.51	0.28169	0.84369	0.56200	199.51%
0.94	0.61869	0.77567	0.15698	25.37%
2.43	0.45259	0.51552	0.06293	13.90%
2.55	0.32964	0.69328	0.36364	110.31%
3.00	0.69224	0.69461	0.00237	0.34%
3.65	0.67200	0.68769	0.01569	2.33%
Participant #3				
0.16	0.69352	0.80663	0.11311	16.31%
0.55	0.24865	0.76823	0.51958	208.96%
0.99	0.68509	0.90365	0.21856	31.90%
1.74	0.78069	0.88084	0.10015	12.83%
2.45	0.51082	0.85329	0.34247	67.04%
2.54	0.47968	0.93808	0.45840	95.56%
3.63	0.71609	0.75672	0.04063	5.67%
Participant #4				
0.14	0.64868	0.83795	0.18927	29.18%
0.47	0.35283	0.17869	-0.17414	-49.36%
1.72	0.91247	0.89776	-0.01471	-1.61%
2.00	0.29950	0.47220	0.17270	57.66%
2.50	0.71261	0.79519	0.08258	11.59%
3.05	0.35149	0.30987	-0.04162	-11.84%
3.63	0.64073	0.86979	0.22906	35.75%
Participant #5				
0.50	0.84169	0.89253	0.05084	6.04%
1.05	0.60105	0.89155	0.29050	48.33%
1.71	0.82231	0.97659	0.15428	18.76%
2.43	0.66176	0.70702	0.04526	6.84%
2.55	0.65247	0.90437	0.25190	38.61%
3.07	0.64104	0.54319	-0.09785	-15.26%
3.64	0.66619	0.89781	0.23162	34.77%

The worst results from this experiment came from participant #4. It is difficult to determine what would have caused the results to be as far off from the results of the other participants. The first cause and the easiest to obtain a solution for was human error. Participant #4 was asked to redo the test so that a new group of data was obtained. Immediately after the data was collected from this experiment, it was visually obvious looking at a chart of the data that this set was much improved and contained less user caused noise. This new data was analyzed in the same manner as the previous data. Tables 14 and 15 show a comparison of the individual regression results and the PCA regression results from participant #4 for each of the two experiments. It can be seen that there was a large improvement from the first experiment to the second experiment and that the results from the second experiment are consistent with the results from the other participants in the experiment. Charts, showing the predicted versus actual glucose values from the new experiment for participant #4, can be found in Appendix D along with the results from the previous experiment.

Table 14: Comparison results for participant #4

Frequency (GHz)	Regular Regression	First Difference Regression	Difference	% Difference
First Experiment				
0.14	0.64868	0.83795	0.18927	29.18%
0.47	0.35283	0.17869	-0.17414	-49.36%
1.72	0.91247	0.89776	-0.01471	-1.61%
2.00	0.29950	0.47220	0.17270	57.66%
2.50	0.71261	0.79519	0.08258	11.59%
3.05	0.35149	0.30987	-0.04162	-11.84%
3.63	0.64073	0.86979	0.22906	35.75%
Second Experiment				
0.14	0.74369	0.78153	0.03784	4.84%
0.47	0.24777	0.68178	0.43401	63.66%
1.72	0.63118	0.78280	0.15162	19.37%
2.00	0.60515	0.61360	0.00845	1.38%
2.50	0.49404	0.43364	-0.06040	-13.93%
3.05	0.51865	0.72353	0.20488	28.32%
3.63	0.92197	0.92657	0.00460	0.50%

Table 15: PCA comparison results for participant #4

Participant	Original PCA	First Difference PCA	Difference	% Difference
Participant #4-1	0.336	0.402	0.066	19.60%
Participant #4-2	0.257	0.708	0.451	175.59%

After taking more data for participant #4 and seeing that the results were much improved and were more consistent with the results of the other participants in the study composite charts were made that include the data from every participant from the PCA regression after the first difference method was applied. These charts show that, by analyzing each participant's data sets individually using PCA after applying the first difference method, a correlation exists between the predicted glucose values from the regression and the actual glucose values. Figure 50 shows the composite chart from the first regression before outliers were removed and figure 51 shows the composite chart after the outliers were removed and another regression was performed.

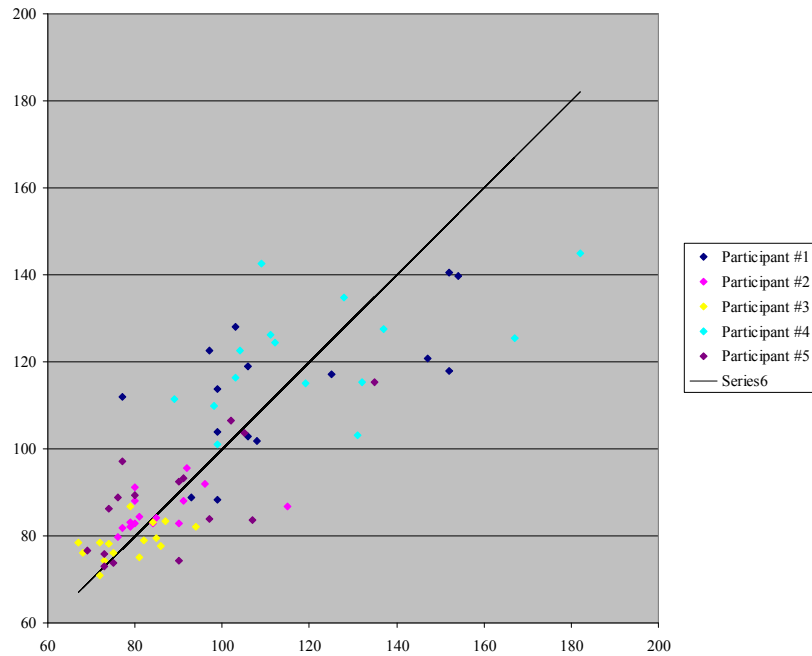


Figure 50: Composite regression results before outliers were removed (predicted versus actual glucose values in mg/dL)

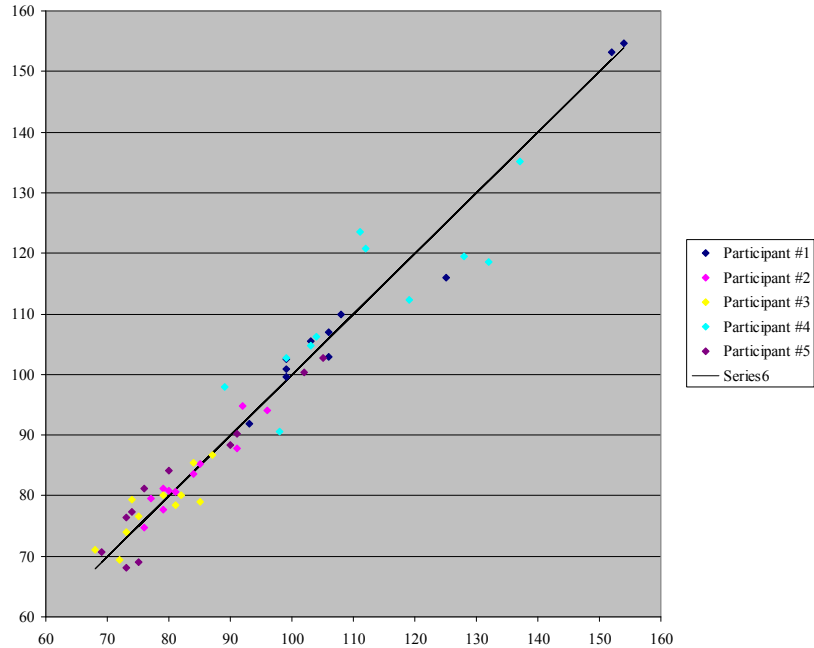


Figure 51: Composite regression results after outliers were removed (predicted versus actual glucose values in mg/dL)

Although the results from the third experiment are greatly improved over the results from all previous experiments, they are not consistent enough for the development of a calibration algorithm. For a calibration algorithm to be realized even for individual users, the regressions would need to provide better R Square values, in the neighborhood of 0.90, over multiple tests for each user. In future experiments sets of data would need to be taken for each user multiple times over a long period of time to determine if R Square values from each set of data meet the requirement. By taking multiple sets of data, the participants would become more accustomed to the device, which would decrease the human error as seen with participant #4 in this experiment.

CHAPTER EIGHT

Conclusions and Final Recommendations

This study presented an improved design of a microwave resonant sensor for correlating $|S_{21}|$ trace data to blood glucose levels and the possibility of developing a calibration for a non-invasive glucose sensing device. The experiment of the “Soda Test” confirmed a correlation between $|S_{21}|$ trace data and blood glucose levels in an unchanging environment over a short period of time. Through the experimentation, data gathering, and data analysis process for developing a calibration algorithm it was found that a calibration cannot be developed at this time. As the various experiments progressed over time new techniques and ideas were brought forth and implemented in order to improve the results of the tests. It was determined that the best way to analyze the data was by applying the first difference method and then performing PCA on the data sets for each participant individually. The results from the regressions on the PCA data provide information and a means for developing a calibration algorithm, but there are many things still to be done before the calibration algorithm can be realized.

Over the course of the study, many modifications were made to the design of the non-invasive sensing device to improve its function and consistency. However, there are still many things that could further improve the design and increase the performance of the resonant sensor and device. The first recommendation would be a better placement for the force sensor. As was found during the study, a placement directly underneath the resonant sensor is not an ideal place for the force sensor because it interfered with the physical

properties of the resonant sensor. Therefore, it was moved to the underside of the metal plate, supporting the resonant sensor. This placement does not affect the resonant sensor in any way and allows for sufficient pressure measurements, but the pressure measurements are not a direct reflection of the force applied by the thumb. In future experiments, it would be desirable to be able to determine the exact thumb pressure and, therefore, there would have to be a change in the placement of the force sensor or a different type of sensor would have to be implemented. Slight thumb movements on the resonant sensor had a large effect on the response of the sensor and it was the most common problem encountered in all of the tests. This was improved throughout the experimentation process; however, thumb movement remains a large problem in creating noise in the signal. The thumb mold and guide developed in this study would have to be redesigned in order to minimize thumb movement further. It is possible that a different material could be used for the mold that encompasses more of the thumb. A guide could also be made that tightened around the user's thumb during use which would be functional for thumbs of various sizes. Another part of the body could possibly be used as a testing area, but the thumb appears to be the best place since the thumb can be taken and placed on the sensor instead of requiring the sensor to be taken to the body. It is easier to consistently place the thumb in the exact same place on the sensor in each test than to place the sensor on the exact same place on the body.

The design of the sensor was not changed greatly from the sensor in Mr. Green's study, but many things could be changed in regards to the current sensor to improve its measurements of blood glucose levels. More research can be done on the best configuration of the sensor, including the type of substrate, the number of curves in the spiral, the thickness of the substrate, the width of the traces, and the shape of the sensor. For a flat sensor

placement the sensor should be made out of a more rigid substrate since a flexible material allows for changes in the physical properties of the sensor which then affects the response of the sensor. However, there is a possibility that a more flexible material should be used because it better conforms to the contours of the thumb. If this were the case, the sensor would have to be carefully mounted on an equally curved metal piece in such a way that there is no possibility that the sensor could physically change after mounting. With a more flexible sensor the traces would have to be narrowed and a substrate with a higher dielectric would have to be used. Besides working with and changing the current sensor configuration, it is very possible that a different sensor configuration would give better results. Many different configurations were designed and tested in Mr. Green's study, but there are many other configurations that were not examined. By using a circuit board etching machine to create the sensors it would be immensely easier to create and test many different sensor configurations.

It was determined, from the results of the analyses, that a calibration for the device, for all participants as a group, is possible but not likely. Also, it was found that the device would have to be calibrated separately for each user. The reason that it is difficult to create an algorithm for all users, as a group, is mainly due to the fact that all people are physically different. Body fat percentages, the flow of blood and volume of blood through the test site, water content in the tissues, and skin thickness all effect the sensor's response and all vary greatly from person to person. A calibration algorithm could be created for each individual user, but most likely the device would have to be recalibrated fairly often depending on environmental changes such as temperature and humidity. This could cause the device to possibly require recalibration every day. These problems are also encountered in a

calibration for all users as a group and are compacted with all of the factors that cause one individual to differ from another. Even after a calibration algorithm is found it would be quite difficult to determine the extent of recalibration until the device is very thoroughly tested and all other issues resolved. With the advance of other devices that use microwaves to non-invasively measure biological parameters there is hope that there could be a universal calibration that could be made to accommodate any user.

The use of a microwave sensor for measuring biological parameters, specifically blood glucose levels, is very advantageous since these types of sensors are very robust and can take measurements in the blood without requiring contact with the blood. The results from the experiments in chapter 7 show that a microwave resonant sensor can be used to track changes in blood glucose levels but there are still many small factors that, when combined together, greatly affect the performance of the sensor. There is much more research and testing that needs to be done before a calibration for a non-invasive sensor to measure glucose levels can be fully realized.

APPENDICES

APPENDIX A

Circuit Schematic, Board Layout, and Device Bill of Materials

Circuit Schematic

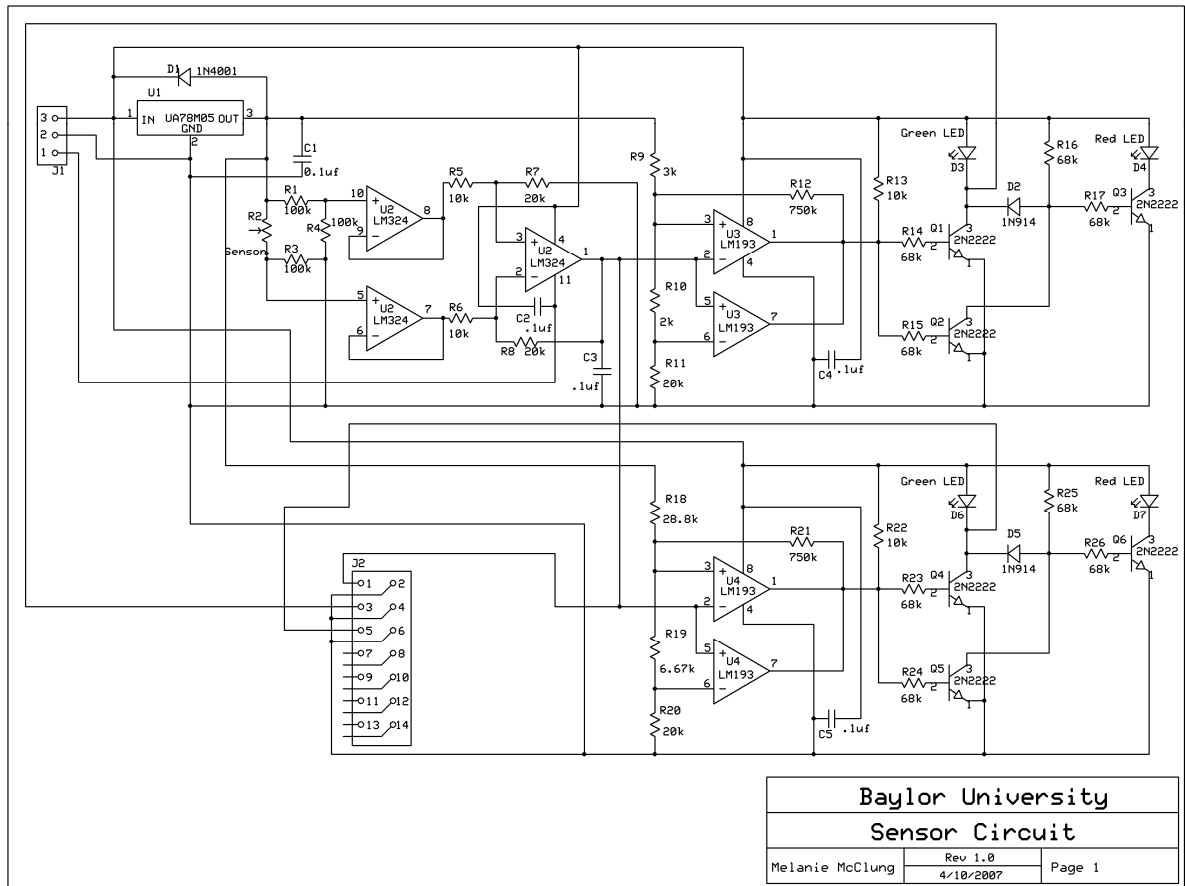


Figure A.1: Circuit schematic

Circuit Board Layout Views

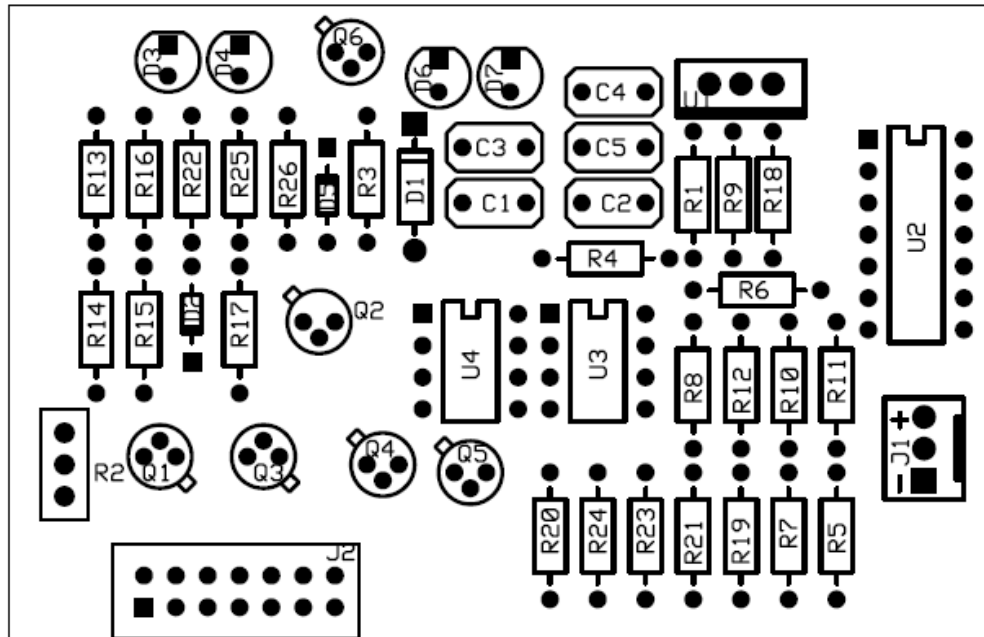


Figure A.2: Silkscreen view of the circuit board showing pads and part labels

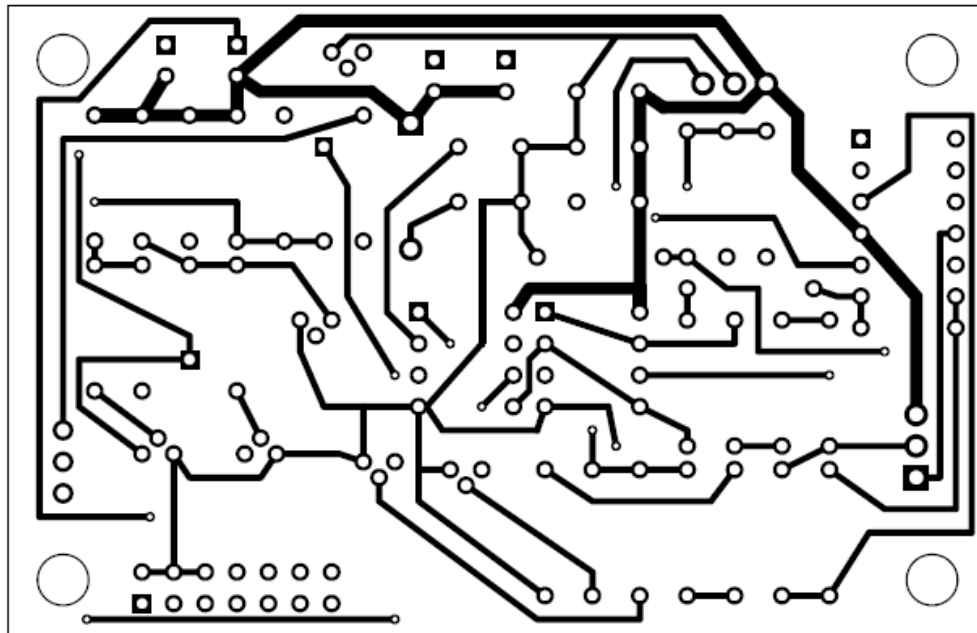


Figure A.3: Circuit board layout showing pads and top copper layer

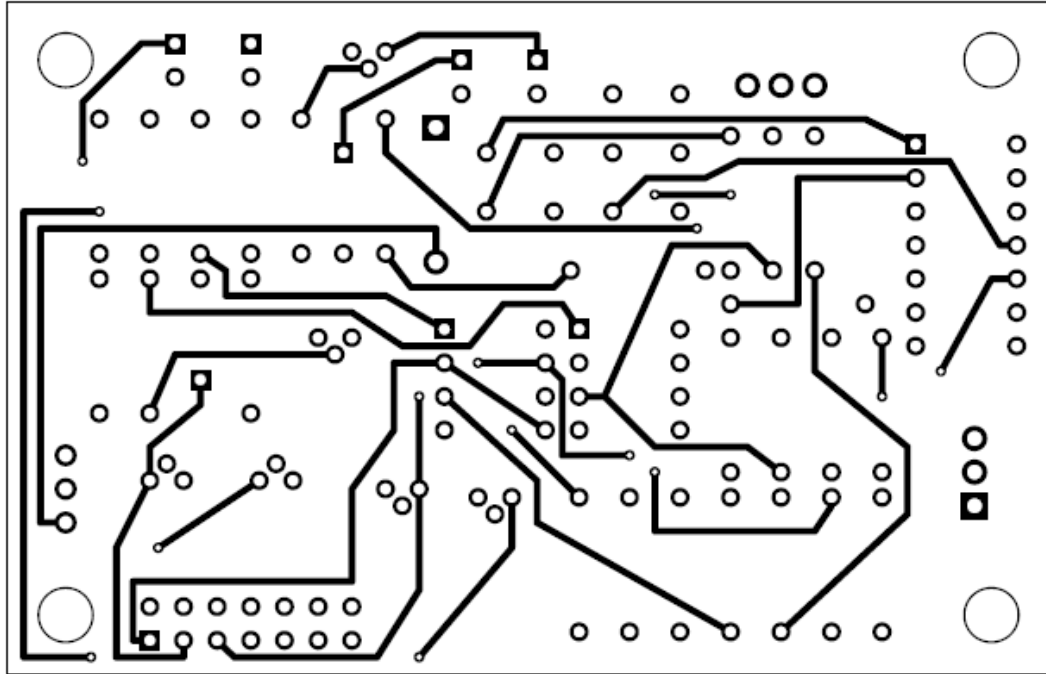


Figure A.4: Circuit board layout showing pads and bottom copper layer

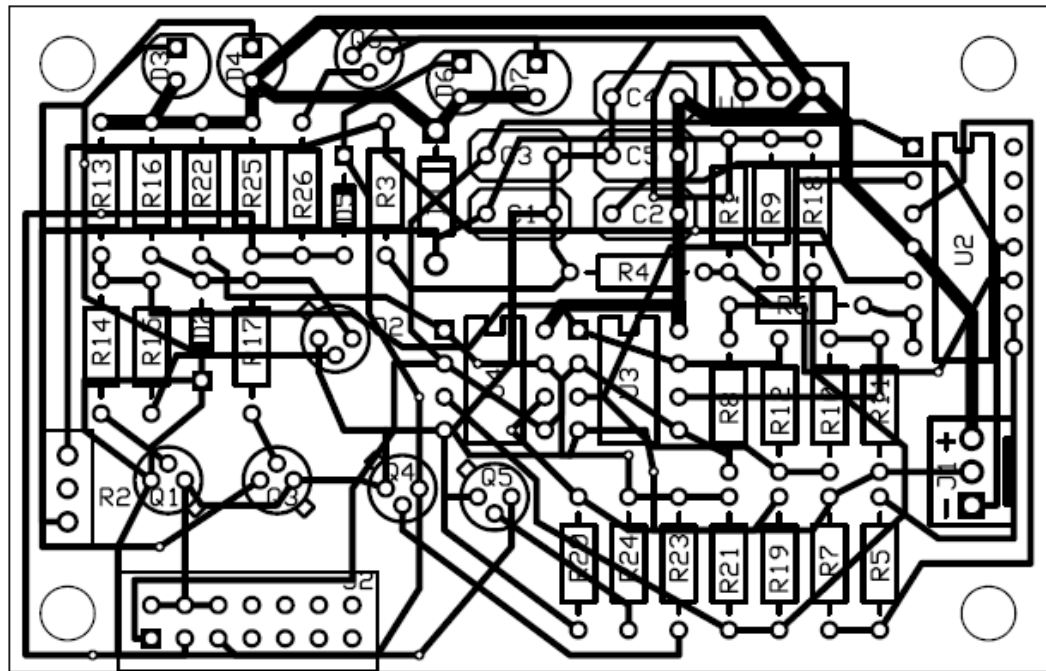


Figure A.5: Circuit board layout showing top copper layer, bottom copper layer, silkscreen, pads, and part labels

Circuit and Device Bill of Materials

Table A.1: Circuit and device bill of materials

Part #	Part Name	Manufacturer	Manufacturer Part #	Allied Part #
C1	0.1uf	Vishay	1C10X7R104K050B	507-0211
C2	0.1uf	Vishay	1C10X7R104K050B	507-0211
C3	0.1uf	Vishay	1C10X7R104K050B	507-0211
C4	0.1uf	Vishay	1C10X7R104K050B	507-0211
C5	0.1uf	Vishay	1C10X7R104K050B	507-0211
D1	1N4001	ON Semi.	1N4001	568-0274
D2	1N914	Vishay	1N914	431-0618
D3	Green LED	Dialight	609-1212-120	511-0131
D4	Red LED	Dialight	609-1112-120	511-0125
D5	1N914	Vishay	1N914	431-0618
D6	Green LED	Dialight	609-1212-120	511-0131
D7	Red LED	Dialight	609-1112-120	511-0125
J1	3-pin screw terminal	Phoenix Contact	1725669	409-0011
J2	14-pin header	Tyco	103240-7	512-1744
Q1	2N2222	STMicro.	2N2222	248-1004
Q2	2N2222	STMicro.	2N2222	248-1004
Q3	2N2222	STMicro.	2N2222	248-1004
Q4	2N2222	STMicro.	2N2222	248-1004
Q5	2N2222	STMicro.	2N2222	248-1004
Q6	2N2222	STMicro.	2N2222	248-1004
R1	100k	SEI		832-1110
R2	Sensor	Tekscan	A201	
R3	100k 1/4W	SEI		832-1110
R4	100k 1/4W	SEI		832-1110
R5	10k 1/4W	SEI		832-1118
R6	10k 1/4W	SEI		832-1118
R7	20k 1/4W	SEI		832-1614
R8	20k 1/4W	SEI		832-1614
R9	3k 1/4W 1%	SEI		832-1308
R10	2k 1/4W 1%	SEI		832-1620
R11	20k 1/4W 1%	SEI		832-1614
R12	768k 1/4W	SEI		832-1542
R13	10k 1/4W	SEI		832-1118
R14	68k 1/4W	SEI		832-1510
R15	68k 1/4W	SEI		832-1510
R16	68k 1/4W	SEI		832-1510
R17	68k 1/4W	SEI		832-1510
R18	28.7k 1/4W 1%	SEI		832-1298
R19	6.65k 1/4W 1%	SEI		832-1486
R20	20k 1/4W 1%	SEI		832-1614

Table A.1: Circuit and device bill of materials (cont.)

Part #	Part Name	Manufacturer	Manufacturer Part #	Allied Part #
R21	768k 1/4W	SEI		832-1542
R22	10k 1/4W	SEI		832-1118
R23	68k 1/4W	SEI		832-1510
R24	68k 1/4W	SEI		832-1510
R25	68k 1/4W	SEI		832-1510
R26	68k 1/4W	SEI		832-1510
U1	LM7805CT	National Semi.	LM7805CT	288-0001
U2	LM324	TI	LM324	735-1154
U3	LM193 or LM393	National Semi.	LM393	288-1371
U4	LM193 or LM393	National Semi.	LM393	288-1371
Wire	Flat Cable 14 Conductors	3M	3365/14	618-4214
Wire connector	14-pin connector	Sareva/FCI	71600-014LF	518-2301
Connectors	SMA - panel mount	S.M. Electronics	1358-000-K051-003	
Sensor				
Connector	3-pin socket	3M	CHG-1003-001010-KCP	618-1844
Connector	2-pin socket	3M	CHG-1002-001010-KCP	618-1840
Switch	Switch, Toggle, Subminiature, Bat Lever, Threaded Bushing, Solder Lug, SPDT, On-None-On	NKK Switches	M2012SS1W01-RO	870-0375
Data Board	C/C++ programmable controller	Tern Inc.	586-Engine	
ADC	8 ch. 12-bit ADC (AD7852)	Tern Inc.	586-Engine Accessory	
Power Supply		Condor	HAD12-0.4-A+	744-9555
Enclosure	Rack; Aluminum; 6 in.; 12 in.; 8 in.; Black Textured; 0.05 in.; Tapping Screw	Bud	CS-11210-BT	736-1310
Heat Shrink	Kit, Tubing; 3/32 in.; 2:1; Polyolefin; Assorted	3M	FP-301-3/32-ASSORT	617-0260
TTS Paper	Toner Transfer System Paper	Pulsar (Digi-key)	182-1003-ND	
TRF	Toner Cover Film	Pulsar (Digi-key)	182-1022-ND	
Copper board	Double Sided	Rogers	RO3006	
Coversheet		Rogers	2001CFH0	
Bonding Film (glue)		Rogers	2001BF00	
Power Cable		Volex	17250 10 B1	626-3523
Connector	cable inlet	Volex	17252A 0 B1	626-9997
Connector	D-sub 10-pin	3M	8309-6000	618-4204
Connector	SMA bulkhead feedthru		132170	319-0185

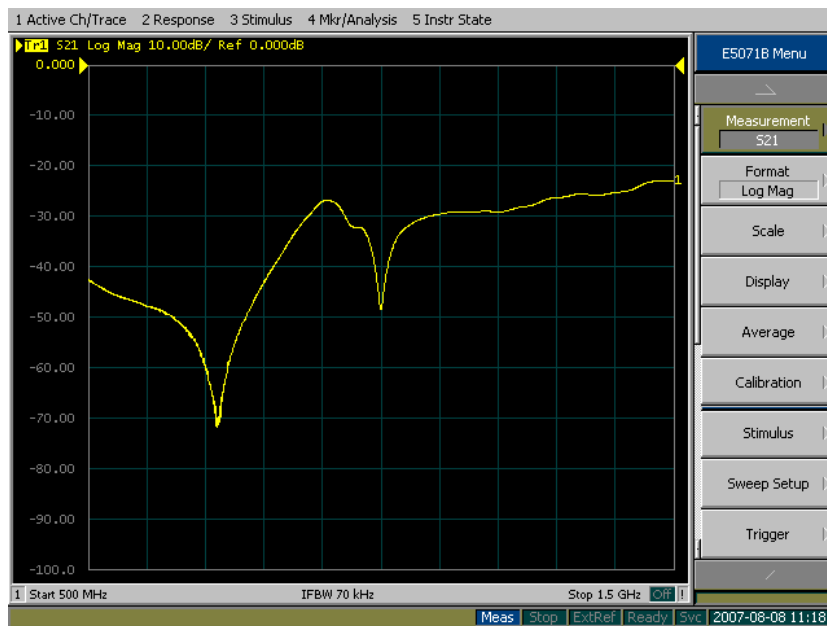
APPENDIX B

Device Instructions, Checklist and Consent Form

Device Instructions

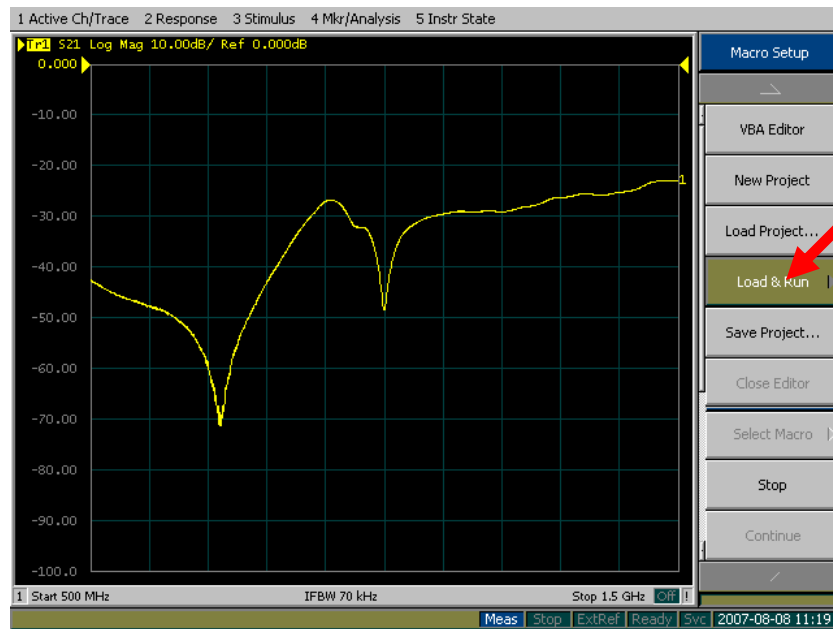
How to Use the Blood Glucose Sensing Device

1. Turn on the VNA and the Glucometer device (switch in the 'up' position and red light on).
2. After you see this screen:

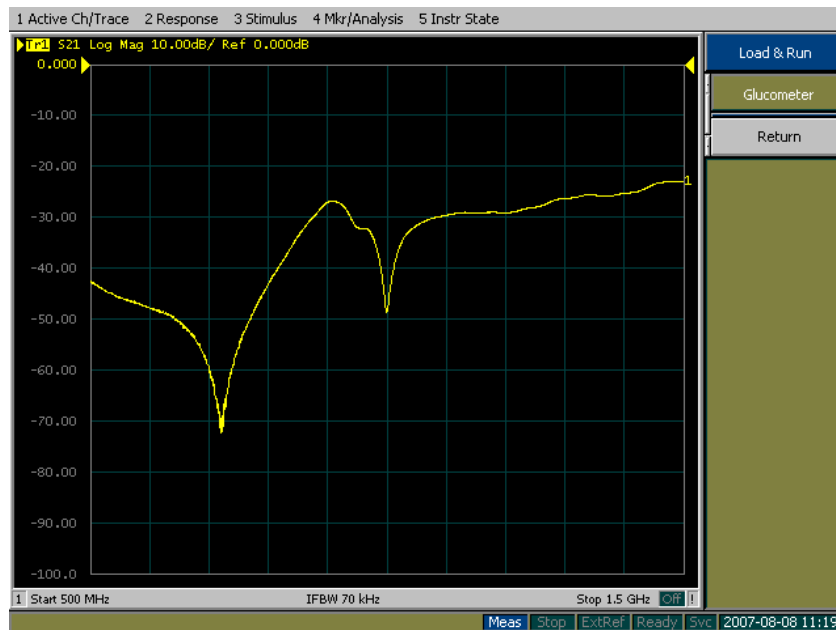


Press the button on the face of the VNA that says Macro Setup.

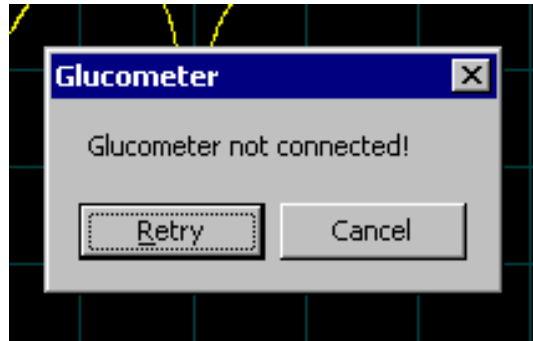
3. On the right side in the screen find and click on the button in the menu that says Load & Run.



4. Click on the button labeled Glucometer.

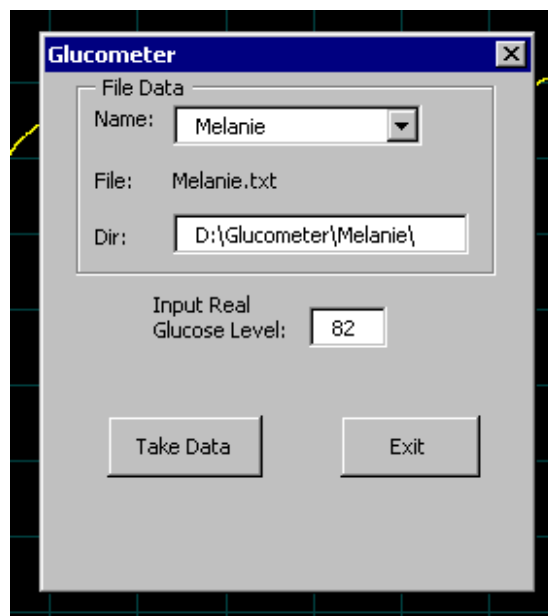


5. If you get a message that says “Glucometer not connected!” check to make sure that the device is turned on (switch in the ‘up’ position and red light on). Then click the Retry button.



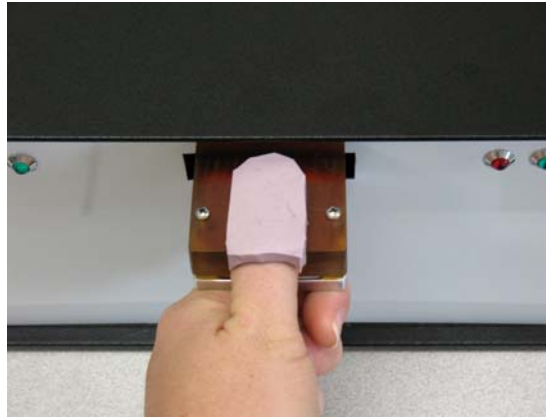
If this still does not work check to make sure that the USB to serial plug is connected to the port in the rear of the device nearest the cables from the VNA. Then click Retry.

6. Type your name into the provided text box or select it from the pull down menu. If you have the same name as another user please also type the initial of your last name or your whole last name at the end of your first name. Make sure the selected directory is D:\Glucometer\YourName\
7. Test your blood sugar with the One Touch Ultra Smart glucometer that is provided. Type in your actual glucose value that you measured into the box on the screen.

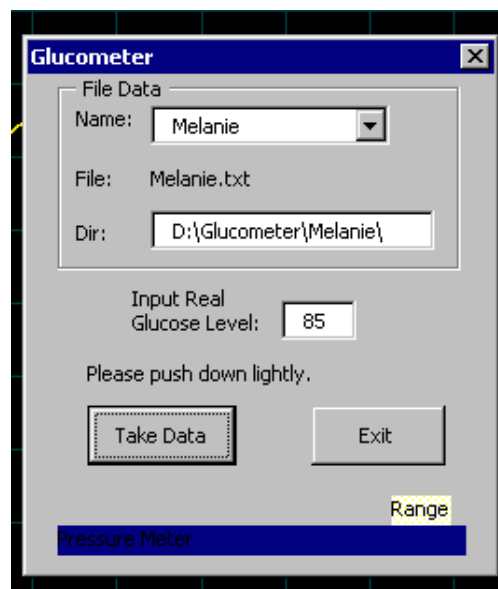


8. Click the take data button.

9. Place your thumb on the sensor with your molded guard over the top of your thumb.



10. Follow the directions on the screen firstly pressing down on the sensor with a light pressure until the status bar is inside of the marked range for 2 seconds. The VNA will make a beeping noise after it takes the data.



11. The VNA will then ask for you to apply a higher pressure until the status bar is inside of the new marked range for 2 seconds. The VNA will make a beeping noise when finished.
12. If you are the last user, exit the program and turn off the VNA, otherwise the next user follows steps 6-12.

Checklist of Information and Instructions Given to Every Participant in the Test

Instructional Checklist for Individual Conducting the Test:

- _____ 1.) Make a finger mold for the participant.
- _____ 2.) Designate a place for the mold in the plastic box by labeling a slot in the box with the participant's name.
- _____ 3.) Demonstrate how to put the lancet into the blood sampler lancing device.
- _____ 4.) Demonstrate the use of the blood sampling device.
- _____ 5.) Demonstrate how to place test strip into the Ultra Smart glucometer. Note when it is time to place blood onto strip.
- _____ 6.) Demonstrate how to find and load glucometer program on the VNA.
- _____ 7.) Show the participant the written instructions for using VNA and sensing device.
- _____ 8.) Describe the process of the program on the VNA for taking data.
- _____ 9.) Ask if the participant has any questions and answer them.
- _____ 10.) Do a run-through test with the participant going through all of the steps.
- _____ 11.) During run-through make sure participant knows and understands what they are doing so they are capable of doing further tests on their own.
- _____ 12.) Show the participant where and how to dispose of used lancet and test strip.
- _____ 13.) Show the participant how to leave testing area set-up for next participant.

Consent Form

**CONSENT FORM
AND
INFORMATION ABOUT**

Collection of Calibration Data for a Noninvasive Glucose Sensor

**Microwave Applied Metrology Laboratory
Department of Electrical and Computer Engineering
Baylor University**

You are being requested to participate in a research study to continue the development of a noninvasive electrical permittivity sensor to measure glucose in the blood. Low-level electrical signals similar to those produced by a cell phone are being studied as a means of sensing glucose levels in blood by simply placing a small sensor against the skin.

This is currently a non-funded research project. The laboratory will not receive payment from an outside source for the costs related to the conduct of this study.

Before you agree to volunteer to take part in this research study, it is very important that you understand the purpose of the study and the nature of the tests and procedures you will be asked to undergo.

This project is not connected with any teaching exercise nor will the internet be used to collect any data.

Minors will not be asked to participate in this study.

Purpose and Background

The purpose of this research study is to evaluate the effectiveness of using low-level electromagnetic signals to measure the dielectric properties (also called the electrical permittivity) of blood as a means of monitoring blood sugar. An important step in the project is to gather precise data on the electrical properties of blood versus glucose level. The data that we collect will be used to develop a calibration algorithm such that the sensor will provide an accurate glucose reading.

You will be one of approximately 50 subjects in this research study.

Procedures

As a first step in the data collection process you will be asked to use a conventional glucometer to measure the glucose level in a small sample of your blood obtained by pricking your finger with a small lancet. This procedure is that performed routinely by diabetic patients in managing their blood glucose levels.

Secondly, we will be measuring and recording the response of an electrical sensor upon which you will be asked to place your thumb for approximately ten seconds. The electrical signal from the sensor will be of such low intensity that you will feel no sensation or experience any effect whatsoever.

Length of Study and Number of Visits

You will be asked to repeat the procedure at random intervals of time at your convenience for a minimum of 10 trials.

Exclusions

There are no exclusions.

Discomfort and Risks

You will experience the discomfort of pricking your finger for the purpose of extracting a small sample of blood for each experimental trial.

Reproductive Risks

There are no reproductive risks associated with this study.

Benefits

The potential benefit is the development of a meter that will measure blood sugar without having to prick fingers.

Alternative Therapies

Not applicable.

Confidentiality

Your participation in this research study will be kept confidential in accordance with applicable law; however, your records related to this study may be accessed by the following:

- the Baylor University Institutional Review Board (The Baylor IRB has reviewed this project for the purpose of protecting your rights.)
- local, state and federal agencies (such as the Office for Human Research Protections and the U.S. Food and Drug Administration) when required by law.

You will not be identified in any publication or presentation of findings resulting from the study.

Cost and Compensation

There will be no cost to you or payment to you if you take part in this study.

Compensation or Medical Treatments for Research-Related Adverse Events

None.

Whom to Contact for Questions or Emergencies

You may contact Dr. Randall Jean, Associate Professor of Electrical and Computer Engineering, Baylor University, at 254-710-4194 or Baylor's University Committee for Protection of Human Subjects in Research. The chairman is Dr. Matthew S Stanford, One Bear Place #97334, Waco, Texas 76798-7334, phone number 254-710-2236.

Participation

Participation in this study is voluntary.

Right to Withdraw

You may withdraw from participation in the study at any time. Your participation may be terminated at any time without your consent.

New Findings

Any new findings developed during the course of your participation in the study, which may be related to your willingness to participate, will be provided to you.

Statement of Consent

The research study has been explained to me and I have had an opportunity to read this consent form and have all of my questions answered. I have been informed that I may leave the study at any time. I freely agree to take part in this research. A signed copy of this consent form will be given to me.

Printed Name of Subject

Signature

Date

Statement of Person Obtaining Consent

I have carefully explained to the subject the nature of the study. I hereby certify that to the best of my knowledge the subject signing this consent form understands clearly the nature, demands, risks and benefits involved in participating in this study. A medical problem or language or educational barrier has not prevented a clear understanding of the subject's involvement in this study.

Printed Name of Person
Obtaining Consent

Signature

Date

07/13/2007

APPENDIX C

Excel Data and Regression Results for the “Soda Test”

Table C.1: Table of low pressure and high pressure glucose values and frequencies where the minimum value of the null occurs

Low Pressure		High Pressure	
Glucose	Frequency	Glucose	Frequency
85	3801350168.770	85	3801162645.330
85	3801162645.330	85	3801912739.090
87	3802100262.530	87	3801912739.090
83	3802100262.530	83	3795724465.560
102	3794036754.590	102	3793849231.150
113	3794224278.030	113	3792349043.630
148	3791036379.550	148	3791598949.870
151	3790661332.670	151	3787660957.620
129	3794036754.590	129	3789723715.460
128	3792536567.070	128	3789911238.900
131	3793661707.710	131	3789536192.020
127	3792911613.950	127	3790286285.790
113	3793849231.150	113	3790848856.110
113	3791973996.750	113	3790661332.670
109	3794411801.480	109	3792349043.630
103	3794036754.590	103	3791786473.310
97	3793286660.830	97	3792349043.630

Table C.2: Regression output for low pressure data

Regression Statistics	
Multiple R	0.830651587
R Square	0.689982059
Adjusted R Square	0.669314197
Standard Error	12.2747187
Observations	17

ANOVA					
	<i>df</i>	<i>SS</i>	<i>MS</i>	<i>F</i>	<i>Significance F</i>
Regression	1	5029.969214	5029.969	33.38429665	3.64559E-05
Residual	15	2260.030786	150.6687		
Total	16	7290			

Table C.2: Regression output for low pressure data (cont.)

	<i>Coefficients</i>	<i>Standard Error</i>	<i>t Stat</i>	<i>P-value</i>	<i>Lower 95%</i>	<i>Upper 95%</i>
Intercept	17389.25762	2990.22528	5.815367	3.40357E-05	11015.74333	23762.77
X Variable 1	-4.55247E-06	7.87909E-07	-5.77791	3.64559E-05	-6.23186E-06	-2.9E-06

Table C.3: Residual output for low pressure data

<i>Observation</i>	<i>Actual Y</i>	<i>Predicted Y</i>	<i>Residuals</i>	<i>Standard Residuals</i>
1	85	83.72763999	1.27236	0.107056447
2	85	84.58133469	0.418665	0.035226524
3	87	80.31286117	6.687139	0.562656258
4	83	80.31286117	2.687139	0.226096021
5	102	117.0217336	-15.0217	-1.263929555
6	113	116.1680389	-3.16804	-0.266558979
7	148	130.6808489	17.31915	1.457234403
8	151	132.3882383	18.61176	1.565994735
9	129	117.0217336	11.97827	1.007852046
10	128	123.8512912	4.148709	0.349072602
11	131	118.729123	12.27088	1.032472319
12	127	122.1439018	4.856098	0.408592389
13	113	117.8754283	-4.87543	-0.410218825
14	113	126.4123753	-13.4124	-1.128518057
15	109	115.3143441	-6.31434	-0.531289289
16	103	117.0217336	-14.0217	-1.179789495
17	97	120.4365124	-23.4365	-1.971949543

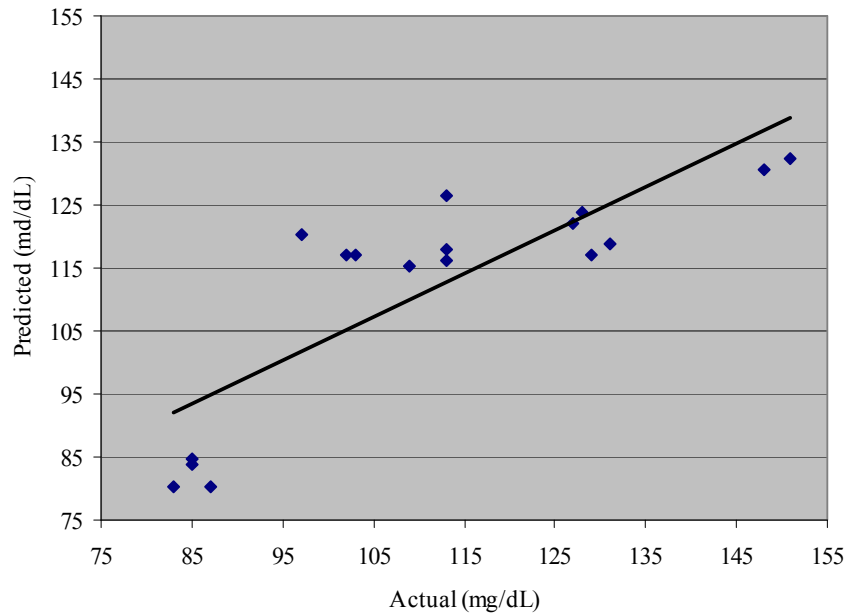


Figure C.1: Chart plotting the predicted values of glucose against the actual measured values of glucose. (Low)

Table C.4: Regression output for high pressure data

<i>Regression Statistics</i>	
Multiple R	0.806305453
R Square	0.650128484
Adjusted R Square	0.626803716
Standard Error	13.03984497
Observations	17

ANOVA					
	<i>df</i>	<i>SS</i>	<i>MS</i>	<i>F</i>	<i>Significance F</i>
Regression	1	4739.436647	4739.437	27.87288135	9.25929E-05
Residual	15	2550.563353	170.0376		
Total	16	7290			

	<i>Coefficients</i>	<i>Standard Error</i>	<i>t Stat</i>	<i>P-value</i>	<i>Lower 95%</i>	<i>Upper 95%</i>
Intercept	14797.59418	2781.639665	5.319738	8.57733E-05	8868.66961	20726.52
X Variable 1	-3.8716E-06	7.33331E-07	-5.27948	9.25929E-05	-5.43466E-06	-2.3E-06

Table C.5: Residual output for high pressure data

<i>Observation</i>	<i>Actual Y</i>	<i>Predicted Y</i>	<i>Residuals</i>	<i>Standard Residuals</i>
1	85	80.99481865	4.005181	0.317222599
2	85	78.09075208	6.909248	0.547233543
3	87	78.09075208	8.909248	0.705639653
4	83	102.0493013	-19.0493	-1.508762859
5	102	109.3094677	-7.30947	-0.578932176
6	113	115.1176009	-2.1176	-0.167720459
7	148	118.0216674	29.97833	2.374375523
8	151	133.268017	17.73198	1.404427229
9	129	125.2818339	3.718166	0.294490114
10	128	124.5558173	3.444183	0.272789795
11	131	126.0078505	4.992149	0.395393488
12	127	123.1037839	3.896216	0.308592215
13	113	120.925734	-7.92573	-0.627742347
14	113	121.6517507	-8.65175	-0.685245083
15	109	115.1176009	-6.1176	-0.484532679
16	103	117.2956508	-14.2957	-1.132259218
17	97	115.1176009	-18.1176	-1.43496934

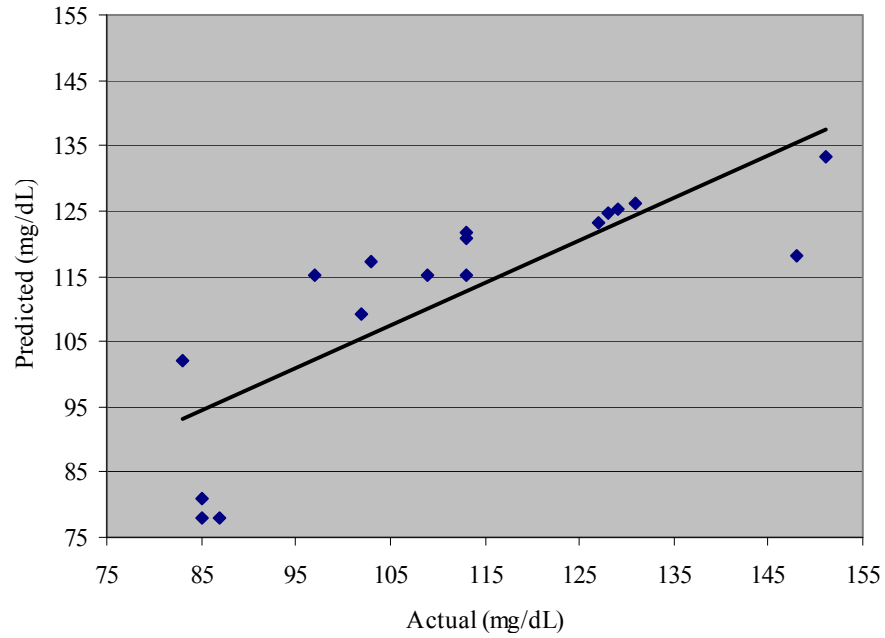


Figure C.2: Chart plotting the predicted values of glucose against the actual measured values of glucose. (High)

Table C.6: Table of low pressure and high pressure glucose values and frequencies where the minimum value of the null occurs after four data points were removed from the data set based on their standard residual values. These points are highlighted in tables C.3 and C.6.

Low Pressure		High Pressure	
Glucose	Frequency	Glucose	Frequency
85	3801350168.770	85	3801162645.330
85	3801162645.330	85	3801912739.090
87	3802100262.530	87	3801912739.090
83	3802100262.530	102	3793849231.150
113	3794224278.030	113	3792349043.630
129	3794036754.590	129	3789723715.460
128	3792536567.070	128	3789911238.900
131	3793661707.710	131	3789536192.020
127	3792911613.950	127	3790286285.790
113	3793849231.150	113	3790848856.110
113	3791973996.750	113	3790661332.670
109	3794411801.480	109	3792349043.630
103	3794036754.590	103	3791786473.310

Table C.7: Regression output for modified low pressure data

<i>Regression Statistics</i>	
Multiple R	0.894056314
R Square	0.799336692
Adjusted R Square	0.781094573
Standard Error	8.494716566
Observations	13

<i>ANOVA</i>					
	<i>df</i>	<i>SS</i>	<i>MS</i>	<i>F</i>	<i>Significance F</i>
Regression	1	3161.93	3161.930003	43.8181932	3.76E-05
Residual	11	793.7623	72.16020954		
Total	12	3955.692			

	<i>Coefficients</i>	<i>Standard Error</i>	<i>t Stat</i>	<i>P-value</i>	<i>Lower 95%</i>	<i>Upper 95%</i>
Intercept	15556.67469	2333.78	6.665870598	3.53472E-05	10420.06	20693.29
X Variable 1	-4.06965E-06	6.15E-07	-6.619531191	3.76294E-05	-5.4E-06	-2.7E-06

Table C.8: Residual output for modified low pressure data

<i>Observation</i>	<i>Actual Y</i>	<i>Predicted Y</i>	<i>Residuals</i>	<i>Standard Residuals</i>
1	85	86.49197	-1.491966329	-0.183444379
2	85	87.25512	-2.255121985	-0.277278009
3	87	83.43934	3.560656294	0.437799682
4	83	83.43934	-0.439343706	-0.054019405
5	113	115.4919	-2.491881335	-0.306388701
6	129	116.255	12.74496301	1.567054017
7	128	122.3603	5.639717762	0.69343021
8	131	117.7813	13.2186517	1.625296301
9	127	120.834	6.166029074	0.758142697
10	113	117.0182	-4.018192647	-0.494055959
11	113	124.6497	-11.64974921	-1.432392253
12	109	114.7287	-5.728725638	-0.704374153
13	103	116.255	-13.25503699	-1.629770047

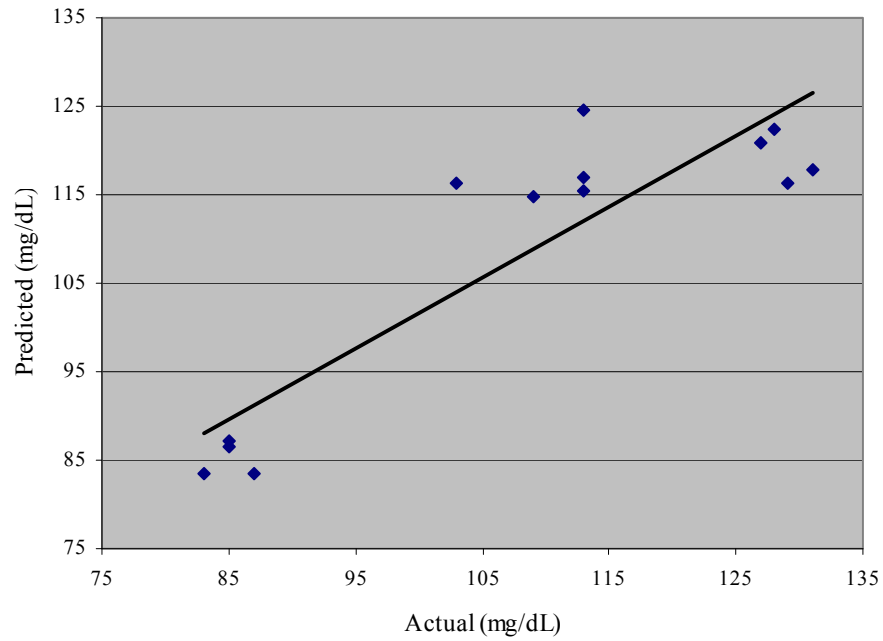


Figure C.3: Chart plotting the predicted values of glucose against the actual measured values of glucose. (Second regression - low)

Table C.9: Regression output for modified high pressure data

<i>Regression Statistics</i>	
Multiple R	0.919334545
R Square	0.845176006
Adjusted R Square	0.831101098
Standard Error	6.849288483
Observations	13

<i>ANOVA</i>					
	<i>df</i>	<i>SS</i>	<i>MS</i>	<i>F</i>	<i>Significance F</i>
Regression	1	2817.037	2817.036643	60.04841924	8.83E-06
Residual	11	516.0403	46.91275272		
Total	12	3333.077			

	<i>Coefficients</i>	<i>Standard Error</i>	<i>t Stat</i>	<i>P-value</i>	<i>Lower 95%</i>	<i>Upper 95%</i>
Intercept	12269.16624	1569.159	7.818941951	8.11518E-06	8815.47	15722.86
X Variable 1	-3.20531E-06	4.14E-07	7.749091511	8.83235E-06	-4.1E-06	-2.3E-06

Table C.10: Residual output for modified high pressure data

<i>Observation</i>	<i>Actual Y</i>	<i>Predicted Y</i>	<i>Residuals</i>	<i>Standard Residuals</i>
1	85	85.24888	-0.248875334	-0.037951651
2	85	82.84459	2.155410206	0.328684146
3	87	82.84459	4.155410206	0.633669383
4	102	108.6907	-6.690659415	-1.020276174
5	113	113.4992	-0.499230495	-0.076128965
6	129	121.9142	7.085770082	1.080527634
7	128	121.3132	6.686841467	1.019693965
8	131	122.5153	8.484698697	1.293853922
9	127	120.111	6.888984269	1.05051925
10	113	118.3078	-5.307801576	-0.809400561
11	113	118.9089	-5.908872961	-0.90105951
12	109	113.4992	-4.499230495	-0.68609944
13	103	115.3024	-12.30244465	-1.876031999

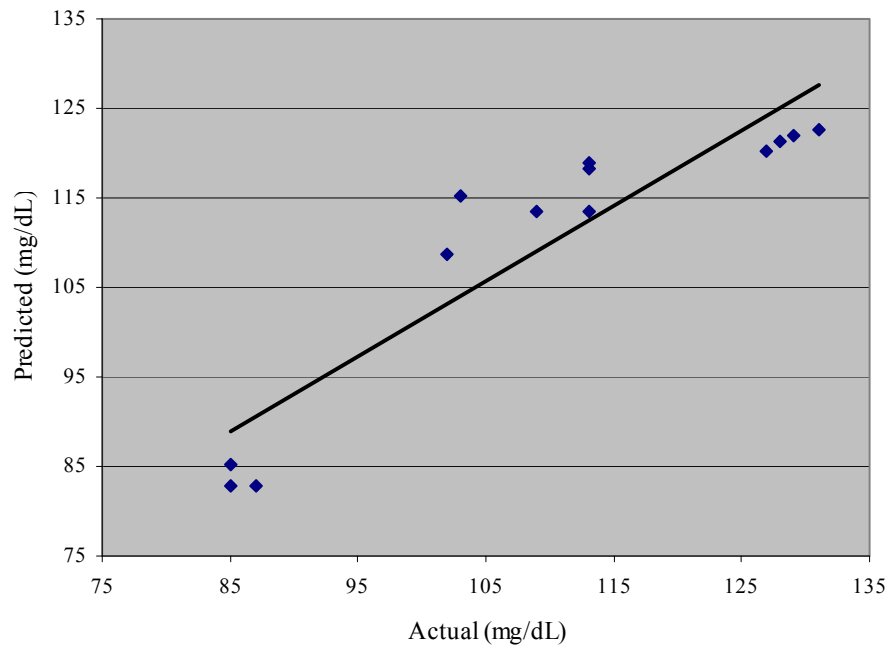


Figure C.4: Chart plotting the predicted values of glucose against the actual measured values of glucose. (Second regression - high)

APPENDIX D

Excel Data and Regression Results for Developing a Calibration Algorithm

Regression Data for Participants with the Least Noisy Data Sets

Table D.1: R Square values and their corresponding frequencies

Frequency (GHz)	R Square Value
1.05	0.89235
2.44	0.79288
3.66	0.85210

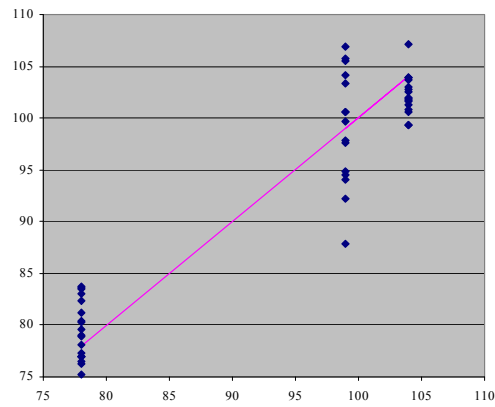


Figure D.1: Predicted values of glucose versus actual values of glucose for least noisy participants at 1.05 GHz

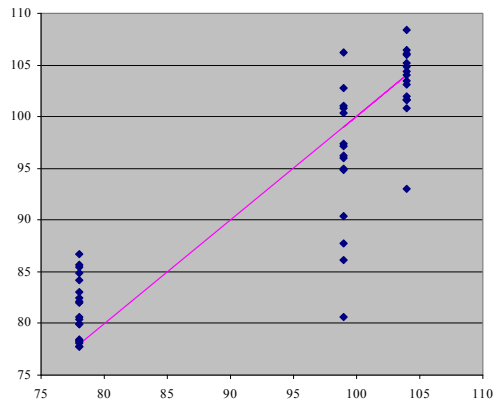


Figure D.2: Predicted values of glucose versus actual values of glucose for least noisy participants at 2.44 GHz

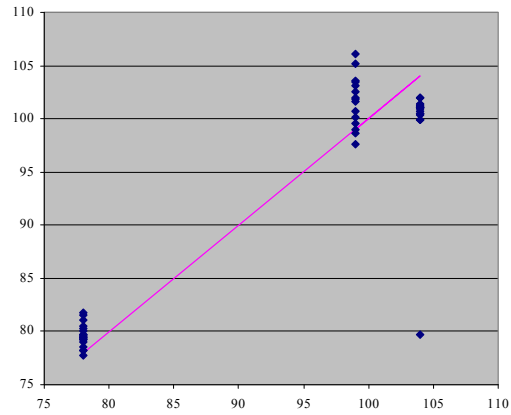


Figure D.3: Predicted values of glucose versus actual values of glucose for least noisy participants at 3.66 GHz

Regression Data for All Participants from Twenty-in-a-Row Test

Table D.2: R Square values and their corresponding frequencies

Frequency (GHz)	R Square Value
0.53	0.82687
0.97	0.97264
2.6	0.96846

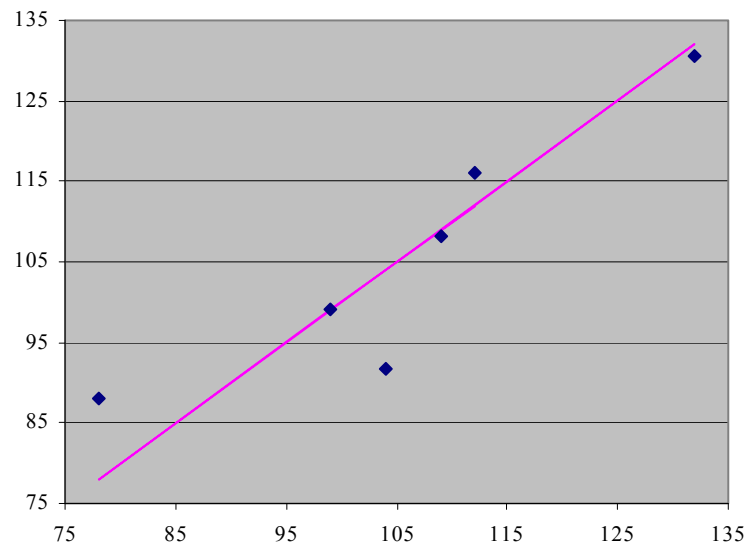


Figure D.4: Predicted values of glucose versus actual values of glucose for all participants at 0.53 GHz

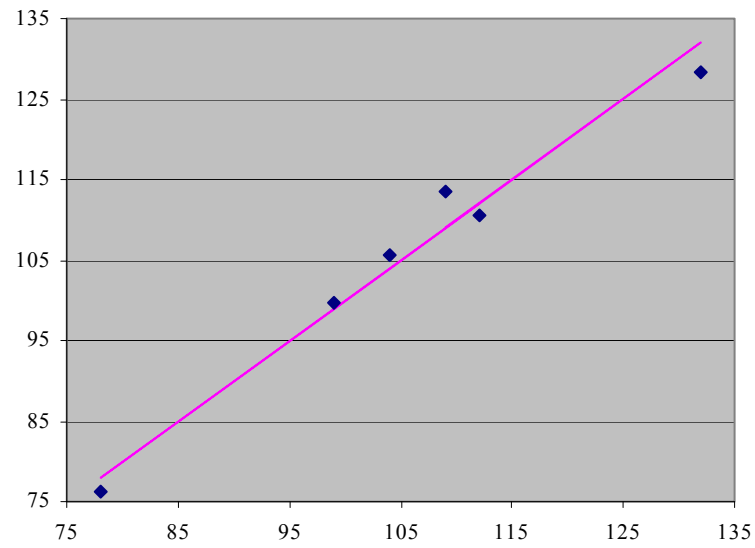


Figure D.5: Predicted values of glucose versus actual values of glucose for all participants at 0.97 GHz

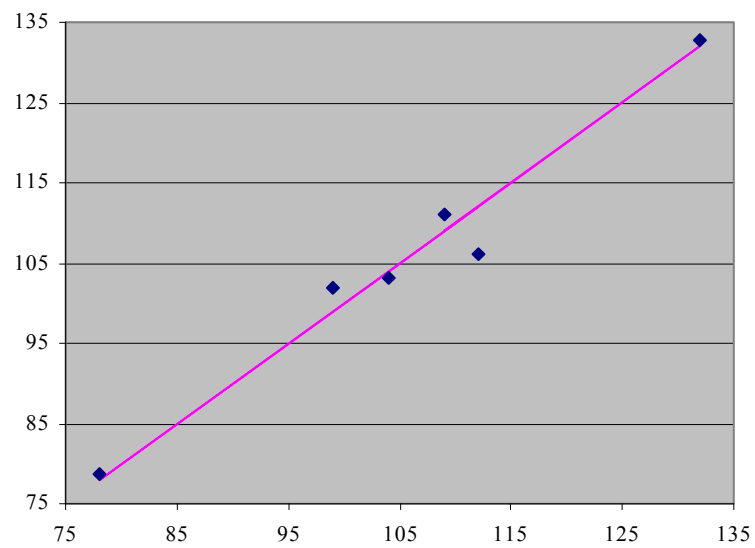


Figure D.6: Predicted values of glucose versus actual values of glucose for all participants at 2.60 GHz

Second Regression Results and Charts for all Participants from Second Experiment

Group

Table D.3: R Square values and their corresponding frequencies for the whole group

Frequency (GHz)	R Square Value
0.30	0.36884
0.47	0.40426
1.00	0.25859
1.70	0.11962
2.40	0.35552
3.02	0.35422
3.65	0.26831

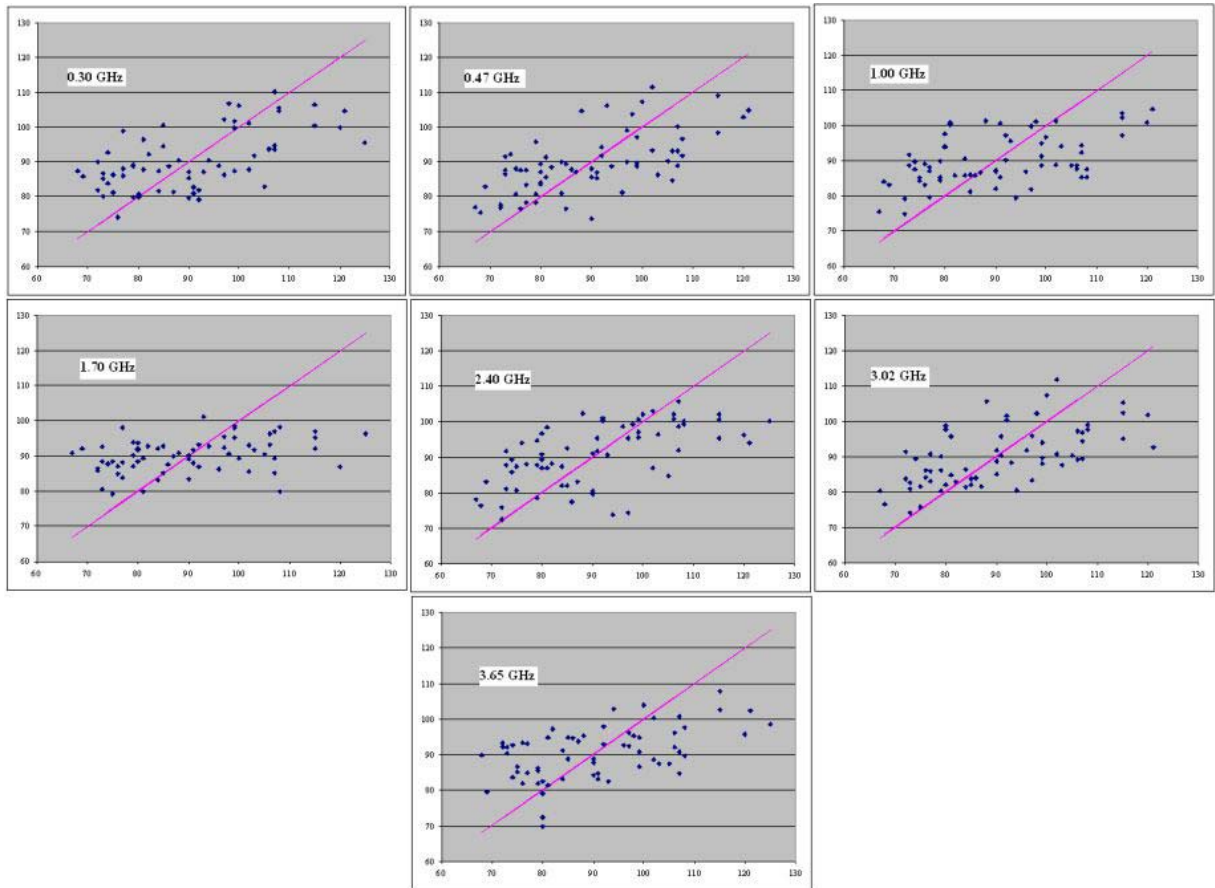


Figure D.7: Group predicted glucose values versus actual glucose values (mg/dL)

Participant #1

Table D.4: R Square values and their corresponding frequencies for participant #1

Frequency (GHz)	R Square Value
0.58	0.61039
1.05	0.90840
1.60	0.59002
1.75	0.89527
2.43	0.57555
2.50	0.23776
3.63	0.73125

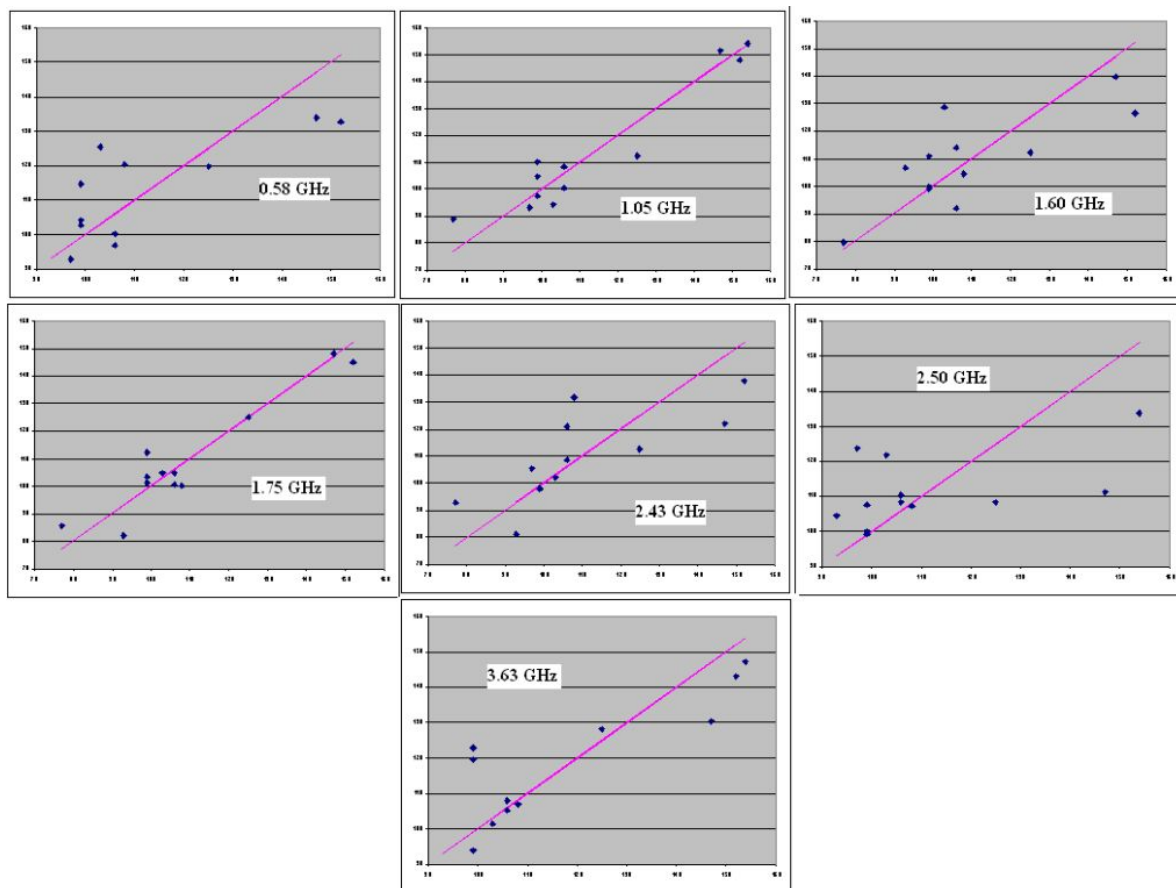


Figure D.8: Participant #1 predicted glucose values versus actual glucose values (mg/dL)

Table D.5: R Square values and their corresponding frequencies after the first difference method was applied for participant #1

Frequency (GHz)	R Square Value
0.58	0.67228
1.05	0.90875
1.60	0.67411
1.75	0.96362
2.43	0.74118
2.50	0.52326
3.63	0.59387

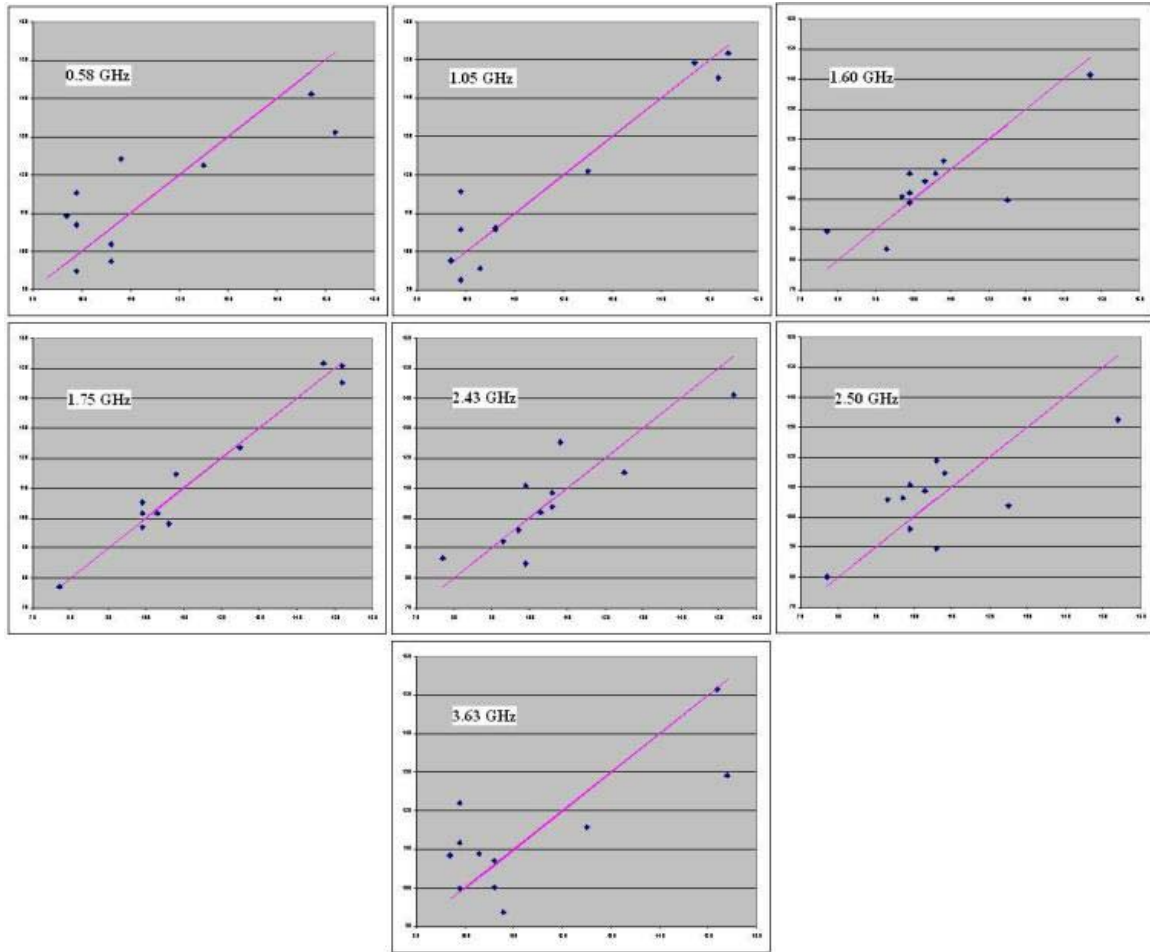


Figure D.9: Participant #1 predicted glucose values versus actual glucose values (mg/dL) after the first difference method was applied

Participant #2

Table D.6: R Square values and their corresponding frequencies for participant #2

Frequency (GHz)	R Square Value
0.14	0.58761
0.51	0.28169
0.94	0.61869
2.43	0.45259
2.55	0.32964
3.00	0.69334
3.65	0.67200

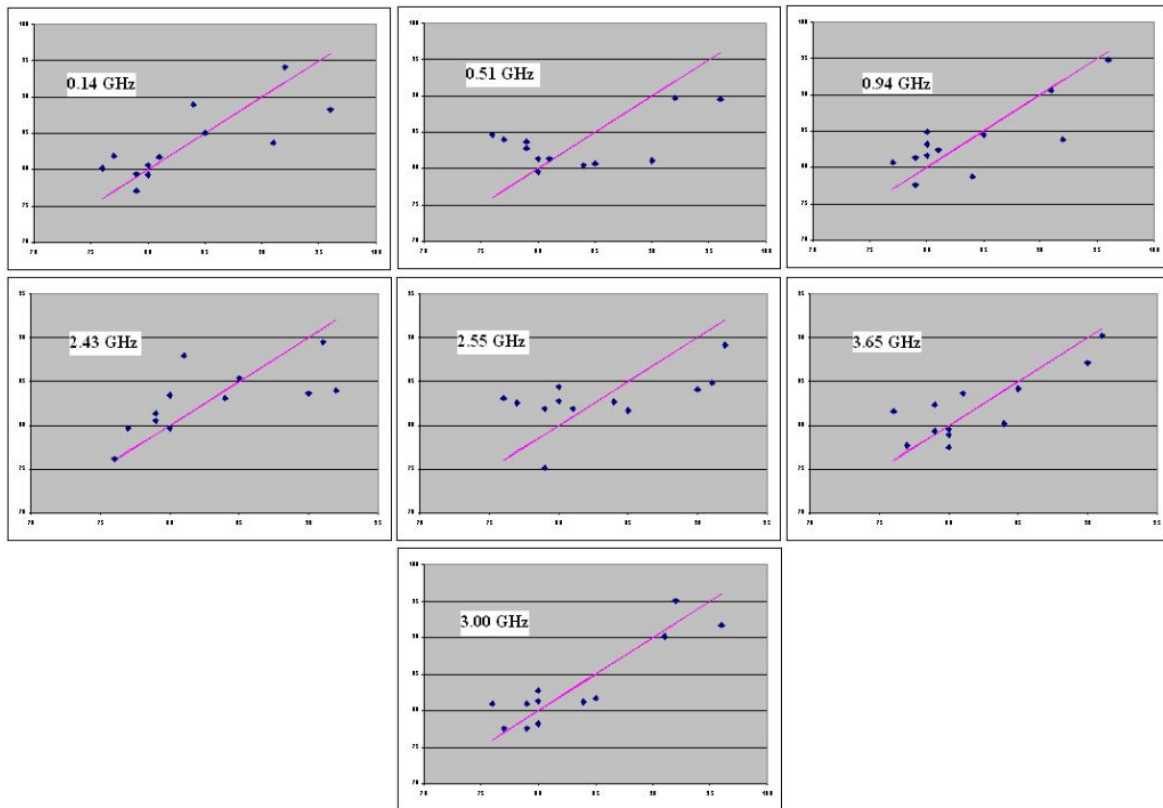


Figure D.10: Participant #2 predicted glucose values versus actual glucose values (mg/dL)

Table D.7: R Square values and their corresponding frequencies after the first difference method was applied for participant #2

Frequency (GHz)	R Square Value
0.14	0.80384
0.51	0.84369
0.94	0.77567
2.43	0.51552
2.55	0.69328
3.00	0.69461
3.65	0.68769

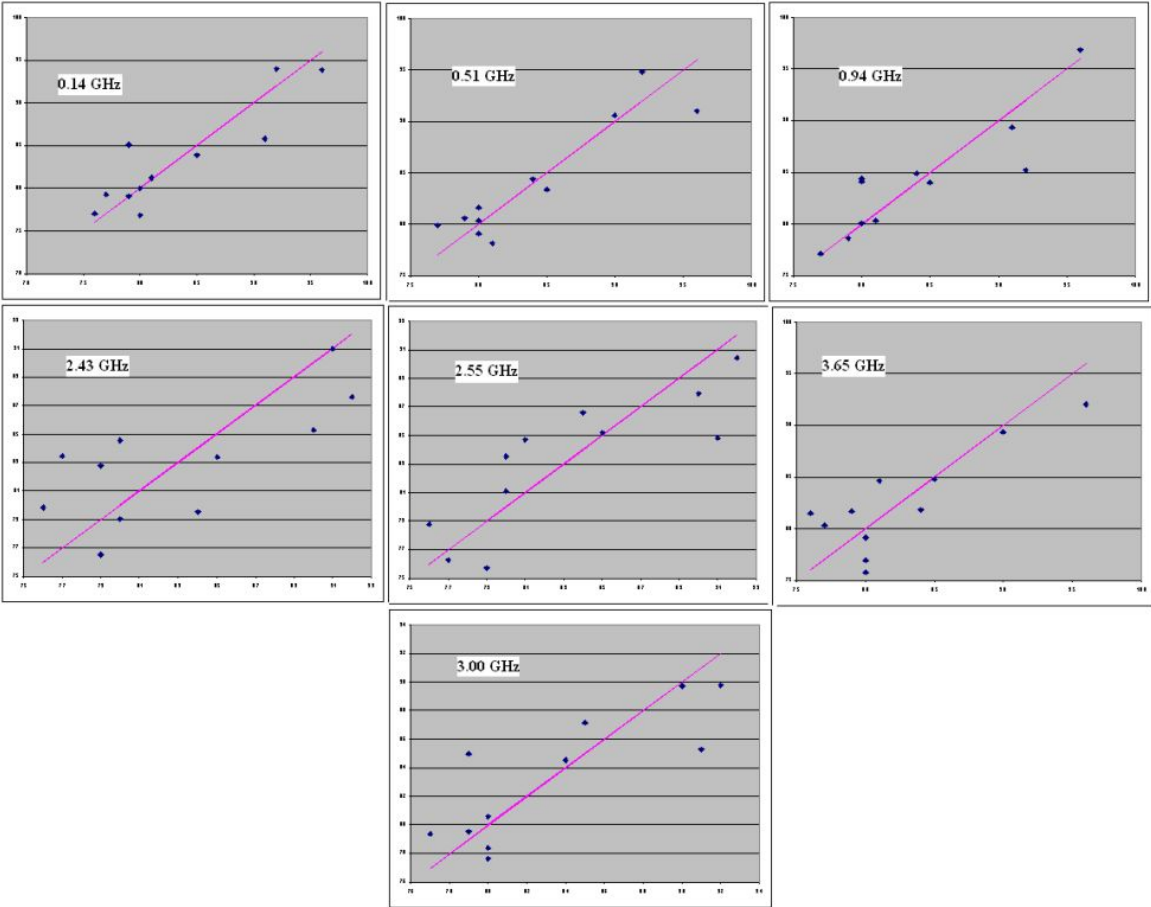


Figure D.11: Participant #2 predicted glucose values versus actual glucose values (mg/dL) after the first difference method was applied

Participant #3

Table D.8: R Square values and their corresponding frequencies for participant #3

Frequency (GHz)	R Square Value
0.16	0.69352
0.55	0.24865
0.99	0.68509
1.74	0.78069
2.45	0.51082
2.54	0.47968
3.63	0.71609

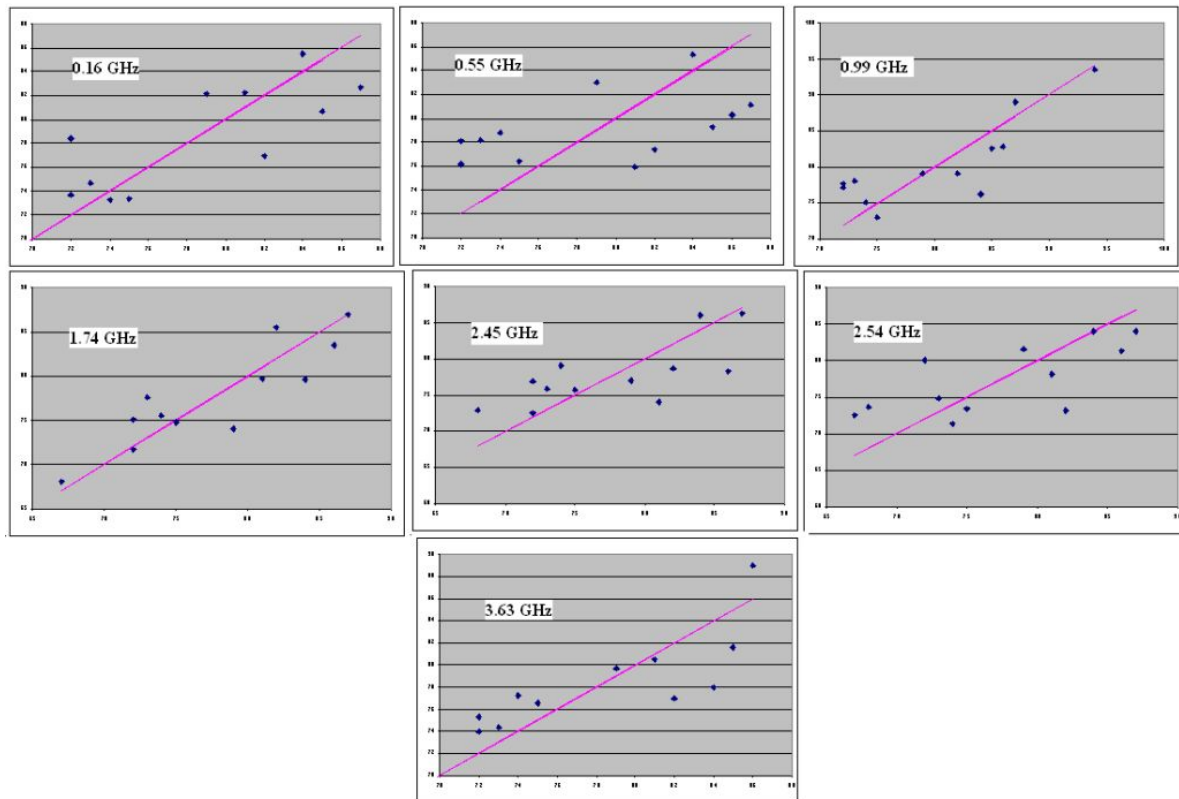


Figure D.12: Participant #3 predicted glucose values versus actual glucose values (mg/dL)

Table D.9: R Square values and their corresponding frequencies after the first difference method was applied for participant #3

Frequency (GHz)	R Square Value
0.16	0.80663
0.55	0.76823
0.99	0.90365
1.74	0.88084
2.45	0.85229
2.54	0.93808
3.63	0.75672

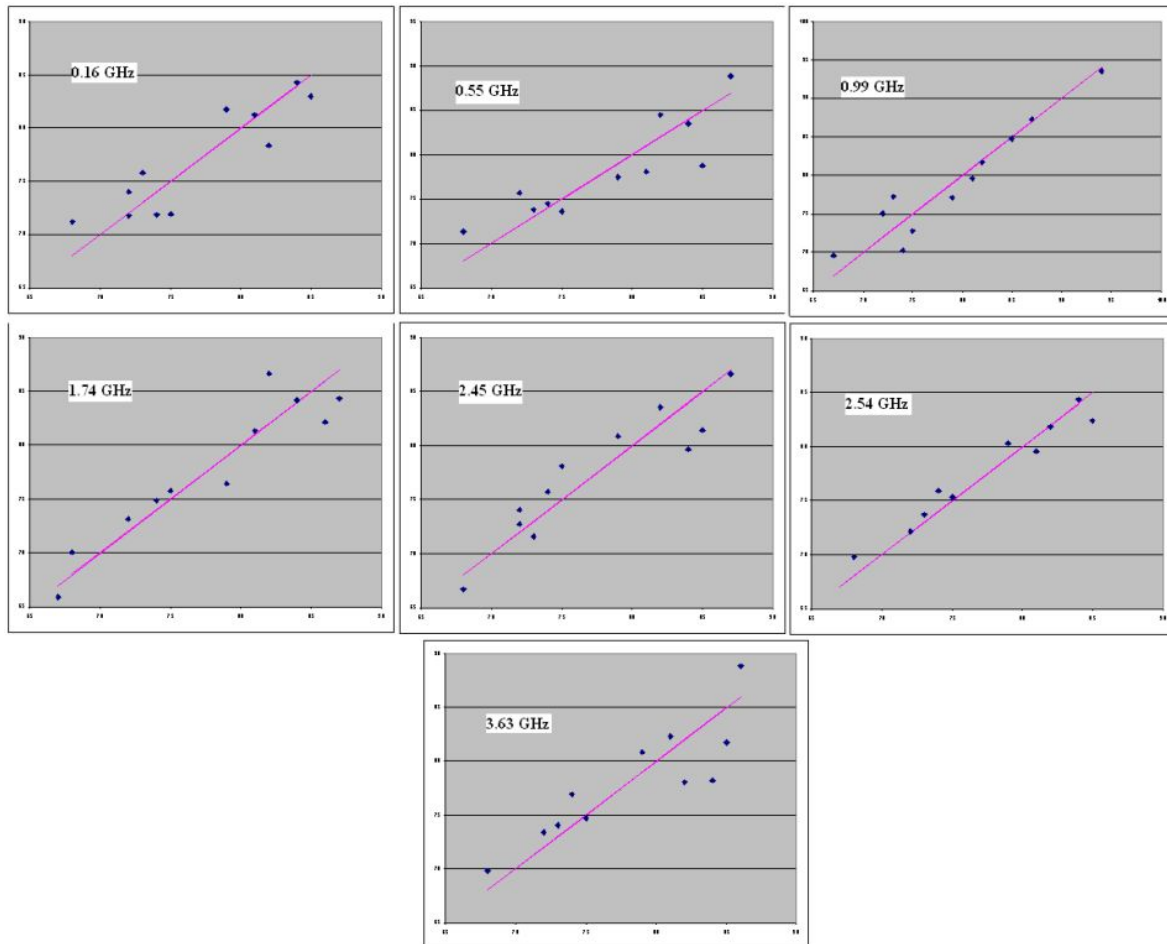


Figure D.13: Participant #3 predicted glucose values versus actual glucose values (mg/dL) after the first difference method was applied

Participant #4

Table D.10: R Square values and their corresponding frequencies for participant #4

Frequency (GHz)	R Square Value
0.14	0.64868
0.47	0.35283
1.72	0.91247
2.00	0.29950
2.50	0.71261
3.05	0.35149
3.63	0.64073

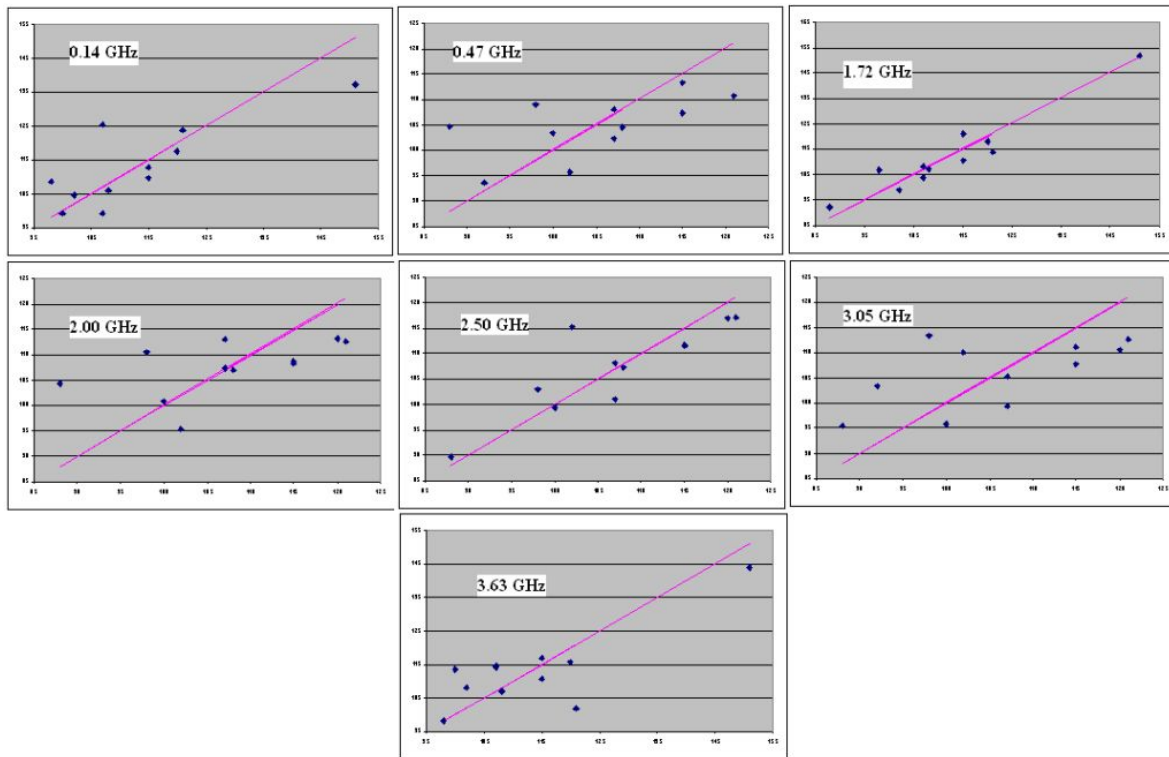


Figure D.14: Participant #4 predicted glucose values versus actual glucose values (mg/dL)

Table D.11: R Square values and their corresponding frequencies after the first difference method was applied for participant #4

Frequency (GHz)	R Square Value
0.14	0.83795
0.47	0.17869
1.72	0.89726
2.00	0.47220
2.50	0.79519
3.05	0.30987
3.63	0.86979

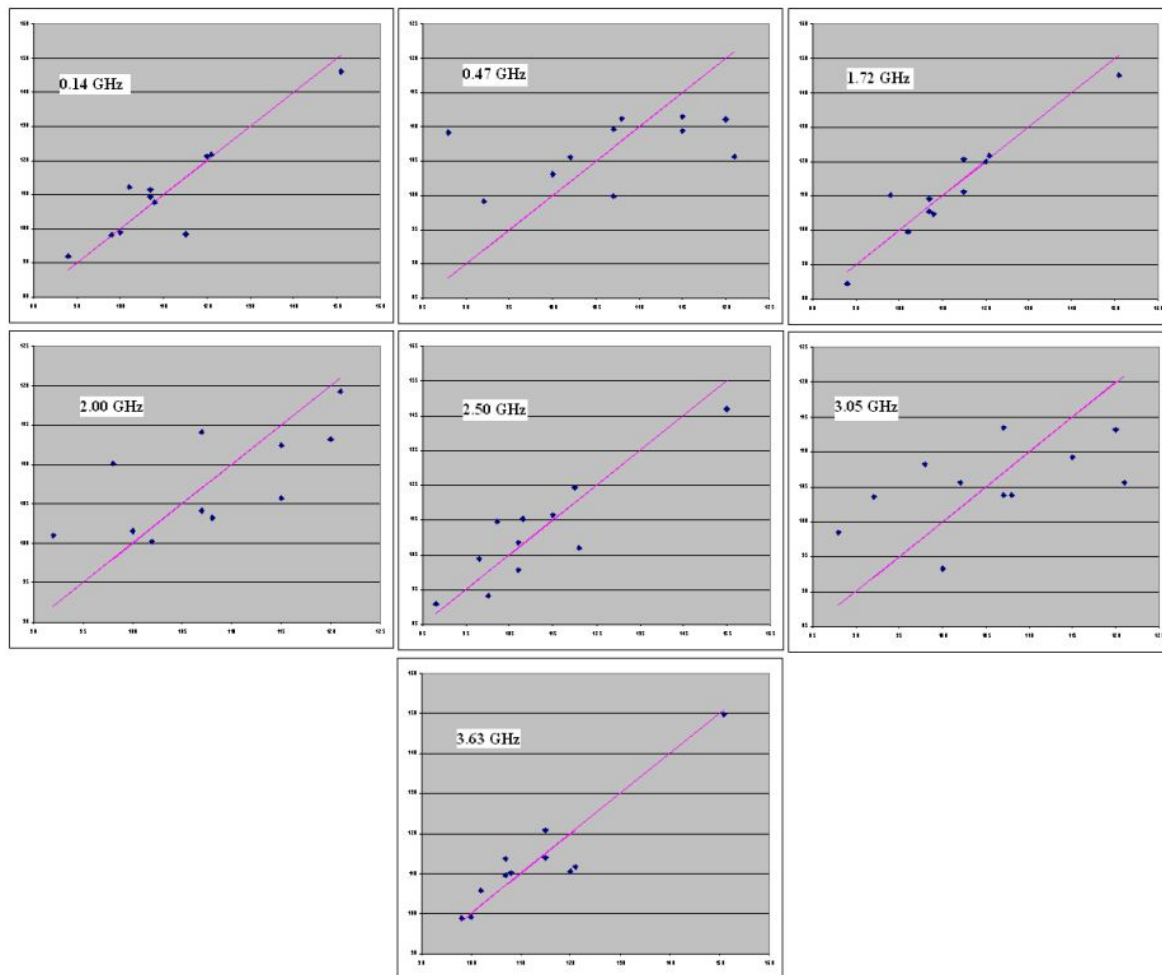


Figure D.15: Participant #4 predicted glucose values versus actual glucose values (mg/dL) after the first difference method was applied

Participant #5

Table D.12: R Square values and their corresponding frequencies for participant #5

Frequency (GHz)	R Square Value
0.50	0.84169
1.05	0.60105
1.71	0.82231
2.43	0.66176
2.55	0.65247
3.07	0.64104
3.64	0.66619

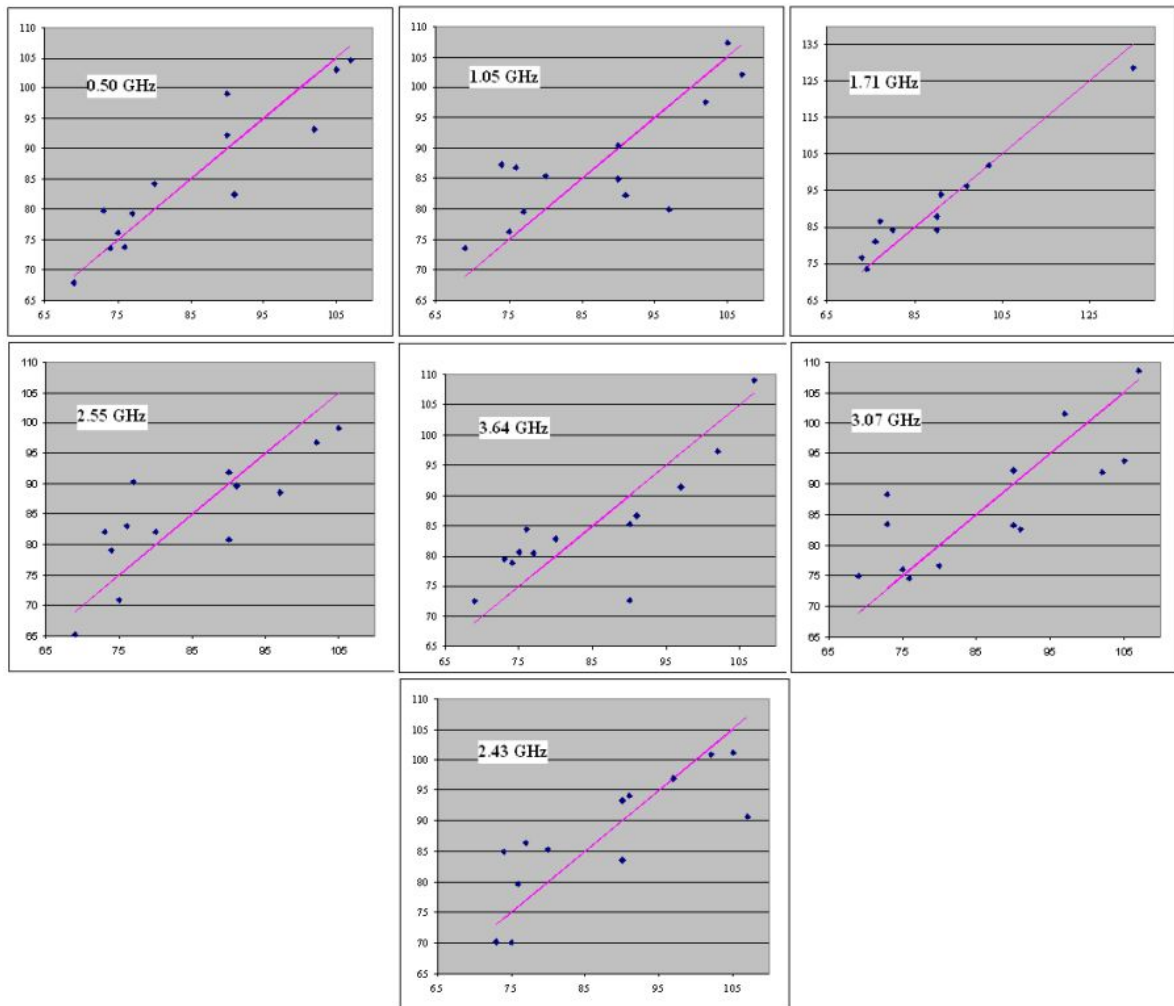


Figure D.16: Participant #5 predicted glucose values versus actual glucose values (mg/dL)

Table D.13: R Square values and their corresponding frequencies after the first difference method was applied for participant #5

Frequency (GHz)	R Square Value
0.50	0.89253
1.05	0.89155
1.71	0.97659
2.43	0.70702
2.55	0.90437
3.07	0.54319
3.64	0.89787

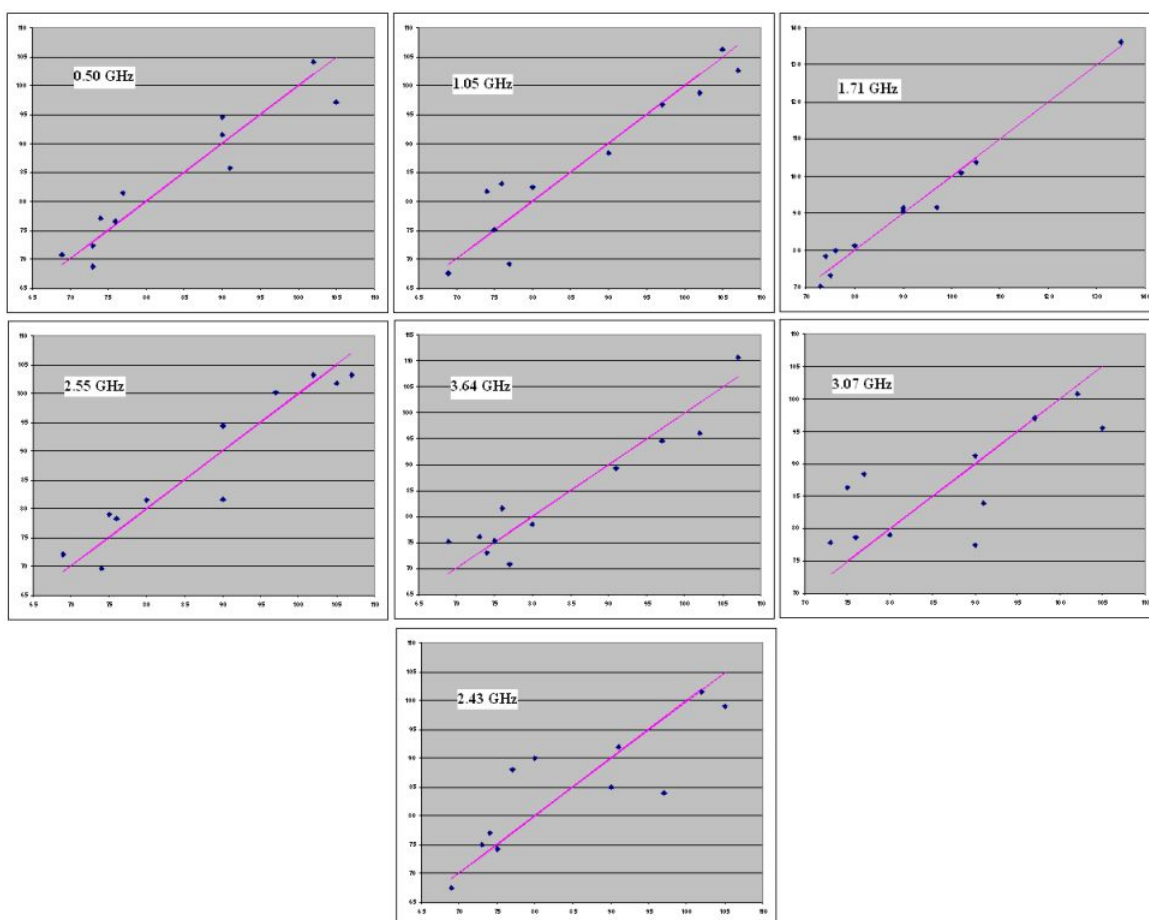


Figure D.17: Participant #5 predicted glucose values versus actual glucose values (mg/dL) after the first difference method was applied

Participant #4-2

Table D.14: R Square values and their corresponding frequencies for participant #4-2

Frequency (GHz)	R Square Value
0.14	0.74369
0.47	0.24777
1.72	0.63118
2.00	0.60515
2.50	0.49404
3.05	0.51865
3.63	0.92197

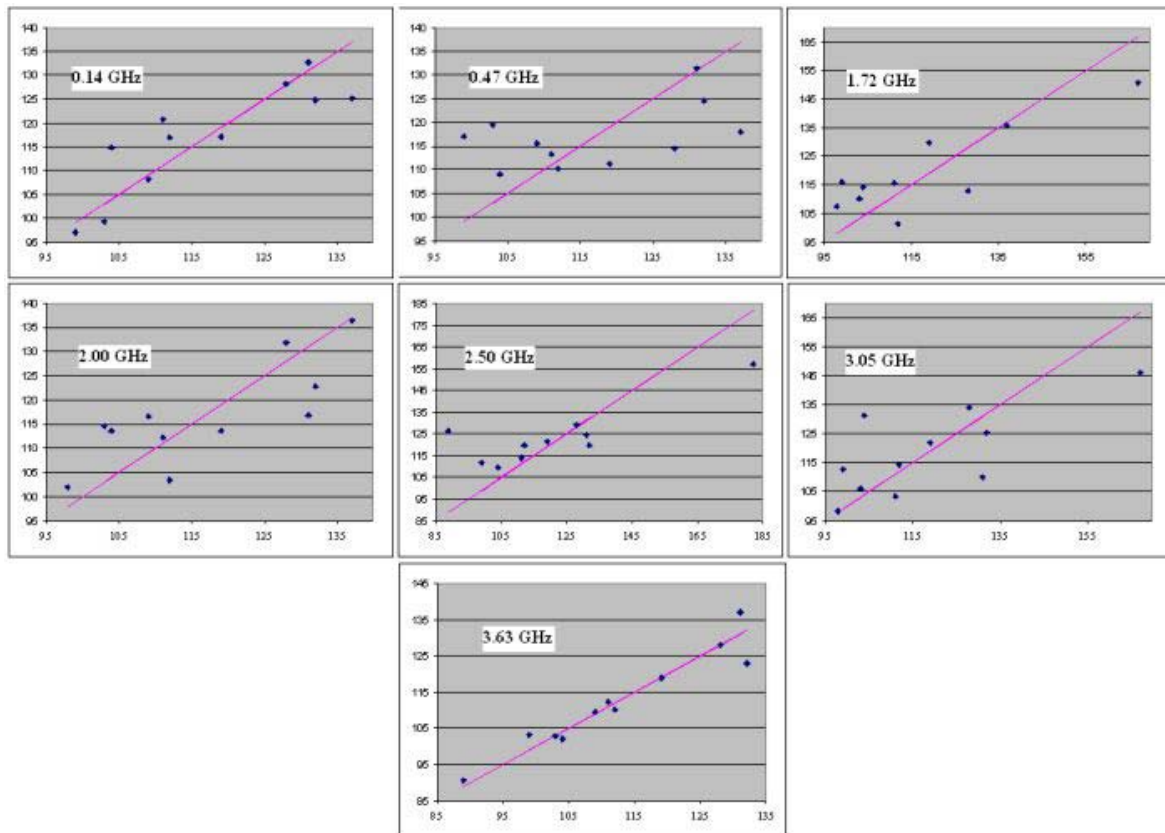


Figure D.18: Participant #4-2 predicted glucose values versus actual glucose values (mg/dL)

Table D.15: R Square values and their corresponding frequencies after the first difference method was applied for participant #4-2

Frequency (GHz)	R Square Value
0.14	0.78153
0.47	0.68178
1.72	0.78280
2.00	0.61360
2.50	0.43364
3.05	0.72353
3.63	0.92657

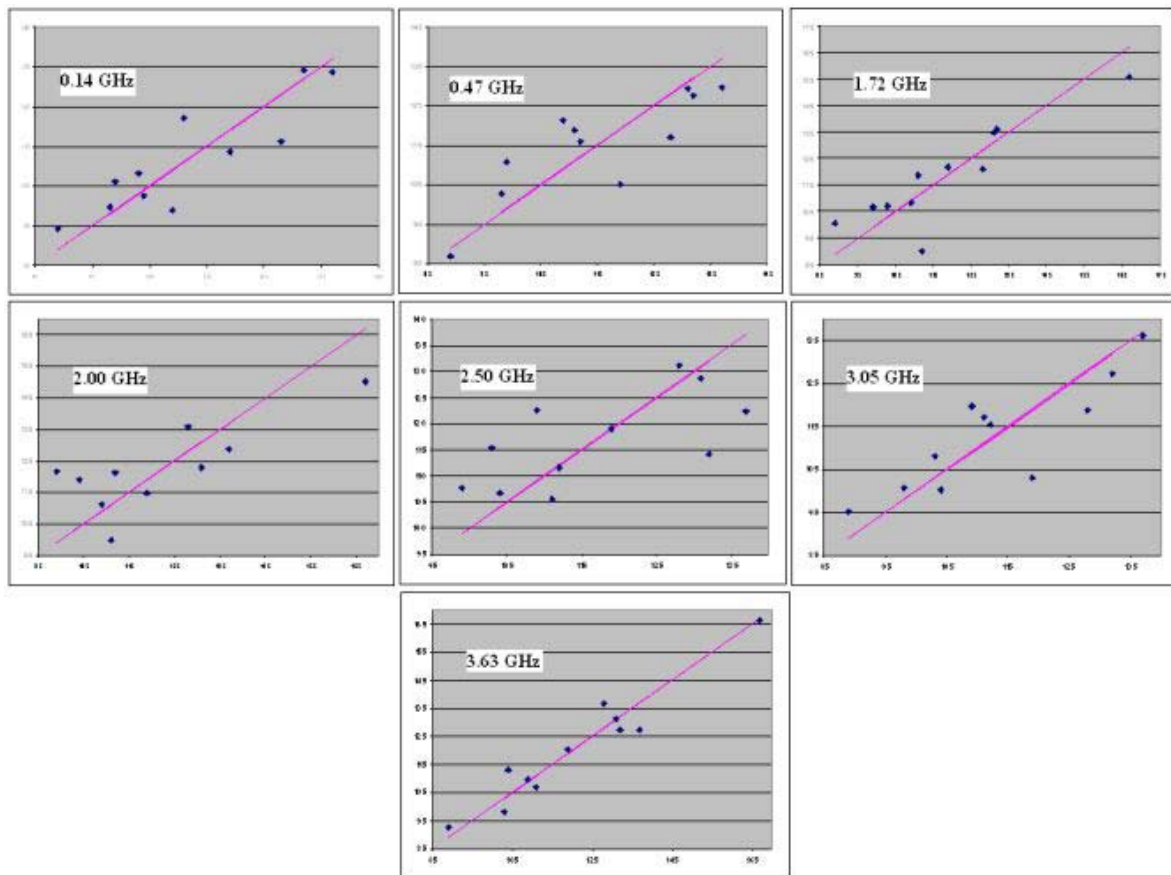


Figure D.19: Participant #4-2 predicted glucose values versus actual glucose values (mg/dL) after the first difference method was applied

PCA Results from the Second Experiment

Table D.16: R Square values for each participant after PCA was applied

Participant	<i>R Square</i>
Participant #1	0.429
Participant #2	0.318
Participant #3	0.803
Participant #4	0.336
Participant #4-2	0.257
Participant #5	0.350

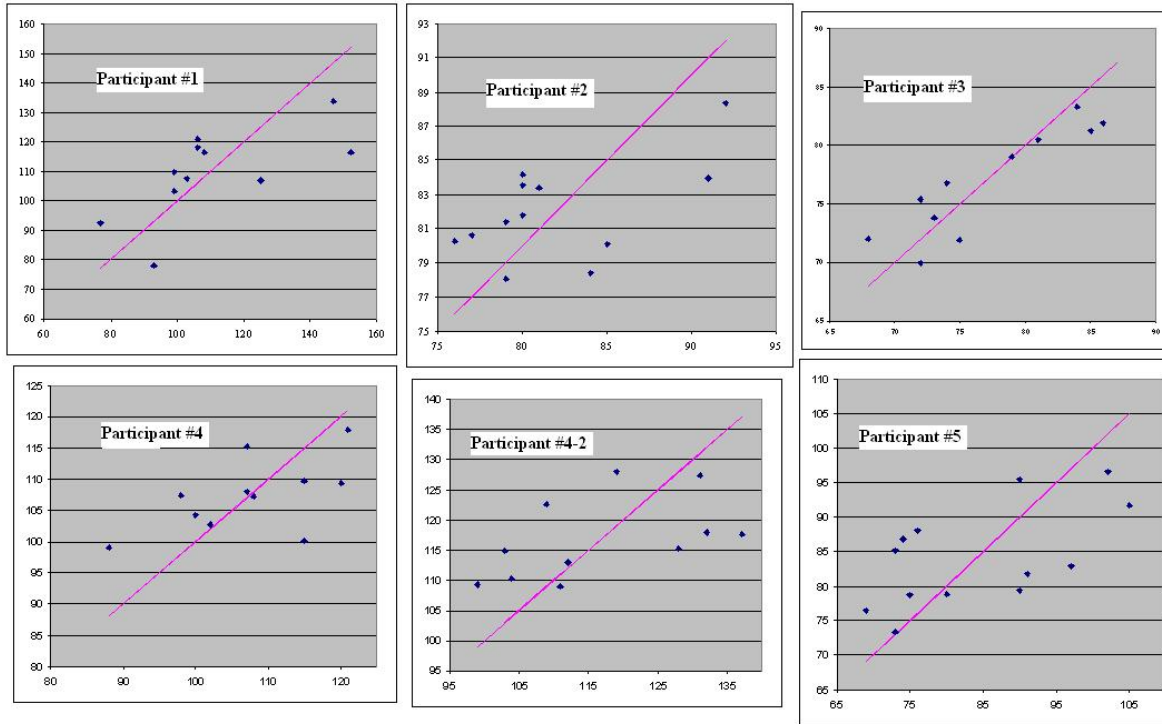


Figure D.20: Predicted glucose values versus actual glucose values (mg/dL) after PCA was applied

Table D.17: R Square values for each participant after the first difference method and PCA were applied

Participant	<i>R Square</i>
Participant #1	0.974
Participant #2	0.915
Participant #3	0.741
Participant #4	0.402
Participant #4-2	0.708
Participant #5	0.911

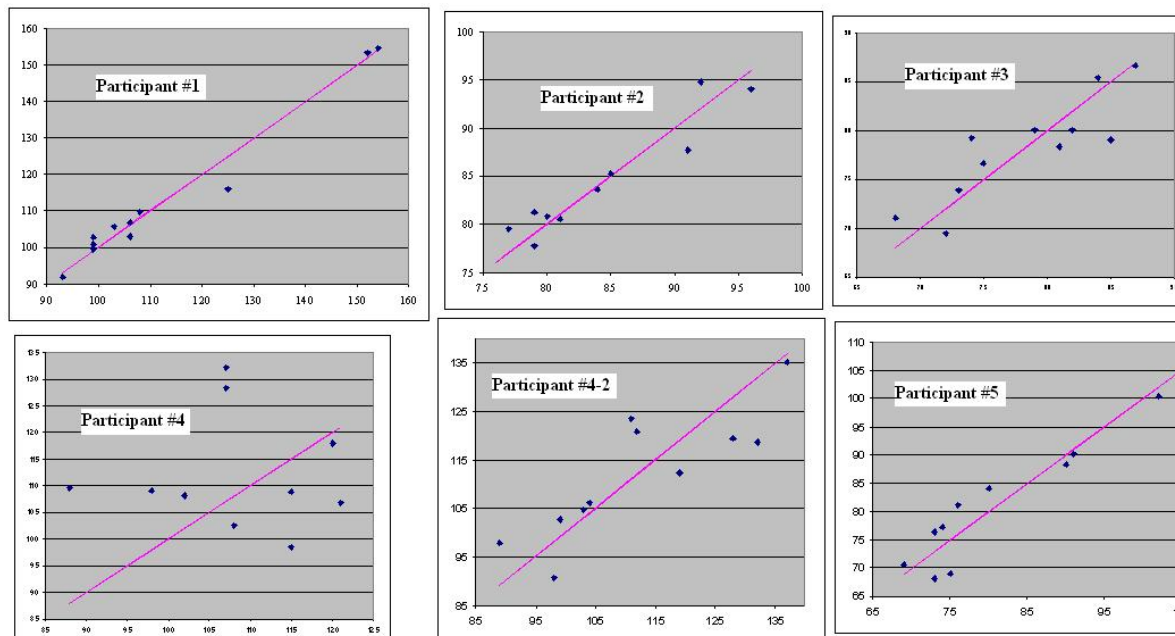


Figure D.21: Predicted glucose values versus actual glucose values (mg/dL) after the first difference method and PCA were applied

BIBLIOGRAPHY

- [1] Centers for Disease Control and Prevention, National Institutes of Health, and American Diabetes Association, "National Diabetes Fact Sheet, 2005." [Online] 2006(November 1), Available: <http://www.diabetes.org/uedocuments/NationalDiabetesFactSheetRev.pdf>
- [2] A. Rosen, M.A. Stuchly and A. V. Vorst, "Applications of RF/microwaves in medicine," *IEEE Trans. Microwave Theory Tech.*, vol. 50, pp. 963-974, 2002.
- [3] American Diabetes Association, "Economic Costs of Diabetes in the U.S. in 2002," in *Diabetes Care*, vol. 26, pp. 917-932, 2003.
- [4] R. Badugu, J.R. Lakowicz and C.D. Geddes, "A Glucose Sensing Contact Lens: A Non-Invasive Technique for Continuous Physiological Glucose Monitoring," *Journal of Fluorescence*, vol. 13, no. 5, pp. 371-374, Sept 2003.
- [5] American Diabetes Association, "All About Diabetes." [Online] 2006(November 1), Available: <http://www.diabetes.org/about-diabetes.jsp>
- [6] *Merriam-Webster's Medical Dictionary*. Springfield, Massachusetts: Merriam-Webster, Inc., 2006.
- [7] Norman Endocrine Surgery Clinic, "Normal Regulation of Blood Glucose," Norman Endocrine Surgery Clinic, 2002. [Online] 2006(November 5), Available: <http://www.endocrineweb.com/insulin.html>
- [8] Medline Plus Medical Encyclopedia, "Glucose Test," U.S. National Library of Medicine and National Institutes of Health. [Online] 2006(November 3), Available: <http://www.nlm.nih.gov/medlineplus/ency/article/003482.htm>
- [9] Anonymous (2007, October 4, 2007). Glucose Meter. [Online]. 2007(October 4), Available: http://en.wikipedia.org/wiki/Glucose_meter
- [10] Sherman, Marie, "How Do Blood Glucose Meters Work?" Chem 13 News, Ursuline Academy, pp. 5-6, Dec. 2006. [Online] (July 17), Available: http://www.chem13news.uwaterloo.ca/issues/343/343_dec_2006_pages_5-6.pdf
- [11] "Glucose Meters & Diabetes Management" Us. Food and Drug Administration, June 14, 2005. [Online] 2007 (July 5), Available: <http://www.fda.gov/diabetes/glucose.html>

- [12] WebMD, "Home Blood Glucose Test," A-Z Health Guides. [Online] 2006(November 3), Available: http://www.webmd.com/hw/diabetes_1_2/hw226531.asp
- [13] "Review Criteria Assessment of Portable Blood Glucose Monitoring In Vitro Diagnostic Devices Using Glucose Oxidase, Dehydrogenase or Hexokinase Methodology. (Draft Version)," U.S Food and Drug Administration Center for Radiological Health, Feb. 28, 1997. [Online]. 2007(July 10), Available: <http://www.fda.gov/cdrh/ode/gluc.html>.
- [14] A.P Kretz and D. Styblo, "Toward Continuous Blood Glucose Monitoring," *Medical Device Link*, June 2003. [Online] 2007 (July 10), Available: <http://www.device-link.com/mddi/archive/03/06/003.html>
- [15] Calisto Medical, "Glucoband – Non-invasive Medical Telemetry," Calisto Medical, Inc., 2004-2006. [Online] 2006(November 7), Available: <http://www.calistomedical.com/eng/?p=glucoband>
- [16] Cygnus, "Brochure: Glucowatch – Automatic Glucose Biographer," Cygnus Inc, Redwood City, California, Oct. 2002. [Online] 2006(November 7), Available: http://www.glucowatch.com/us/pdfs/patient_brochure1.pdf
- [17] Anonymous, "Breakthrough technology allows non-invasive, pain-free glucose testing," in *The SPIE Magazine of Photonics Technologies and Applications*, October 24, 2005. [Online] 2006(November 7), Available: http://oemagazine.com/newscast/2005/102405_newscast01.html
- [18] Anonymous, "Study Shows Non-Invasive Device Outperforms fasting Glucose and A1C for Diabetes Screening," Medcompare Medical News, September 29, 2006. [Online] 2006(November 7), Available: <http://www.medcompare.com/news.asp?newsid=153324>
- [19] R.W. Waynant and V.M. Chenault, "Overview of Non-Invasive Fluid Glucose Measurement Using Optical Techniques to Maintain Glucose Control in Diabetes Mellitus," *Leos Newsletter*, vol. 12, no. 2, April 1998.
- [20] A. Tura, A. Maran and G. Pacini, "Non-invasive Glucose Monitoring: Assessment of Technologies and Devices According to Quantitative Criteria," *Diabetes Research and Clinical Practice*, April 6, 2006.
- [21] L.C. Shen and J.A. Kong, *Applied Electromagnetism*, 3rd ed. Boston: PWS Pub. Co., pp. 606, 1995.
- [22] N.N. Rao, *Elements of Engineering Electromagnetics*, 2nd ed. Englewood Cliffs, New Jersey: Prentice-Hall, Inc., 1987.

- [23] Anonymous (2006, November 11, 2006). Water. [Online]. 2006(November 15), Available: <http://en.wikipedia.org/wiki/Permittivity>
- [24] D.K. Cheng, *Fundamentals of Engineering Electromagnetics*, 1st ed. Reading, Massachusetts: Addison-Wesley Publishing Company, 1993.
- [25] Pethig, R., "Dielectric Properties of Body Tissues," *Clinical Physics and Physiological Measurements*, vol. 8, pp. 5-12, 1987.
- [26] Sischa, F., "Basics of S-Parameters, part 1," Agilent Technologies Characterization Handbook, May 2002. [Online] 2006(November 15), Available: http://eesof.tm.agilent.com/docs/iccap2002/MDLGBOOK/1MEASUREMENTS/3VNA/3SPAR/1SparBasics_1.pdf
- [27] Agilent Technologies, "85070E Dielectric Probe Kit 200 MHz to 50 GHz Technical Overview," [Online], 2006(November 12) Available: <http://cp.literature.agilent.com/litweb/pdf/5989-0222EN.pdf>
- [28] Jefferies, J., "Waveguides and Cavity Resonators," University of Surrey, Department of Electrical Engineering, Jan. 14, 2005. [Online] 2006(November 14), Available: <http://www.ee.surrey.ac.uk/Personal/D.Jefferies/wguide.html>
- [29] Anonymous Electromagnetic Problems, "Introduction to Rectangular Waveguides." [Online]. 2006(November 16), Available: <http://www.ee.bilkent.edu.tr/~microwave/programs/magnetic/rect/info.htm>
- [30] K. Saeed, A.C. Guyetts, I.C. Hunter, R. D. Pollard, "Microstrip Resonator Technique for Measuring Dielectric Permittivity of Liquid Solvents and for Solution Sensing," *IEEE/MTT-S International Microwave Symposium 2007*, pp. 1185-1188 2007, June 2007.
- [31] B.R. Jean, "Guided Microwave Spectrometry for In-line Analysis of Flowable Materials," in *RF & Microwave Sensing of Moist Materials, Food, and other Dielectrics*, vol. 7, K. Kupfer, A. Kraszewski and R. Knochel Eds. Weinheim:Wiley, 2001.
- [32] "IEEE standard for safety levels with respect to human exposure to radio frequency electromagnetic fields, 3 kHz to 300 GHz," *IEEE Std C95.1, 1999 Edition*, 1999.
- [33] Anonymous (2007, October 4, 2007). Thermography. [Online]. 2007(October 4), Available: <http://en.wikipedia.org/wiki/Thermography>
- [34] O.G. Martinsen, S. Grimnes and H.P. Schwan, "Interface phenomena and dielectric properties of biological tissue," in *Encyclopedia of Surface and Colloid Science* Anonymous Marcel Dekker, Inc., 2002, pp. 2643-2652.

- [35] S. Gabriel, R.W. Lau and C. Gabriel, "The Dielectric Properties of Biological Tissues: III. Parametric Models for the Dielectric Spectrum of Tissues," *Physics in Medicine and Biology*, vol. 41, pp. 2271-2293, April 1996.
- [36] K Ismail, D.K. Ghodaonkar, M.S. Mohamed Said, Z. Awang, and E. Mazlina, "Microwave Characterization of Human Blood using Dielectric Waveguide Measurement System," in *Proceedings of the XXVIIIth URSI General Assembly in New Delhi (October 2005)*, International Union of Radio Science, 2005. Available: [http://www.ursi.org/Proceedings/ProcGA05/pdf/K01.5\(0870\).pdf](http://www.ursi.org/Proceedings/ProcGA05/pdf/K01.5(0870).pdf)
- [37] Y. Nikawa and D. Someya, "Non-invasive measurement of blood sugar level by millimeter waves," *Microwave Symposium Digest 2001 IEEE MTT-S International*, vol. 1, pp. 171-174, May. 2001.
- [38] J.H. Park, C.S. Kim, B.C. Choi and K.Y. Ham, "The correlation of the complex dielectric constant and blood glucose at low frequency," *Biosensors and Bioelectronics*, vol. 19, pp. 321-324, Dec 15. 2003.
- [39] B.H.V. Borges and L.E.M. de Barros Jr., "Design of Optical Bio-Sensor Using Polymetric Waveguide," *IEEE MTT-S IMOC 1999 Proceedings*, pp. 66-69, 1999.
- [40] A. Caduff, E. Hirt, Y. Feldman, Z. Ali and L. Heinemann, "First human experiments with a novel non-invasive, non-optical continuous glucose monitoring system," *Biosensors and Bioelectronics*, vol. 19, pp. 209-217, May 15, 2003.
- [41] E.C. Green, "Design of a Microwave Sensor for Non-Invasive Determination of Blood-Glucose Concentration." Master's thesis, Baylor University, 2005.
- [42] L. R. Ballew, "A Microwave Radiometer System for Use in Biomedical Applications." Master's thesis, Baylor University, 2006.